Master's thesis

NTNU
Norwegian University of Science and Technology
Faculty of Engineering
Department of Civil and Environmental Engineering

Mari Elisabeth Jensvold Ørbæk

Smart Thermal Energy System for Modern Apartment Buildings

Master's thesis in Energy and Environmental Engineering
Supervisor: Armin Hafner
December 2020

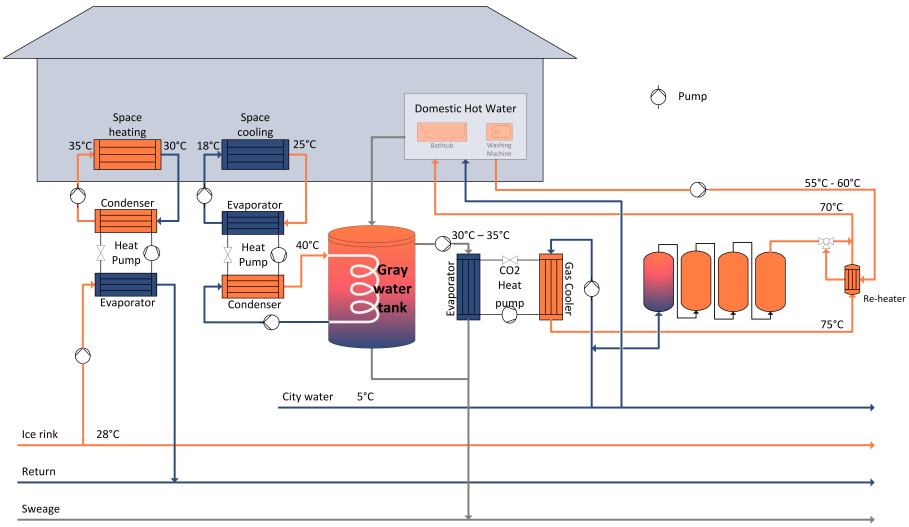

NTNU
Kunnskap for ei betre verd

Mari Elisabeth Jensvold Ørbæk

Smart Thermal Energy System for Modern Apartment Buildings

Master's thesis in Energy and Environmental Engineering
Supervisor: Armin Hafner
December 2020

Norwegian University of Science and Technology
Faculty of Engineering
Department of Civil and Environmental Engineering

NTNU
Kunnskap for ei betre verd

Task for Thesis

At Leangen in Trondheim, a new building area is to be built. The building area will follow high standards of energy efficiency, thus needs a good energy profile. In order to achieve this, a smart and energy efficient delivery system for both heating and cooling, and for space and tap water, will be used. This will be done through a local low-temperature grid, utilizing excess heat from different sources.

The building area is going to be divided into 13 zones, each with it's own energy central. This thesis will include providing an energy profile for one of these zones, including a description of its energy demand.

Different sources of energy will also be evaluated, with a focus on the use of excess heat from the gray water the building area is producing, and a local ice rink. This thesis will look into different studies of utilizing this method, and compare it with other sources and ways of covering the energy demand.

The heating and cooling demands will be covered by the help of heat pumps. This thesis will use the modeling language Modelica to simulate a heat pump. The simulation will use the surplus heat from the sources found, and calculate how much energy it is possible to deliver. It will also explore the possibilities of storing this as thermal energy.

The following tasks are to be considered:

- Reviewing of relevant literature
- Modeling an ammonia heat pump in Dymola
- Use the simulation tool SIMIEN to calculate the energy profile of a single building and a whole substation
- Evaluate different heat sources, with focus on gray water
- Simulate a tank to hold gray water in the simulation tool COMSOL Multiphysics
- Perform an economic analysis of the different energy delivery methods
- Analyze the results in terms of system performance, energy consumption, and thermal energy storage potential
- Summary of report
- Draft version of a scientific paper based on the main findings of the Thesis
- Proposal for further work

Preface

This thesis was written in the year of 2020, in a time when the corona virus ravaged the world. This thesis has experienced ups and downs, and has been an incredible journey to work with. When I now hand it in, it concludes my 5 years studying at NTNU in Trondheim.

I would like to thank my supervisor, Armin Hafner, and my co-supervisor, Hanne Kauko, for helping me achieving my goals for this thesis. They have been a huge support and great discussion partners, and given me valuable guidance through the whole process. I want to thank Marcel Ulrich Ahrens and Ignat Tolstorebrov at NTNU, for being great mentors in building the systems of this thesis in the simulation tools.

Finally, I would like to give a special thanks to my family, who has stood by my side this whole year. They have been an invaluable emotional support that I could not have been without.

Mari Elisabeth Jensvold Ørbæk
Trondheim
December 2020

Abstract

At Tungavegen 1 in Trondheim, an old, rundown racecourse will soon be transformed into a new, future-oriented residential area. The area will consist of apartment buildings, common areas, office buildings, and more. The goal is for it to be completed by 2050. These buildings are going to have a massive energy demand for space heating and cooling, as well as for heating of tap water. This thesis will evaluate different methods of providing this energy, in the most efficient manner.

The area will be built into 13 zones, and to get an understanding of how much energy Tungavegen 1 will need, one of these zones has been simulated in the simulation tool SIMIEN. The energy profile is a result of construction and equipment requirements of a low energy consuming building, taken from the TEK17 standard. The energy demands for space heating, domestic hot water heating and space cooling, are 29.5 kWh/m^2, 30.0 kWh/m^2 and 10.4 kWh/m^2, respectively.

Every zone will contain an energy central, providing and distributing energy to all the buildings within the specific zone. An energy central will consist of heat pumps, thermal energy storage tanks, gray water tanks, and general pipes and circulation pumps. Different methods of integrating the appliances have been presented and evaluated.

The energy supply for heating of space, will primarily be delivered through a local low-temperature thermal distribution system. This local grid will contain water that has been heated up by excess heat from a local ice rink, and will pass through all the 13 energy centrals. Together with a heat pump, this will be used to provide enough heat the heat up the entirety of the zones.

In addition to this, gray water produced by the buildings will be gathered in a tank, and used as a heat source for the heating of domestic hot water. This will be done in the same manner as for space heating, with the help of a heat pump. The temperature elevation of domestic hot water is much larger than for space heating, and therefor will require a different heat pump.

In order to create an optimized energy efficient building area, heat pumps were evaluated in order to deliver hot water to the facilities requiring higher temperatures than what can be delivered by the low-temperature distribution system. Both CO_2 and ammonia heat pumps were discussed, but only the ammonia heat pump was evaluated in detail. It was evaluated that space heating and cooling will need a heat pump able to deliver 140 kW and 112 kW, respectively.

Another major topic that has been inspected in this theses, is the integration of a space cooling circuit and the gray water tank. The implementation of a space cooling circuit, will require a separate heat pump, and will produce energy in form of heat in the same way as the ice rink. Therefore, an integration of pipes within the walls of the gray water tank was looked at, to see if this could be a viable heat sink for the space cooling circuit.

The gray water tank was of concrete, and since this material has a very low conductivity, there was not a high heat transfer rate. It was found that the tank could only provide between 10 kW and 25 kW, which is not much compared to the potential of 112 kW. Instead, other solutions, like having an external heat exchanger or dumping the heat in the return circuit of the local thermal grid, were evaluated

as more efficient.

This thesis has kept in focus the enormous potential of waste heat. Some of the biggest challenges facing our earth, is how much energy humans are consuming. If smarter solutions are chosen, where spilled energy gets new life as a heat source, our planet might be saved.

Sammendrag

I et område i Trondheim, Tungavegen 1, vil en gammel nedslitt veddeløpsbane snart bli omgjort til et nytt og fremtidsrettet boligområde. Området vil blant annet bestå av rekkehus, leiligheter, fellesområder og kontorbygg. Målet er at området skal være ferdig utbygd innen 2050. Disse bygningene vil ha et enormt energibehov for oppvarming og nedkjøling, samt oppvarming av springvann. Denne masteroppgaven har evaluert forskjellige metoder for å levere den nødvendige energien på en mest mulig effektiv måte.

Området skal bygges i etapper og deles inn i 13 soner. For å få en forståelse av hvor mye energi som trengs i Tungavegen 1, ble en av disse sonene, B1, simulert i simuleringsverktøyet SIMIEN. Energiprofilen ble basert på krav til konstruksjon og utstyr for et lavenergibygg, hentet fra TEK17-standarden. Energibehovet for romoppvarming, varmtvann og kjøling, er her henholdsvis 29.5 kWh/m^2, 30.0 kWh/m^2 og 10.4 kWh/m^2.

Hver sone vil ha en energisentral som tilfører og distribuerer energi til alle bygningene i den spesifikke sonen. En energisentral vil bestå av varmepumper, lagringstanker for termisk energi, gråvannstanker, rørsystem og sirkulasjonspumper. Ulike metoder og mulige oppsett for systemet ble presentert og evaluert i oppgaven.

Energiforsyningen for oppvarming av rom, vil i hovedsak bli levert gjennom et lokalt lav-temperatur distribusjonssystem. Det lokale nettet vil bestå av vann som er oppvarmet av overskuddsvarme fra den lokale skøytebanen i området. Det oppvarmede vannet vil distribueres gjennom rørsystemet for hele området og de 13 energisentralene. Sammen med en varmepumpe vil dette oppvarmede vannet gi nok energi til å varme opp den enkelte sonen.

I tillegg til dette, vil man samle gråvann fra bygningene i en gråvannstank. Spillvarmen fra gråvannet vil benyttes som varmekilde for å varme opp varmtvann til husholdningene. Dette vil gjøres på samme måte som ved romoppvarming, ved hjelp av en varmepumpe. Temperaturløftet for varmtvann er mye høyere en for romoppvarming, og det må derfor benyttes en annen type varmepumpe for å få til dette.

For å skape et optimalt energieffektivt område, ble varmepumper evaluert for de delene der det var nødvendig med høyere temperaturer enn det som kunne bli levert av et lav-temperatur distribusjonssystem. Både CO_2 og ammoniakk varmepumper ble vurdert, men bare ammoniakk varmepumper ble evaluert i detalj. Videre ble det beregnet at en varmepumpe for oppvarming og kjøling vil trenge en pumpe som kan levere henholdsvis 140 kW og 112 kW.

Et annet hovedtema som ble sett på i denne oppgaven, var å integrere en romkjølingskrets med en gråvannstank. Implementering av en romkjølingskrets vil kreve en egen varmepumpe og vil produsere energi i form av varme på samme måte som den lokale skøytebanen. Det ble derfor sett på en integrering av rør inne i veggene på gråvannstanken for å se om dette ville være et egnet varmesluk i romkjølingskretsen.

Oppgaven har sett på en gråvannstank av betong, og siden dette materialet har lav varmeledningsevne, var varmeoverføringshastigheten lav. Det ble funnet at tankene bare kunne gi mellom 10 kW og 25 kW, noe som er lavt i forhold til

potensialet på 112 kW. Andre løsninger ble vurdert, og det ble funnet ut at en ekstern varmeveksler eller å dumpe varmen i returkretsen til den lokale termiske sentralen, ville være mer effektivt.

Denne masteroppgaven har fokusert på potensialet rundt spillvarme. En av de største utfordringene jorden står overfor, er det enorme energiforbruket vi mennesker har. Med smarte løsninger der man gjenbruker energien i spillvarme til oppvarming, har man gjort mye for å redde planeten vår.

Contents

List of Figures

List of Tables

Nomenclature

ΔT_{SH}	Superheat temperature	K
ΔT	Temperature difference	K
δ	Degree	°
Δ_P	Operating pressure	bar
ΔT_{lm}	Log mean temperature difference	K
$\dot{m}$	Mass flow	kg/s
$\dot{Q}$	Heat transfer rate	kW
$\dot{Q}_C$	Heat transfer in condenser	kW
$\dot{Q}_E$	Heat transfer in evaporator	kW
$\dot{Q}_{GC}$	Heat transfer in gas cooler	kW
$\dot{W}$	Compressor power	kW
η	Efficiency	–
η_{is}	Isentropic efficiency	–
μ	Dynamic viscosity	kg/m s
Φ	Total heat flux	kW
ρ	Density	kg/m^3
τ_w	Shear stress	Pa
ε	Roughness	mm
φ	Heat flux	W/m^2
ζ_b	Drag coefficient	–
A	Surface or cross sectional area	m^2
c_p	Specific heat capacity	kJ/kg K

C_{comp}	Cost of electricity in the compressor	NOK
C_{elect}	Electricity cost	NOK
$C_{reduced}$	Reduced cost	NOK
C_{tot}	Total cost	NOK
COP	Coefficient of Performance	–
D	Diameter	m
d	Thickness	m
D_{pipe}	Pipe diameter	m
E	Energy consumption	kWh
f	Darcy friction factor	–
g	Gravitational acceleration	$9.81\,\mathrm{m/s^2}$
G_{fee}	Variable grid fee	NOK/kWh
GR_{fixed}		NOK
GR_{var}	Variable grid rent	NOK/kWh
H	Height	m
h	Specific enthalpy	kJ/kg
h_c	Convective heat transfer coefficient	$\mathrm{W/m^2\,K}$
i	Discounting rate of return on an alternative investment	–
k	Thermal conductivity	$\mathrm{W/m\,K}$
L	Length	m
m	Mass	kg
NPV	Net present value	NOK
P	Pressure	bar
P_{crit}	Critical pressure	bar
P_C	Pressure in condenser	bar
P_E	Pressure in evaporator	bar
P_{GC}	Pressure in gas cooler	bar
Q	Heat capacity or demand	J

R	Thermal resistance	W/K
R_t	Net inflows and outflows for a single period	NOK
Re	Reynolds number	–
S	Savings	NOK/kWh
T	Temperature	°C
t	time periods	–
T_C	Condensation temperature	°C
T_E	Evaporation temperature	°C
T_{crit}	Critical temperature	°C
T_{pipe}	Pipe temperature	°C
U	Thermal transmittance	$\mathrm{W/m^2\,K}$
U-value	Heat transfer coefficient	$\mathrm{W/m^2\,K}$
V	Volume	$\mathrm{m^3}$
v	Fluid velocity	m/s
v_{avg}	Average fluid velocity	m/s
Q_{SH}	Space heating demand	kWh

Chapter 1

Introduction

1.1 Background and Motivation

Greenpeace recently sued the government of Norway for not taking enough responsibility for their ruining of our environment. They lost. Australia almost burnt down last winter. Money was raised in order to put out the fire, but close to nothing was raised in order to prevent it from happening again. Instead, companies keep drilling for oil in the Australian waters. They continue doing this because there is still so much money in the oil industry, because we are still dependent on the energy it provides. No one is willing to change their behavior. This cannot continue.

The energy demand for houses covers a share of 40 % of the total energy use in Norway [52]. Further, 80 % of this is estimated to be needed to cover the heating of space. The constant growth in energy demand, as well as the massive use of non-renewable energy sources like oil, indicates a future where the energy demand cannot be reached. This is a huge problem. Especially with the continued growth of environmental challenges that we are facing. The greatest effort the building sector can do in order to do their part for the environment, is contributing to reduce the energy need for new building areas.

To deal with this matter, the United Nations has made 17 goals, called the Sustainability Goals, going towards 2030. The seventh goal deals with energy, and promises to ensure affordable, reliable, sustainable and modern energy for everyone [62]. A future problem can be the continued growth in the worlds population.

In order to reach this goal, the building sector needs to do their part. This thesis will therefore go through measures that can lower the energy need of building drastically, both by reducing the need for general energy, but also by producing their own heat and energy. The goal is to do this without compromising the actual energy use of the building.

This is why houses with low energy consumption and renewable delivery methods for energy is an important measure to take. At Leangen in Trondheim, a building area is going to be built with this is mind.

1.2 Scope and Outline of Thesis

With the knowledge of needing to reduce the energy footprint of buildings in mind, this thesis continues. Because, how can this be done?

One obvious solution is reducing the energy need by simply reducing the energy use. Turning off the heating equipment in all buildings and stop using technical equipment. Turning off stoves and washing machines, is a very efficient way of reducing the need for energy. However, reducing the standards of living is not something many people are willing to compromise with, and is therefore not a very long term solution.

Another solution could be installing solar panels to cover the total energy use. This, however, would be very costly and quite space consuming, and is thereby not a optimal solution for the future.

So the question becomes: how can the energy demand of a building decrease, without having to compromise the standards of living or it becoming a huge economical burden?

This thesis will answer this question by the following points:

- Reviewing a variety of literature
- Introducing the building area of Leangen
- Defining a reference building zone and estimating its energy profile
- Investigating different sources of energy, with special notice to excess heat from gray water with help from COMSOL
- Investigating the use of heat pumps through the use of the simulation tool Dymola
- Making cost analyses and comparing different energy methods

The thesis contains 7 chapters where these points will be covered. Several of the chapters include sections and subsections, which are all covered in the table of contents. The 1st chapter is the current chapter, covering the introduction. The 2nd chapter deals with the literature review and explains all the theory needed for the rest of the thesis. The 3rd chapter is the method section of the thesis, describing how all the results have been found, and touches upon the strengths and weaknesses of the methods. The 4th chapter presents the results and analyses them. The 5th chapter presents discussions of the findings presented in the previous chapter. The 6th chapter concludes the discussion from the previous chapter. The 7th and last chapter comprises a suggestion of tasks that can take the concept of this thesis even further.

1.3 Limitations of Thesis Parameters

There are some factors in this thesis that can be seen as limitations.

First of all, Tungavegen 1 is going to be built step-wise, and standards and technologies will probably improve from the first building is built, until the last one. Because of this, the findings in this thesis might not be applicable for the later stages of the process.

Specifications for Tungavegen 1 has changed throughout the period of the making of this thesis, and will most likely change again before the first building is standing. This has affected the results in this thesis, and will also affect the reliability of the findings in this thesis in comparison with what will actually happen at Tungavegen 1.

Another limitation, is that all simulations performed in this thesis are just that, simulations, and not based on actual measurements. This means that the finding in this thesis are solely theoretical, and real life cases might differ.

Chapter 2

Theory

The second chapter of this thesis, presents the theory it is based on. The chapter starts with explaining how district heating and local thermal grids work, the benefits of it, and how it can be used to regulate the thermal environment in buildings. Then, the concepts behind heat transfer and pressure drop will be explained. The thesis will then present different methods for how thermal energy grids can be made even more sustainable and environmental friendly, through the help of heat sources, heat pumps, and thermal energy storage. The chapter then closes with a brief evaluation of how to calculate the costs relating to these systems.

2.1 Heat Distribution

Reaching sustainability goal 7 means providing affordable, reliable, clean, sustainable and modern energy for everyone [62]. One method of doing this, which is already highly distributed in Trondheim, is the use of district heating [65]. In this section, the concept of district heating will be explained, as well as how it can help with the sustainability goals.

2.1.1 Principles of District Heating

District heating is a system for distributing energy from a centralized energy plant, through systems of insulated pipes for commercial and residential heating requirements. The main purpose of district heating, is the heating and distribution of water. Underground pipes are used for transportation of heated water between a producer and an end user, usually within the same area. A district heating system consists of several centrals, where the water is distributed to several buildings. [13]

Once the water reaches a building, the heat from the water can be used for the heating of space, usually through underfloor heating systems or radiators. Heating of tap water is another area of use for this energy. Both of these methods will be explored more thoroughly later in this chapter.

The heat sources for the production plant include combustion of waste, bio fuel, gas, oil and electricity. Heat pumps are also common parts of district heating, and using more than one of these components together ensures a reliable supply of energy to the end user.

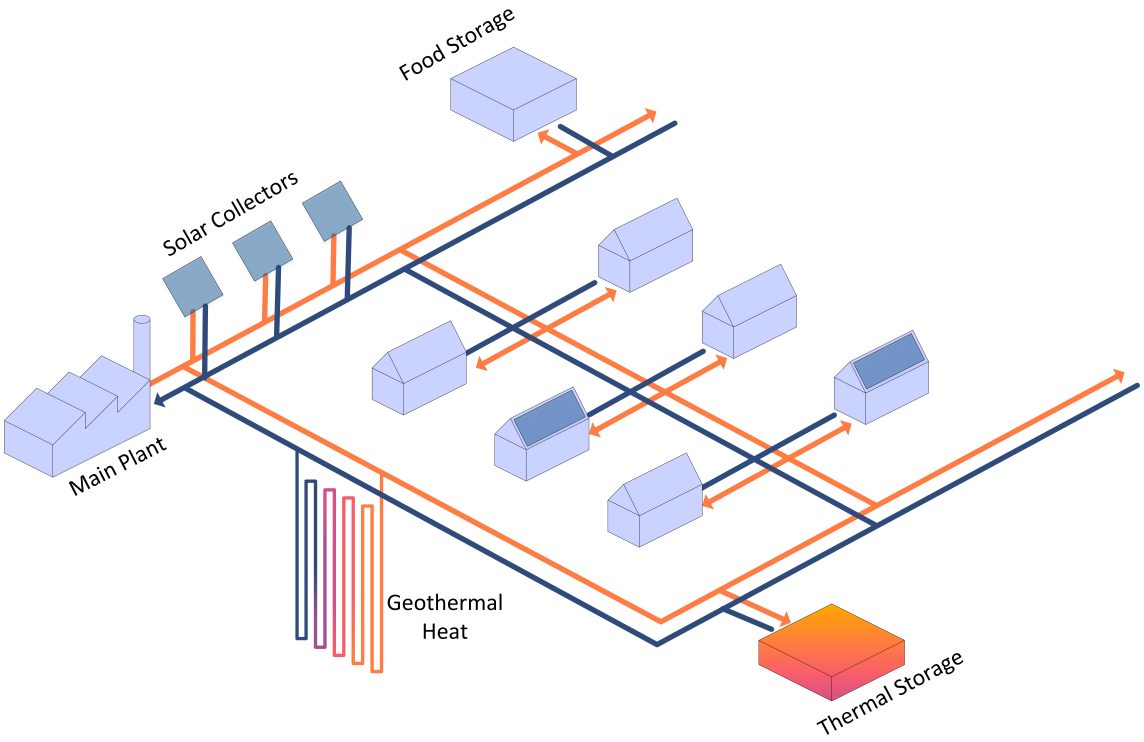

Figure 2.1: *Simplified district heating system*

Figure 2.1 shows a local district heating network, with a main plant, or producer, to the left and all the houses it provides heated water for to the right. The figure also includes solar collectors, thermal storage and heating wells, which can all integrate with the district heating system.

The fact that district heating can integrate a hand full of different energy sources in the same system, gives this method a huge advantage over more conventional methods. It allows for the use of highly renewable heat sources, like solar and geothermal heat, and, which will be the main focus for heat source in this thesis, the use of excess heat from various processes.

2.1.2 Development of District Heating

District heating involves a centralized heat generator, which distributes heat to remote locations. The carrier of heat is a heated medium circulating in underground pipes. Since the start in the late 1800s, district heating systems have undergone a huge development. Each generation of district heating are represented by better, safer and more efficient methods of distributing the heated medium. [31]

The first generation of district heating, involved steam as heat carrier. This system was introduced in the 1880s, and used very high temperatures of over 200 °C. This is now an outdated solution, because it resulted in relatively low efficiencies, due to the heat losses caused by the steam, and could lead to explosions if leakage occurred.

The second generation was formed in 1930s and used pressurized hot water.

These required large on-site plants, but used lower temperatures, though still usually above 100 °C. The efficiency was better, though still quite low.

The third generation from the 1970/80s used pre-insulated pipes and was able to utilize off-site constructions. The heat carrier was pressurized water, where the temperatures were lower than 100 °C and the efficiency had reached even better standards.

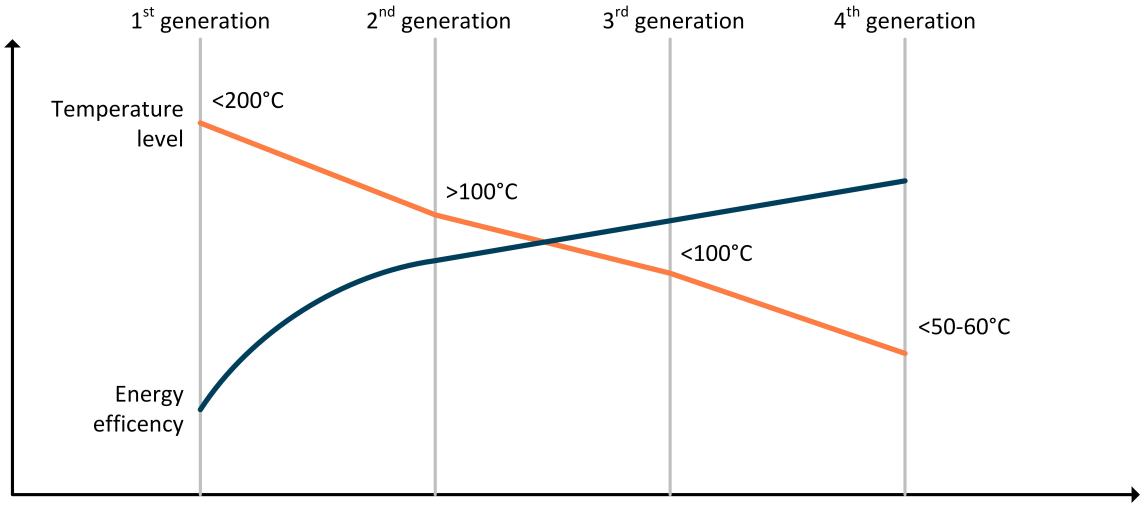

Figure 2.2: *The generations of district heating and temperature and effectiveness levels*

The ongoing trend throughout these three generations, has been the lowering of the heat carrier's temperature. This is mainly because the heat losses increase with the temperature, which again cause lower efficiencies, as summarized in figure 2.2. Therefore, the next generation of district heating, known as 4th Generation District Heating (4GDH), will continue this trend and should be able to implement an even lower temperature, while still being able to deliver enough heat for space heating and domestic hot water (DHW). In addition, the system should be able to do this with the minimum amount of losses to ensure the best efficiencies as possible.

Another feature of this 4GDH system, which also is the most important feature, is that it does not only focus on what we need here and now, but also on what the needs in the future will be. As cities are getting smarter and more energy efficient, it is also important for a better district heating system to be able to cooperate and integrate with its functions. This includes being able to combine smart electricity, thermal and gas grids in one united solution, as well as having the ability to recycle energy from other energy sources, like solar power, geothermal energy or other sources that might come. Additionally, it should ensure everything mentioned can be done in a cost efficient manner. [31]

The 4GDH is the DH system that is in development right now. The most essential difference between the 3rd and the 4th generation, is that temperatures now can get as low as 40 °C to 50 °C, which lowers the thermal losses significantly. In addition, it opens up for the integration of "weaker" and renewable sources, like excess heat from buildings, and solar and geothermal heat. [41]

2.1.3 Low-Temperature Thermal Grids

Studies show that up to one third of the heat losses can be eliminated by lowering the temperatures in the distribution systems [26]. This is why lowered temperatures are preferable.

However, there are limitations for how low the temperatures can be set. One is related to the temperatures needed in the building. For instance, tap water usually needs a temperature of at least 50 °C. The temperature levels needed for space heating vary greatly from country to country, depending on the climate. For the Scandinavian countries, radiators should have a temperature of around 50 °C, and floor heating around 30 °C. [28]

Regarding the return temperature, a lower supply temperature usually means an increase in the return temperature. This is because the lower temperature needs to be compensated with a higher flow rate, giving the water less time to transfer heat. However, it is preferred to reach a lower temperature in both supply and return pipes, to achieve lower losses. [28]

Another limitation on how low the temperature can get, is regarding sanitizing in the equipment handling water. To prevent Legionella formation in water, a temperature of above 60 °C is required. It doesn't mean the water needs to be this warm at all times, but all equipment needs to be exposed to high temperature once in a while. Studies show that Legionella will be killed by exposure to 60 °C for longer than 25 minutes, and 70 °C for longer than 10 minutes. [69]

The 4GDH is made for the future. It will have the flexibility of connecting a various set of appliances, such as renewable and recycled heat sources, as well as thermal energy storage (TES). A main feature of the 4GDH is the use of low temperature heat sources which secures the ability to connect to other smart energy systems that are more efficient and open to more variety. [29]

2.1.4 Components of Low-Temperature Thermal Grids

Distribution systems using water, consists of a number of different components. This section will introduce the most important ones, being heat exchangers, piping systems, controlling equipment, and circulation pumps.

Heat Exchangers

To transfer heat from one medium to another, a heat exchanger is needed. Simply explained, a heat exchanger is a component that allows two media to run through it, where one transfers heat to the other. The two media are never in direct contact with each other, but can be separated by, for instance, pipes or plates. [2]

There are several different types of heat exchangers. Two of them will be explained in this section. Evaluating how much energy is needed is crucial for choosing the right heat exchanger, and deciding the size of it. Related calculations and how they can be used, will be introduced in section 2.3.

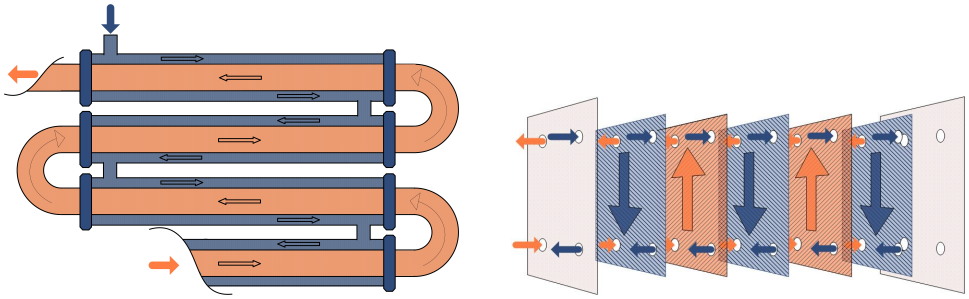

(a) Tube and Tube *(b)* Plate

Figure 2.3: *Examples of heat exchangers*

Tube and Tube Heat Exchanger A tube and tube heat exchanger exist of one tube within another tube, where the outer tube has a slighter bigger diameter than the inner. Figure 2.3a shows an example of how this can look. This design is especially applicable for systems operating with high temperature and pressure levels, and low mass flows.

Plate Heat Exchanger A plate heat exchanger consists of multiple parallel plates on top of each other. These plates form channels between one another, making the liquid flow in streams. Two inlet and two outlet holes let the two liquids flow through the plate heat exchanger. The fish bone pattern this results in, like shown in figure 2.3b, ensures a high heat transfer. [58]

Sizes of plate heat exchangers vary greatly. They can have a plate size of a couple of square centimeters, or up to 3 square meters. The number of plates can be as few as 10 plates, but can also be several 100. The biggest sizes of total heat transfer area can reach values of thousands of square meters. [45]

Controller and Regulation Systems

In order to make sure the system stabilizes, and keeps the correct temperatures to deliver the right amount of heat, controllers and regulation systems are needed. They can be used to control the mass flows of the media through valves and pumps within the system. [19]

For a regulation system to work properly, sensors are needed. The sensors used include equipment to measure temperature and pressure levels, mass flows, and enthalpy values to name a few. Further, the system uses valves or compressors, and regulate, respectively, the openings and speeds so that the sensors measure the wanted value.

It is very important to make sure the system stabilizes, to prevent the pressure to keep on growing.

Piping System

The piping system is used to transfer the liquid between the different components. The material and thicknesses used for the pipes depend highly on the chosen fluid. Factors that play a role on the choice of material, are whether or not the fluid is

corrosive or contain particles that will cause the pipes to erode, and the temperature levels the fluid will operate in. The thickness of the pipes will depend on the pressure levels, and how much stress they need to endure. [33]

The flow velocity also plays a role in choosing materials for pipes. The different materials have different velocity requirements, including ranges. To control the flow within a piping system, valves could be used. There are many different types of valves, but, in essence, the more closed the valve is, the more friction it adds.

In order to have systems more complex than just a straight pipe, different fittings are to be used as well. These can be plugs, valves, nipples, and other components, or simply a bend. However, all components and unregularities cause hydraulic resistance to the system, which needs to be taken into consideration when designing the system.

Circulation Pumps

For a district heating system to serve its purpose of delivering heat, the heat carrier needs to be circulating within the system. Circulation pumps ensures this by causing a pressure difference in the pipes to control the mass flow of the carrier. To cause motion in the carrier, the mass flow needs to overcome the hydraulic resistances within the system. [63]

Two of the main parameters of a pump, are the mass flow, $\dot{m}$ [kg/s], and the operating pressure, ΔP [bar]. The mass flow indicates the quantity of fluid that is transported through the pump, from the inlet to the outlet side. The operating pressure defines the amount of energy transferred from the pump to the fluid. These parameters are determining the size and dimensions, and thereof the characteristics, of the circulation pump.

2.1.5 Existing Systems

More and more people are seeing the benefits of sustainable building projects, both environmental and economical. This section includes two examples, one in Norway and one in Sweden, where low temperature thermal grids have been used in order to make sustainable residential buildings.

FutureBuilt at Furuset in Oslo

As a project for improving living conditions in the multicultural suburbs in Oslo, Oslo kommune has started a FutureBuilt project at Furuset in Oslo. The goal is to add more value to the area and the people staying there, and doing this in a sustainable manner. The new project includes building a new area that will provide between 1700-2300 new apartments and 2000-3400 new jobs. [3]

The energy use will be lowered by advanced regulation equipment. It will also use a local waterborne heat distribution system that will be able to utilize excess heat from surrounding area. A criteria for the system is that it has to be innovative, but also can be built in stages in correspondence with the development of the area.

This project consists of several smaller projects, where some of them have already been built. The finished projects include 36 climate neutral residential buildings,

and a passive school building.

Oslo kommune wants this projects to be a model project, and hope it will help inspire climate-friendly environment, and show how sustainability can be accomplished.

Medicon Village in Sweden

Medicon Village, is a cluster in Sweden for companies and organizations researching science for improving the health of people and making their lives better [35]. The interesting part of Medicon Village regarding this thesis, is that it uses ectogrid™.

ectogrid™ is a concept developed by E.ON, and deals with the distribution and reuse of thermal energy. ectogrid™ does this in a smart and energy efficient way, ensuring a sustainable and environmental friendly solution. The ectogrid™ at Medicon Village is the world's very first one to be built. [16]

As shown by the energy staircase in figure 2.4, from an energy efficiency point of view, the higher step of energy that can be utilized, the better [16]. ectogrid™ balances the needs of the different buildings involved, which corresponds to the second best energy utilization on the staircase.

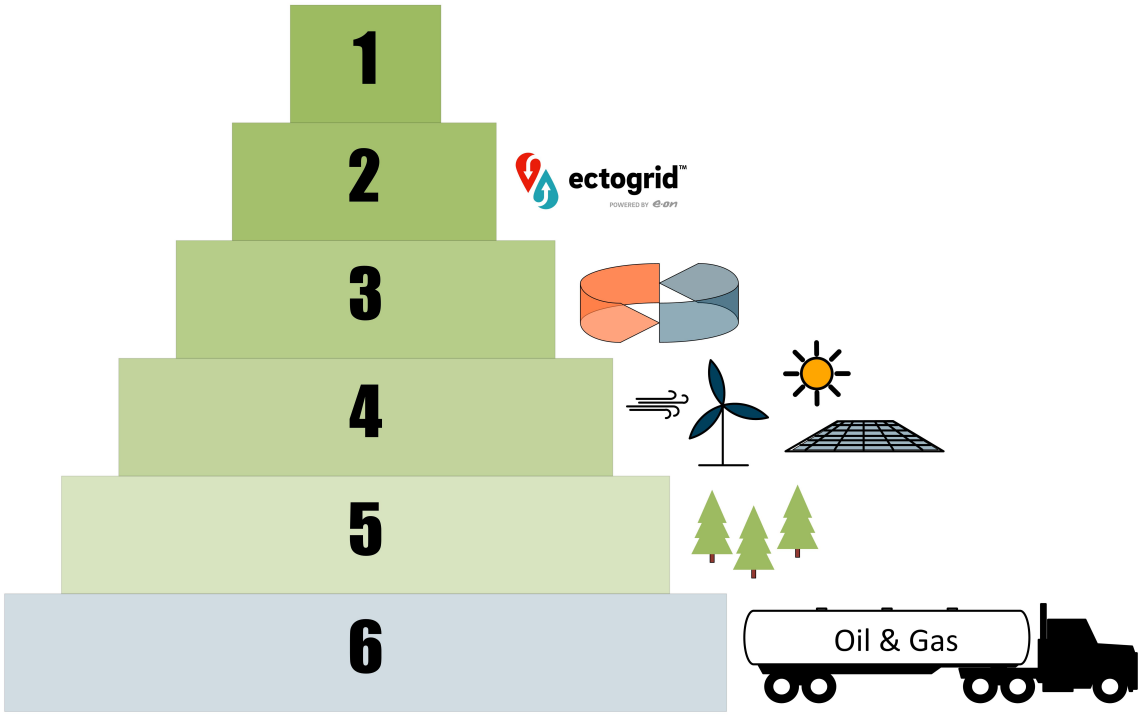

Figure 2.4: *The energy staircase*

One concept ectogrid™ utilizes, is a technology concept called "Vehicle to grid". This concept utilizes the batteries of parked electrical vehicles as "free" and additional energy storage. The other concept is thermal heating systems.

Medicon Village uses the thermal heating system to combine heating and cooling needs, store energy and gather detailed information about its users. This information, in addition to weather forecasts, energy production, energy trading prices and

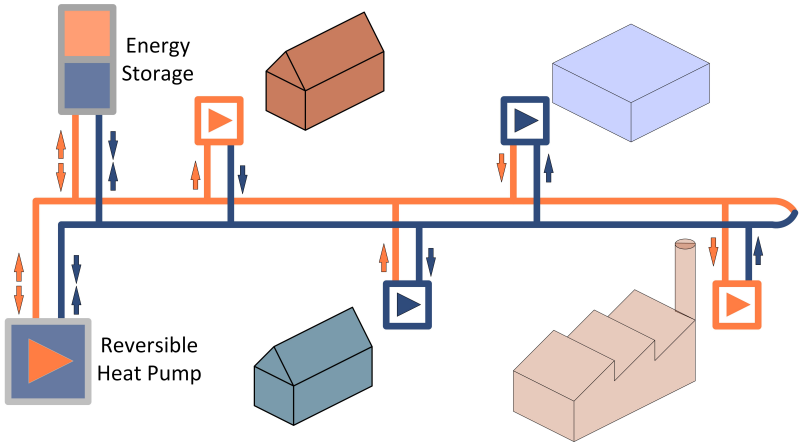

Figure 2.5: *Heating and cooling distribution in ectogrid™ concept*

more, is used to predict the future needs of the area and also optimize the flexibility of the system. [16]

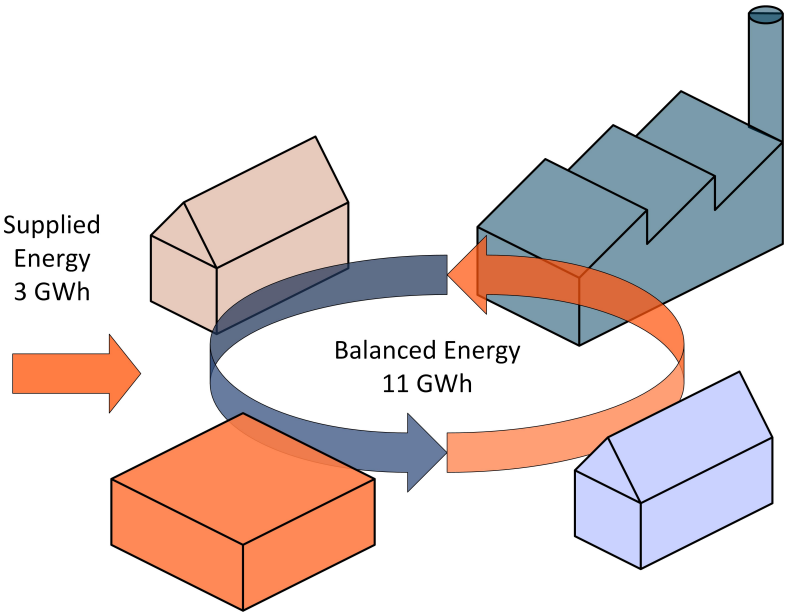

Figure 2.6: *The energy balance of Medicon Village*

Medicon Village had before ectogrid™ an energy consumption equivalent to 10 GWh heating and 4 GWh cooling. Before the building process started, it was estimated that the area had a potential of balancing 11 GWh, leaving only an external supply of 3 GWh [16]. This is illustrated in figure 2.6. This means the new system is able to reduce the electrical bill with 78.6 %

2.1.6 Relating Cost to District Heating

The cost of a district heating system is based on several variables. The size of the pipes used will influence the size of the investment, the bigger the pipes, the higher

cost. Further, the distance from the central to each apartment will have an impact. [21]

There is a wide misconception about waterborne heating systems. The installation costs are about 1000 kroner to 10 000 kroner more than of a conventional heating system. In a larger context, this is not very much money.

Further, the use of district heating with thermal storing of excess heat, is much more cost efficient than using electrical storage in batteries. When comparing investment in full electrical coverage in an apartment and waterborne heating, the electrical system will be 4500 kroner more expensive per kW than waterborne heating. [38]

2.2 Heat Distribution Within a Building

The distribution of heat within a building can be done in numerous different ways. Some ways are more complex than others, and can include other features like space cooling and ventilation. The efficiencies vary greatly between the methods as well. This section will introduce HVAC, underfloor heating and TABS, which are three methods of regulating the thermal conditions of a building.

2.2.1 Heating, Ventilation and Air Conditioning Systems

The most conventional way of regulation the temperatures in a building, are heating, ventilation and air conditioning (HVAC) systems. These systems can be used in large industrial complexes, as well as small apartment buildings, and as the name indicated, the systems can both heat up and cool down a building. [17]

The concept of a HVAC system, is that air is pushed by a fan over coils that are either warmer or colder than the induced air. The air is then, with the reduced or increased temperature, entered into the building to regulate. In buildings with requirements of explosion proofness, the HVAC systems are also obligated to cause a slight over pressure inside the building to prevent unwanted gases to flow into the rooms. [22]

These solutions are quite scalable, and can be designed for either heating or cooling, or it can be designed to do both processes. The cheapest systems only performs one of the two, and include very few fans and fan speeds. The more advanced the system is, the more expensive it will be, but it will also be more efficient. [17]

2.2.2 Waterborne Underfloor Heating

Underfloor heating uses either electrical or hot water circuits installed under the floor construction, like shown in figure 2.7. The coils heat up the floor, which then cause radiant heat to flow into the room. Heating like this can be quite comfortable, and do not include any visible components. The method is also quite energy efficient and is adaptable to many different energy types, whether it being electricity, water, or gas. [66]

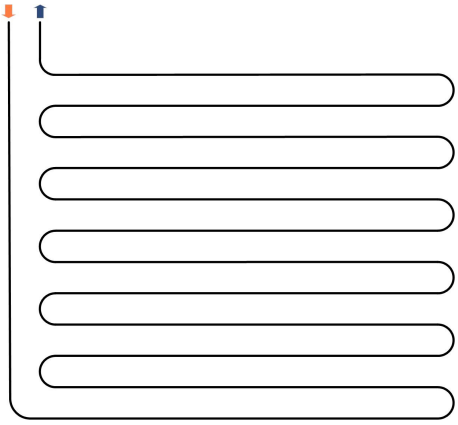

Figure 2.7: *Illustration of how underfloor heating works*

Due to the low temperatures in district heating systems, waterborne underfloor heating is often the preferred solution [28]. Water also has much higher density compared to air, which makes water able to deliver energy to the building at a much higher efficiency. However, unlike a HVAC system, ventilation cannot be included in underfloor heating and needs to be installed as well.

Other benefits of using waterborne underfloor heating, is higher thermal comfort, higher freedom for furniture arrangements, and lower operation temperatures, to mention some. [70]

In newer buildings, the floor surface needs a temperature of 2 to 3 °C higher than the wanted temperature in the room. A floor surface emits about 10 $\mathrm{W/m^2}$ for every degree difference in temperature from the surface to the room. This corresponds to 20 to 30 $\mathrm{W/m^2}$.

2.2.3 Thermally Activated Building Systems

Thermally Active Building System (TABS) is a green and innovative method for controlling the indoor temperatures in a building. The concept of TABS, is that it utilizes the thermal capacity of the building, rather than adding additional components like those of conventional HVAC systems. [6]

TABS uses water pipes that flow through the structure, usually floor or roof, and heats up or cools down the entire construction. By doing this, there will be no need to regulate the rooms differently due to their different loads, because the system instead uses the whole construction mass to regulate room temperatures automatically. Because this solution exploits the thermal storage capacity within the building structure, the system can also reduce the impacts of peak loads. [7]

To use TABS for cooling, ground water or night air temperatures could be utilized [47]. To get the cooling process to work, sun shading is an important factor. TABS are specifically efficient when the night temperatures are low enough to cool down the building to keep low temperatures during the day in summertime. Tubes and heat exchangers can help the night temperatures cool down the building even faster and further, TABS ensure that only energy needed for the distribution of the cooling is needed, not the generation of it.

2.3 Heat Transfer

In thermodynamics, heat is measured as energy. The warmer a medium is, the more energy it contains. When there is a temperature difference either within a medium, or between two different media, the high temperature side will pass over heat to the colder side. Eventually, everything will have the same temperature and reach equilibrium. The phenomenon of moving energy between media is called heat transfer.

Heat transfer can happen through three different methods. These are

- Conduction
- Convection
- Radiation

Conduction refers to the heat transfer within a stationary medium, that being either a fluid or a solid. Convection is heat transfer that happens between a surface and a moving medium at different temperatures. Thermal radiation is the electromagnetic wave any surface emits. [23]

Heat transfer can be presented as heat flux, φ [W/m^2], which is the heat transfer rate for each unit of area. The total heat flux, Φ [W], can also be measured by multiplying φ with the area of which the heat flux is happening.

2.3.1 Conduction

Conduction is, as explained, the heat transfer happening across a stationary medium. This means that we need to look at atomic activity. The basic explanation of conduction is that energy is transferred from particles with higher energy, to particles with lower energy. [23]

Figure 2.8 shows this process through a wall. T_1 [°C] and T_2 [°C] represents the temperatures on respectively the warm and the cold side of the wall. $\dot{Q}_k$ [kW] is the heat transfer rate through the wall. d [m] is the thickness of the wall. A [m^2] is the area of the wall on which the calculations are done.

Thermal conductivity, k [W/m K], is also to be found in the figure. Thermal conductivity defines the medium's ability to transfer heat, and as a general rule, it is larger for solids than for liquids, and the lowest for gases. Thermal conductivity is also highly dependent on temperature, and some values are shown in table 2.1.

With this information, the heat transfer rate through the wall can be found with equation 2.1.

$$\Phi_k = kA\frac{T_1 - T_2}{d} \qquad \text{[kW]} \quad (2.1)$$

2.3.2 Convection

The heat transfer for convection, is due to heat transfer from one area to another caused by the movement of a fluid. This can be done by force or it can happen

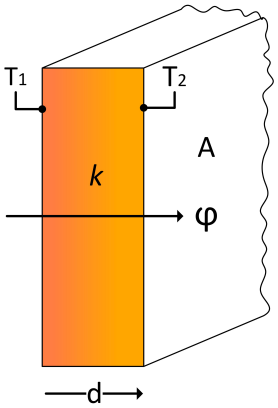

Figure 2.8: *Conductive heat transfer*

Table 2.1: *Some thermal conductivity rates at 300 K and under atmospheric pressure*

	Thermal conductivity k [kW/m K]
Concrete	500
Insulation	34
Water, fluid	613
Water, vapor	19.5
Ammonia	24.7
CO_2	15.2
Air	26.3

naturally. Forced convection is a product of an external force causing the fluid to move. This can be by a fan, mixer or pump. [23]

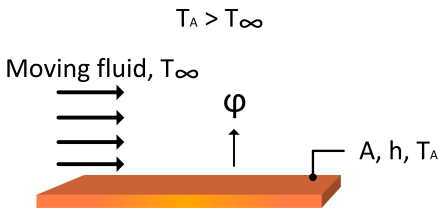

Figure 2.9: *Convective heat transfer*

Natural convection on the other hand, happens by natural buoyancy that is caused by different densities and temperatures of the fluid. When one part of a fluid volume gets heated, the fluid will start to rise and will be replaced by colder fluid that again will rise. This process will continue and contribute to the whole volume getting a higher temperature. This is the phenomena behind natural convection, and is illustrated in figure 2.9.

In order to calculate the heat transfer potential of convection, a value called convective heat transfer coefficient, h_c [W/m^2 K], must be known. The convective heat

transfer coefficient represents the driving force for the heat transfer rate. Typical values for h_c for gases and liquids, as well as for media in phase change, is shown in table 2.2.

Table 2.2: *Convective heat transfer coefficient in different fluids*

Process	Convective heat transfer coef. h_c [W/m^{2}K]
Free convection	
Gases	2-35
Liquids	50-1000
Forced convection	
Gases	25-250
Liquids	100 - 20 000
Convection with phase change	
Boiling	2500-100 000
Condensation	2500-100 000

The heat transfer rate for convection can be calculated by equation 2.2.

$$\Phi_h = h_c \cdot A \cdot \Delta T \qquad [\text{kW}] \quad (2.2)$$

Here the area, A [m^2], of the surface on which the heat transfer is happening, and ΔT [K], the temperature difference between the surface and the moving medium.

2.3.3 Radiation

Thermal radiation is the final method of which heat transfer happens. All surfaces, whether solid or liquid, with a given temperature emits energy to it's surroundings. Two examples of this is the heat that can be felt from either a bonfire or a radiator. [23]

However, thermal radiation can happen in a much smaller scale as well. Figure 2.10 shows the principle of thermal radiation.

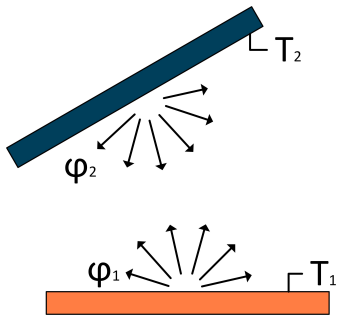

Figure 2.10: *Thermal radiation*

2.3.4 Thermal Resistance

When evaluating the heat transfer through a wall, the concept of thermal resistance, R [K/W], is a convenient tool. Thermal resistance is a measure of the insulation property of a medium, and is dependent on the temperature differences. The thermal resistance can be calculated both for convective and conductive heat transfers. [23]

If the length and surface area of a wall is known, as well as the thermal conductivity, the thermal resistance for the conductive heat transfer can be calculated by equation 2.3.

$$R_{t,cond} = \frac{d}{kA} \qquad [\mathrm{K/W}] \quad (2.3)$$

$R_{t,cond}$ is important to know when calculating the total heat transfer through a composite wall with several parallel layers of different thermal resistances. This will be explained later in this section.

Thermal resistance for convection can be found through equation 2.4, if the surface area and h is known.

$$R_{t,conv} = \frac{1}{hA} \qquad [\mathrm{K/W}] \quad (2.4)$$

Finding the combined thermal resistance of a composite construction is a bit more complex than just adding them together. Instead, they can be combined as shown in equation 2.5.

$$R_{tot} = \frac{1}{h_{c,1}A} + \frac{d}{kA} + \frac{1}{h_{c,2}A} \qquad [\mathrm{K/W}] \quad (2.5)$$

2.3.5 Heat Transfer Through a Wall

When looking at the transfer of heat through a wall and how it affects its surroundings, all heat transfer methods must be considered. Conduction must be used in order to estimate how much heat will flow through it, convection and radiation must be used in order to estimate how quickly the heat rate affects the surroundings. [23]

In order to find out how well energy is transferred through a composite wall, the total thermal transmittance, or the U-value, U [$\mathrm{W/m^2\,K}$], needs to be calculated. The U-value represents the heat transfer rate through a structure, and is usually used in order to estimate how well a wall is insulated, or how fast a heat exchanger can transfer heat. The U-value is a combination of convection and conduction. Figure 2.11 shows how heat transfer happens through a composite wall.

Equation 2.6 shows how the U-value of the example in the figure is calculated. As seen, the equation uses the heat transfer coefficients for both the inner and outer fluids, $h_{c,inside}$ and $h_{c,outside}$, respectively. It also uses the total thermal resistance for both of the wall compositions.

$$U = \frac{1}{\frac{1}{h_{c,inside}} + \frac{d_1}{k_1} + \frac{d_2}{k_2} + \frac{1}{h_{c,outside}}} \qquad [\mathrm{W/m^2\,K}] \quad (2.6)$$

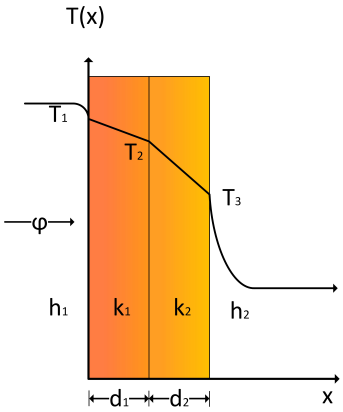

Figure 2.11: *Heat transfer through composite wall*

Here, $h_{c,inside}$ [W/m^{2}K] refers to the heat transfer coefficient of the inner fluid and $h_{c,outside}$ [W/m^{2}K] the same for the outer fluid. These values differ for a substance depending on different factors. d_1 [m] is the thickness of wall 1 and d_2 [m] the thickness of wall 2. k_1 [W/mK] and k_2 [W/mK] are the two parts corresponding thermal conductivities.

2.3.6 Heat Exchangers

To evaluate how much heat a medium is capable of supplying through a heat exchanger, specific heat capacity, c_p [kJ/kg K], must be used. c_p indicates how much energy is needed in order to raise the temperature of 1 gram of a liquid by 1 °C. Specific heat capacity can also be used to evaluate energy flows through the heat exchanger, as shown in equation 2.7. [2]

$$\dot{Q} = \dot{m} \cdot c_p \cdot \Delta T \qquad \text{[kW]} \quad (2.7)$$

The fluids in heat exchangers are in motion, they can be represented with their mass flow, $\dot{m}$ [kg/s], and the energy flow produced, $\dot{Q}$ [kW]. The temperature difference, ΔT [K], indicates the temperature difference of the medium before and after energy transfer, or between the inlet and the outlet of the heat exchanger.

Equation 2.7 stipulates the amount of energy needed in order to elevate the temperature of the cold medium with ΔT, when the $\dot{m}$ and c_p values are known.

The c_p value is dependent on which medium is being used, and at what temperature it is operating. Table 2.3 shows some c_p values for different media under different conditions. All the values are given when the media are under a temperature of 20 °C.

The size needed for the heat exchanger can be calculated using thermal resistance. Figure 2.12 shows a heat exchanger where the two fluids flow through the heat exchanger in two different directions, also known as counter flow. The high temperature side enters the heat exchanger with temperature T_{hi} [°C] and exits with the temperature T_{ho} [°C]. The low temperature medium enters with temperature T_{ci} [°C] and receives a temperature rise to T_{co} [°C].

Table 2.3: *Specific heat capacities at 20°C*

	Specific Heat Capacity c_p [kJ/kg K]
Water	4.18
Ammonia, liquid	4.74
Ammonia, gas	3.02
CO2, liquid	4.26
CO2, gas	4.55

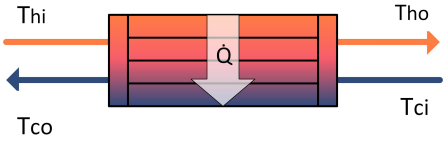

Figure 2.12: *Heat exchanger*

To estimate the size of the heat exchanger, equation 2.8 should be used. The equation states that the energy rate needed $\dot{Q}$ equals to the heat transfer coefficient, U [kW/m^{2}K], times the total transfer area, A [m^2], and the log mean temperature difference, ΔT_{lm} [K]. [2]

$$\dot{Q} = U \cdot A \cdot \Delta T_{lm} \quad \text{[kW]} \quad (2.8)$$

It should be noted that $A = 2\pi r L$ for a cylindrical wall, where r [m] is the radius of the tube and L [m] is its length [33].

T_{lm} in a counter flow heat exchanger is found by following equation 2.9. ΔT_1 is the difference in temperature on the left hand side of figure 2.12, hence $T_{hi} - T_{co}$. ΔT_2 is the temperature difference on the right hand side, hence $T_{ho} - T_{ci}$. [2]

$$\Delta T_{lm} = \frac{\Delta T_1 - \Delta T_2}{\ln \Delta T_1 / \Delta T_2} \quad \text{[K]} \quad (2.9)$$

A similar equation counts for cross flow heat exchangers, where the fluids move perpendicular to one another, but with a correction factor.

2.4 Pressure Drop Calculations

In order to evaluate the need for circulation pump capacity, a series of calculations related to the fluid flow is needed. These calculations involve the length of the pipes carrying the fluid, the optimal diameter of the pipe and other factors. These calculations will in the end determine the pressure drop per meter, thus dictate proper circulation pump capacity.

Circular pipes are able to withstand high pressure differences between the inside and outside, and is therefore often used for transportation of liquids.

2.4.1 Dynamic Viscosity

Dynamic viscosity, μ [kg/m s], is an expression for internal resistance within a fluid, saying something about the horizontal movement of the fluid within. The viscosity is dependent on the temperature of the fluid, and is calculated differently for liquids and gases.

$$\mu = \frac{aT^{1/2}}{1 + b/T} \qquad [\text{kg/m s}] \quad (2.10)$$

Equation 2.10 is the dynamic viscosity for gases, and the constants a and b are found experimentally, while T is the absolute temperature. For water at atmospheric conditions, a and b are approximated to be as follows:

- $a = 1.458 \cdot 10^{-6}$ kg/m s K$^{1/2}$
- $b = 110.4$ K

As indicated by equation 2.10, the viscosity increases with the temperature.
Equation 2.11 is used to calculate the dynamic viscosity of liquids.

$$\mu = a \cdot 10^{b/(T-c)} \qquad [\text{kg/m s}] \quad (2.11)$$

The constants a, b and c are found experimentally. For water, using the following values:

- $a = 2.414 \cdot 10^{-5}$ N s/m^2
- $b = 247.8$ K
- $c = 140$ K

and a T of between 0 °C to 370 °C will give a result with an error of less than 2.5 %. [4]

2.4.2 Reynolds Number

Knowing μ, the Reynolds number, Re [–], can be found, using equation 2.12. The Reynolds number indicates how the fluid flows inside the pipe. The flow is either categorized as laminar or turbulent, depending on Re being above or below 2300. Below 2300 is laminar, and above it is considered turbulent. However, it is not fully turbulent before reaching 4000, thus between 2300 and 4000 the flow is described as transitional. [4]

A laminar flow is characterized by having smooth and ordered lines. Turbulent flows are recognized by unsteadiness and wavering lines. The transitional flow is the transition between laminar and turbulent flows. Laminar flows are mostly present in fluids with high viscosity, like oils, or through narrow pipes. Most flows for heat transfer are therefore turbulent.

$$\text{Re} = \frac{\text{Inertial forces}}{\text{Viscous forces}} = \frac{\rho v_{avg} D}{\mu} \qquad [–] \quad (2.12)$$

ρ [kg/m^3] is the density of the liquid. v_{avg} [m/s] is the velocity of the liquid, and D [m] is the diameter of the pipe.

In a pipe, the velocity varies greatly through the cross section. At the pipe wall, the velocity is equal to zero, and it increases towards the center of the pipe. It is quite difficult to perform calculations for this, and therefore v_{avg} makes the calculations easier. v_{avg} is the average velocity through the whole pipe. An average temperature T is also used. The losses in accuracy caused by these simplifications are minor to the increased convenience.

When the Reynolds number is high, the inertial forces are superior to the viscous forces, meaning the viscous effect cannot prevent the fluctuations happening. For smaller Reynolds numbers the opposite is true, and the fluctuations are overpowered by the viscous forces.

Turbulent flow is preferred for heat transfer, because the movement in the water cause rapid heat transfer.

2.4.3 Shear Stress

In order to evaluate different energy parts of a turbulent flow, shear stress, τ_w [Pa], that reduces the flow speed towards the wall of the pipe needs to be considered. This is related to the velocity profile slope. Figure 2.13 shows this phenomenon.

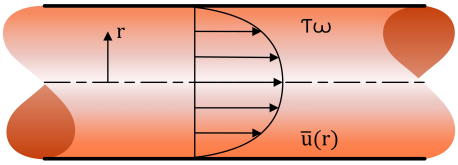

Figure 2.13: *Shear Stress*

2.4.4 Darcy Friction Factor

Further, Darcy's friction factor, f [–], can be found.

$$f = \frac{\text{Wall friction force}}{\text{Inertial force}} = \frac{8\tau_w}{\rho v^2} \qquad [–] \quad (2.13)$$

For laminar flows, the Darcy friction factor is only dependent on the Reynolds number, meaning thereof independent of the roughness of the pipe surface. Therefore equation 2.14 can be used.

$$f = \frac{64}{\text{Re}} \qquad [–] \quad (2.14)$$

This equation is true for when the water is flowing horizontally in a round pipe.

2.4.5 Colebrook Equation

For turbulent flows, evaluating the Darcy friction factor can be a bit more difficult. Many scientist have tried to find a way to find the Darcy friction factor, and Colebrook is one of them. He developed equation 2.15, for evaluating the friction factor

in a fully developed turbulent flow in a pipe, which is dependent of the Reynolds number and the relative roughness, ε/D [−].

$$\frac{1}{\sqrt{f}} = -2.0 \log\left(\frac{\varepsilon/D}{3.7} + \frac{2.51}{\mathrm{Re}\sqrt{f}}\right) \tag{2.15}$$

This equation is difficult to solve, but the matlab script colebrook.m and the excel-paper gives the same results.

Table 2.4: *Roughness values for new commercial pipes*

Material	Rougness ε [mm]
Glass, plastic	0
Concrete	0.9 - 9
Copper	0.0015
Stainless steel	0.002

Table 2.4 shows the values for the roughness of the pipes, though these values have a huge uncertainty of 60 %.

Using the Moody chart, this is easier to evaluate.

2.4.6 Pressure Drop in Straight Pipes

Finally, the total pressure drop can be calculated by equation 2.16. This equation may be applied regardless of pipe cross section, roughness of surface, internal flows, and flow direction.

$$\Delta P = f\frac{L}{D}\frac{\rho v_{avg}^2}{2} \quad \text{[Pa]} \tag{2.16}$$

It is recommended that the total pressure drop in the pipe does not exceed 20 kPa for underfloor heating [70]. Higher pressure drops are acceptable for other applications. In one example for heat exchanger, a pressure drop of 50 kPa was acceptable [4]. 100 kPa is equal to 1 bar.

2.4.7 Pressure Drop in Bends

When using pipes to transfer fluids, bends are often needed to change the direction of the pipes and the fluid flow. Bends of different types cause pressure drops within the fluid, so for calculating the total pressure drop in pipes, bends need to be taken into consideration as well. [24]

Figure 2.14 shows the different factors that play a role when evaluating a pressure drop in a bend. Equation 2.17 shows how the values from the figure are put together in order to evaluate the pressure drop.

$$\Delta P = \zeta_b\frac{\rho v^2}{2} \quad \text{[Pa]} \tag{2.17}$$

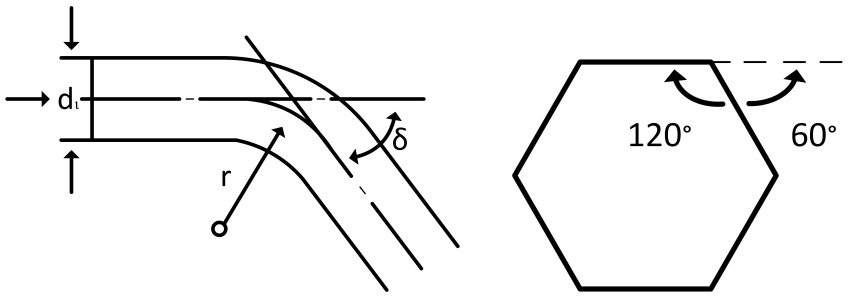

(a) Pressure Drop *(b) Hexagon*

Figure 2.14: *Pressure drop through bends and a hexagon*

The drag coefficient, ζ_b [−], is taken from a graph. It is dependent on the ratio between the radius, r [m], of the bend, and the inner diameter, d_i [mm], of the pipe, found in figure 2.14a. The pressure drop is also dependent on the density and velocity of the fluid within the pipe.

Table 2.5: *Drag coefficient for bends with r/d_i ratio of 5 for smooth pipes*

δ	Drag coefficient ζ_b [−]
45°	0.075
60°	0.085
90°	0.1

Figure 2.14b shows how a bend shown in figure 2.14a would fit for a pipe circuit formed as a hexagon. Every bend adds pressure loss. For a pipe running around a hexagon shaped path, the δ value is 30°, as shown. Table 2.5 shows the ζ_b values for bends in pipes with a r/d_i ratio of 5.

2.5 Building Specifications of a Passive House

Deciding how a building should be built in order to keep energy demands on a preferred level, can be difficult. Wanting to build a low energy or passive building can be one thing, but making sure an energy system will be able to have an optimal performance within the different standards is another. Therefore, different requirements and guidelines should be followed. This section is going to present these. The information mentioned in this section is mostly based on the TEK17 standards made by Direktoratet for byggkvalitet, as well as other standards by Standard Norge.

2.5.1 Building Specifications

When constructing a building of a specific standard, different requirements must be followed. For buildings with low energy consumption, the requirements shown in table 2.6 from TEK17 should be followed [68]. If the goal is to build a building

with close to zero net energy consumption, the passive house standards shown in the same table apply [55].

Table 2.6: *Building requirements for apartment buildings*

	Units	TEK17	Passive Houses
U-value exterior wall	W/m^2K	≤ 0.18	≤ 0.10
U-value roof	W/m^2K	≤ 0.13	≤ 0.08
U-value floor	W/m^2K	≤ 0.10	≤ 0.08
U-value windows and doors	W/m^2K	≤ 0.80	≤ 0.80
Window/door to BRA ratio	-	≤ 0.25	-
HR efficiency in ventilation	-	≥ 0.8	-
SFP-factor ventilation	$kW/m^3/s$	≤ 1.5	≤ 1.5
Air leakage at 50 Pa	h^{-1}	≤ 0.6	≤ 0.6
Normalized thermal bridge value	W/m^2K	≤ 0.07	≤ 0.03

A passive house is a standard used for getting highly energy efficient buildings, and is voluntary. Achieving a passive house standard is done by taking passive measures, like adding additional isolation and ensuring a tight structure with the least amount of holes. In addition, the Norwegian standard includes a requirement of the energy delivery being as independent from oil, gas and electricity as possible. It says that more than 50 % of the heating of water needs to be covered by renewable sources, the rest can be covered by electricity. [27]

Both standards are for apartment and residential buildings. For office buildings, supermarkets and other types of buildings, the values may differ. As seen, some of the values are the same for both energy profiles, but the isolation within the exterior structure needs to be better for the passive house standard. The standards from TEK17 took effect on July 1st 2017, and will become requirements for all new buildings. The passive house standards are voluntary for constructing an even more energy efficient building [68].

2.5.2 Energy Demand

While TEK17 have requirements and recommendations for how to construct buildings in general, the NS 3700 standard presents values that should be used when planning, building and evaluating apartment buildings with very low energy use [54]. Most importantly, the standard can be used to set requirements regarding products and building components used, as well as for the embodiment of the building process, for passive houses and low energy buildings.

Table 2.7 shows the average demands and internal loads of different factors within a residential building when it is operating on an annual basis. The values presented here apply for both low energy consuming buildings and passive houses. It is assumed that highly efficient lighting is used, and that all electrical equipment has a

simple control systems. This is to ensure the lowest contribution from internal loads as possible.

Table 2.7: *Energy demands and internal loads for low energy apartment buildings[54]*

	Operation h/day/week	Power demand [W/m^2]	Energy demand [kWh/m^{2}year]	Internal load [W/m^2]
Lighting	16/7/52	1.95	11.4	1.95
Equipment	16/7/52	3.00	17.5	1.80
Hot water	16/7/52	5.10	29.8	0.00
People	24/7/52	-	-	1.50
Sum	-	-	58.7	-

In addition to the values shown in table 2.7, NS 3700 also has requirements regarding the maximum average space heating demand the two building types can have. Low energy buildings are divided into two different types, class 1 and class 2. Class 2 has the least stringent requirements of 45 kWh/m^2 a year, followed by class 1 where the energy demand cannot exceed 30 kWh/m^2 a year. To be able to reach the requirements of a passive house, only 15 kWh/m^2 a year can be used. These values for maximum energy demand are valid for buildings with a surface area of more than 250 m^2 and an annual outdoor mean temperature of 6.3 °C or more, and are summarized in table 2.8.

Table 2.8: *Annual energy demand for space heating*

	Spesific heating demand [kWh/m^2]
Class 2	45
Class 1	30
Passive House	15

The heating demand presented includes regular space heating and any potential heating batteries for the ventilation. This demand includes covering the heat losses within the building. These are due to transmission, infiltration and ventilation losses. Transmission losses are due to conduction loss through the structure of the building, i.e. the roof, walls, doors and windows. Infiltration and ventilation losses are both due to shifting of air. The difference, however, is that infiltration losses are due to air shifts through cracks and openings of the structure, while ventilation losses are due to introduced air through the ventilation system.

Supplied Temperatures

According to SINTEF, an underfloor heating with a temperature between 35 to 40 °C should be sufficient in order to keep a room temperature of about 23 to 28 °C. This also corresponds to a heat output of 30 to 40 W/m^2 [61]. If radiators are used, low temperature radiators should have a supply temperature of 45 to 55 °C [15].

DHW will be assessed more in depth in section 2.6.3, but includes hot water for showers, washing machines and dishwashers. In order to cover hot water temperatures that these facilities demand, a temperature of 55 to 65 °C should be applied, and to make sure no Legionella is formed, this should be as high as 75 °C. [40]

Space cooling is another temperature demand that needs to be covered. Water tempertaures below 18 °C should be avoided.

2.5.3 Indoor Environment

It is important to consider and evaluate the indoor environment whenever a house that at some point will be occupied by people is being constructed. This section will explain this concept and the different factors that affects it. It will also touch upon how to optimize the conditions. This section is mainly based on the book *Energy Management in Buildings* [42]. TEK17 is also used in this section for different values [68].

Thermal Comfort

Thermal comfort is a term used to describe how the thermal environmental is perceived by the people experiencing it. A lot of factors play a role when determining this, including the metabolism rate performed and clothes worn by these people. The metabolism rate is determined by the unit met and the amount of clothing worn is indicated by the unit clo.

The level of thermal comfort is presented by the two values predicted percentage dissatisfied (PPD) and predicted mean vote (PMV). PPD is a value between 0 and 100 which illustrates the percentage of how many people are dissatisfied with the thermal condition. PMV is an indicator of how hot or cold the people in the room are perceiving the temperature. The value span from -3 to 3, where 0 is neutral, -3 is an indication of the room being too cold and 3 is too warm.

The values of PPD and PMV can be calculated if the room temperature and humidity of the room is known, as well as the mean metabolism and clothes worn by the people in the room. Table 2.9 shows an example of what these values could be for a regular household situation.

Table 2.9: *Thermal comfort for*

	Clothing [clo]	Temperature [°C]	Metabolism [met]	Humidity [%]	PMV [–]	PPD [%]
Summer	0.50	24	1.2	60	-0.18	5.6
Winter	1.0	21	1.2	40	-0.19	5.8

People tend to wear different clothing during winter and summer, hence the difference in clothing and indoor temperature for these periods. Metabolism of 1.2 represents an activity level at the same rate as standing or being relaxed. Humidity also vary through the year, represented by the 40 % and 60 % in the table.

Temperature

There are no regulations regarding indoor temperatures. However, in TEK17 a recommendations for indoor temperatures in rooms for different purposes, are presented. These are shown in table 2.10.

Table 2.10: *Temperatures recommended by TEK17*

Activity level	Light	Medium	Heavy
Temperature [°C]	19-26	16-26	10-26

In addition, they recommend that the operative temperatures, the thermal temperature as experienced by humans, are kept below 22 °C during periods with heating demand. During hot days in summer, the following measures are also recommended to be implemented in order to keep the indoor temperature below 26 °C:

- Reduced window area on the sunlit facade
- Reduced exposed thermal mass
- Added solar shading
- Added windows with opening abilities to ventilate
- Air intake or ventilation placed in order to minimize temperature rise

Following one or two of these measures should, according to TEK17, be enough for a regular residential building to protect the building from overheating.

Ventilation System

A proper ventilation system should be able to keep satisfactory air quality, with special regards to smell, solvents, dust and other contaminations. This is to keep the comfort level of the occupants at a good level, but also to avoid negative health effects. [68]

In order to decode on the dimension of a ventilation system, factors like the size and design of the room, the activity and processes performed, as well as the contamination from people and equipment within the room, should be taken into consideration. Buildings placed in areas with high concentration of contaminants should have sufficient filtering and cleaning equipment as well.

TEK17 also requires a fresh air supply of at least $1.2\,m^3$ per m^2 gross floor area (GFA) in residential buildings. In addition, for bedrooms there should be a minimum of $26\,m^3$ fresh air supply every hour for every people sleeping in the room. Rooms with high production of contamination, like the kitchen and bathrooms, should have an exhaust system that ensures a quick and effective extraction of air.

Daylight Infiltration

According to TEK17, daylight is generally perceived as the best form of illumination, and gives the best and most appropriate form of lighting. Finding a way to optimize the window area without compromising the transmission losses is therefore to be preferred.

2.6 Heat Sources

The most common way of providing a building with energy in Norway, is through electricity. However, in order to achieve what sustainability goal 7 advises, about providing reliable and modern energy for everyone by 2030, a better method must be used. Fortunately, there are plenty of existing heat and energy sources that are not being utilized to its full extent. This section will explain different sources of this type of energy, how they are produced and how they can be used to contribute to heating of a building.

2.6.1 Excess Heat from Cooling Processes

Cooling processes like freezing and refrigeration are highly energy consuming processes and can therefore be quite expensive. Cooling processes work by removing heat from the refrigerated room and disposing it somewhere else. Examples of buildings where freezing and refrigeration often take place are supermarkets, factories and ice rinks. [40]

Figure 2.15 shows the basics of a cooling process, in which air from one area reaches a lower temperature by transferring energy into another area. This happens when air from the inner space from the figure enters the heat pump with a temperature of $-3\,^{\circ}\mathrm{C}$. From there on, it goes through the heat pump and receives a lower temperature of $-5\,^{\circ}\mathrm{C}$. This process will be described more detailed in section 2.7. The main point to take from this however, is that the air now has reached a lower energy level. The laws of thermodynamics ensure that energy cannot disappear, and this energy has instead been transferred to the outdoor air. This is illustrated by showing that the outdoor air enters at temperature of $20\,^{\circ}\mathrm{C}$, and with the added energy receives a temperature of $22\,^{\circ}\mathrm{C}$.

In short terms, the outdoor air receives energy, and for bigger productions this can potentially correspond to very much energy. However, the potential of reusing this energy is equally as big. An example of where this has been done in real life, is described in section 2.6.4.

2.6.2 Solar Collection

A dependable, renewable and ever lasting source of heat and energy, is the sun. Exploiting the sun through absorption has been done for generations, and since it is a free source of energy, it can also be very cheap. A quite simple way of exploit energy from the sun, is through active solar heating. [1]

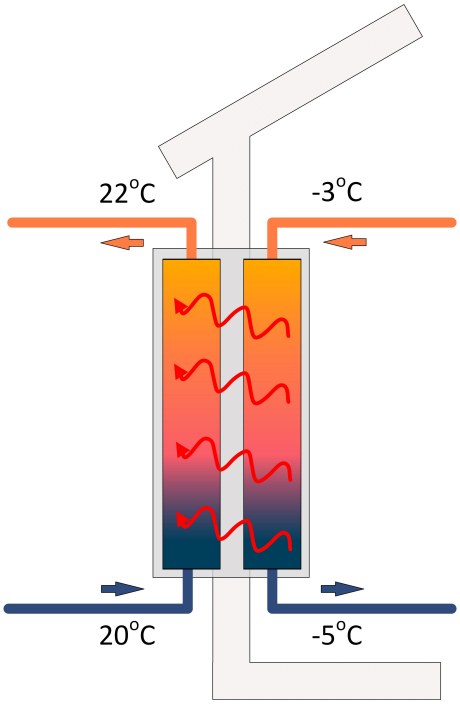

Figure 2.15: *A simple representation of the cooling process*

In simple terms, active solar heating systems, are systems where the sun heats up a liquid before the liquid is guided through the interior space and hot water to increase the temperature. To utilize the heat from the sun, the liquid is run through solar collectors where they get a temperature rise from, for instance, no more than 5.6 °C to 11 °C. Subsequently, the liquid is either run through a heat exchanger for direct heating, or directed to a storage tank. The low temperatures of the liquid ensures the lowest amount of losses possible, and a heat pump can later be used to elevate the water temperature to the preferred level. Components of a system like this include piping, pumps, valves, an expansion tank, heat exchangers, storage tanks, a boiler and controllers. A simplified example is shown in figure 2.16. [1]

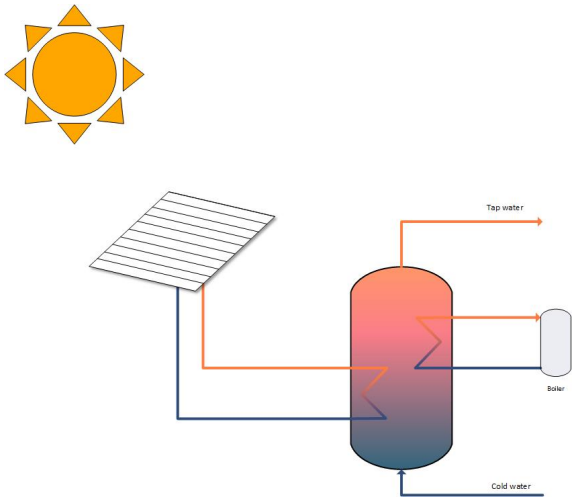

Figure 2.16: *Active solar heating of water*

The distribution of a system like this is much like for regular district heating systems, with low temperature water being the heat carrier. This makes it especially easy to integrate in a bigger low temperature district heating system. The heat can be distributed through underfloor heating, hot water radiators or an air handling unit.

Systems like these are most efficient in cold climates with high solar radiation. Compared to other methods like electricity and boiling of expensive fuel, this solution can be quite cost efficient. In addition, it will keep the emissions down and contribute to reaching the sustainability goals towards 2030.

During summer time, absorption can be a very economical and environmental friendly way of heating up DHW. Using absorption for the winter can be a bit more tricky and requires a whole different set of equipment, but can still give an economical benefit [49].

2.6.3 Gray Water

According to a study performed by SINTEF in 2006, 15 % of all energy demand in a regular residential building located in Norway, is used for the heating of DHW [18]. Further, it is shown that 60 % of the electricity is used for space heating. Combined, this stands for ¾ of the electricity in the building.

For passive houses, however, the hot water demand normally covers a share of 50 % [32]. This is mostly due to the space heating demand being so low because of the improved insulation in these buildings. An illustration of this is shown in figure 2.17. This water includes all water usage, with exception for those buildings using water for space heating as well. The DHW is the water tapped from sinks and showers, or used in washing machines and dishwashers.

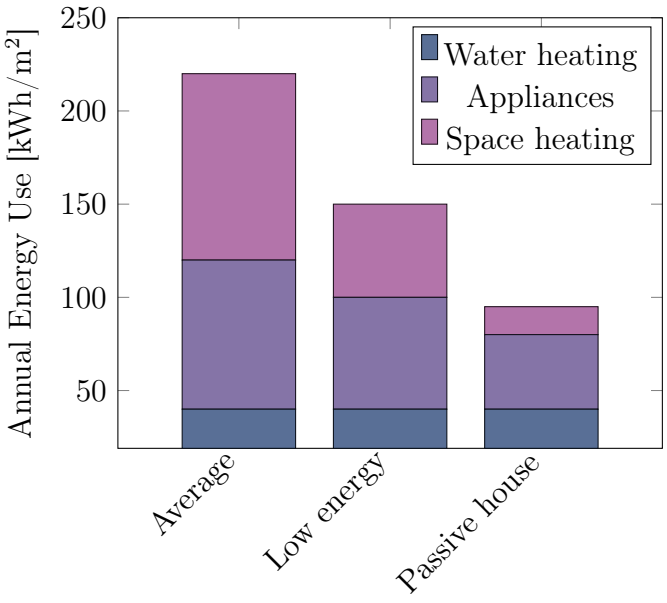

Figure 2.17: *Annual energy use for different building types*

Due to comfort levels for humans, it is very difficult to reduce the water demand

and temperature for water appliances [32]. So, in order to get the net energy demand for the hot water in a building, a different approach is needed. This section will explain a possible approach for this.

When the water has served it's purpose, about 80 to 90 % of the initial heat ends up in the drains as waste water. This represents a huge heat loss in the building sector, and finding a way to reuse this heat in an inexpensive manner, would mean a much lower electricity use for the system. This is where gray water comes in. Gray water is water that has been used for shower and hygiene purposes, washing of dishes and clothes, and making of food. [67]

Water usage in domestic buildings can be divided into three categories, which are shown in table 2.11. Two of these are types of gray water, divided into light load and heavy load. The light load consists of water from showers, bathroom sinks and bathtubs and is by far the easiest to use for gray water heat recovery. The heavy load gray water consists of water from dishwashers, kitchen sinks, and washing machines. Water from these sources require grease traps and removal of sludge before the heat can be recovered, and thereby require a more complex system. [32]

Table 2.11: *Characteristics of water found in domestic sewage systems*

Type	Source	Content
Light load gray water	Shower, bathroom sinks, bathtubs	Shampoo, soap, hair, bacteria, organic particles
Heavy load gray water	Dishwashers, kitchen sinks, washing machines	Surfactants, detergents, phosphates, heavy metals, suspended solids, organic particles, oil, grease, higher pH, bacteria
Black water	Toilets	Feces, urine, toilet paper

The last category of water waste from buildings is black water, which comes from toilets. This water is not suitable for heat recovery due to both high contamination content, and also very low temperatures. Most houses do not have different piping systems for the different water categories, so adding a solution that does, would mean more complex piping than seen in current residential buildings. [32]

Water Usage Calculations

The usage of water in different apartments varies widely depending on who lives there. Factors that affect the usage profile is age, gender and number of occupancy, to mention some. Therefore, it can be quite difficult to predict a normalized curve for this usage. To make it even more difficult, different sources state different water usage.

Oak Ridge National Lab has made an estimation that every person produces about 136 L of waste water every day, where a fraction of 64 % corresponds to the

gray water production [32]. In conclusion, a person produces 87 L of gray water every day.

Heat Recovery

There are two main ways of exploiting gray water from buildings using heat exchangers, either by on-demand or the storage method. On-demand heat recovery means that the gray water heats up incoming fresh water on its way out, as shown in the left illustration in figure 2.18. The heat gained by the fresh water will then be used directly in the building. Heat recovery using storage, on the other hand, heats up water in a tank on its way out. This water can then be used when needed. This is shown in the right illustration in figure 2.18. [64]

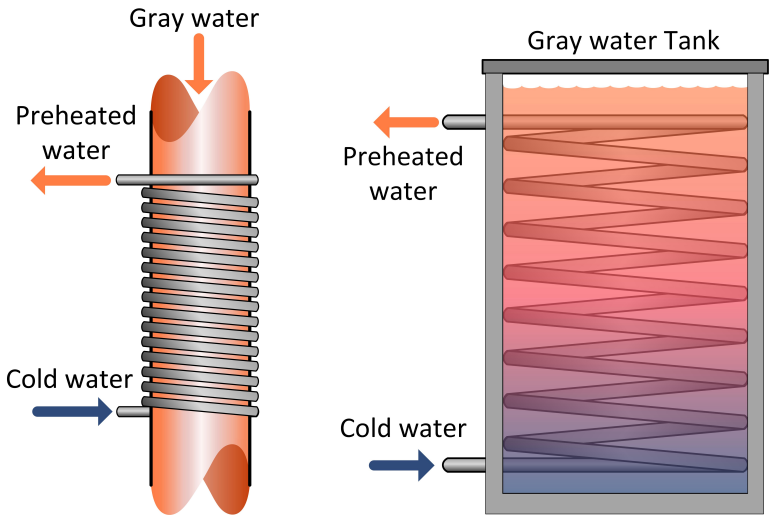

(a) On-demand *(b) Storage*

Figure 2.18: *On-demand and storage waste water heat recovery [64]*

Gray water can deliver a wide range of temperatures. These are highly dependent on the usage behavior of the people living in an apartment, and how many showers or washing cycles they tend to take. A shower normally has an input temperature of about 40 °C, and ends up with about 30 to 38 °C in the drain, depending on the ambient temperature [34]. Dishwashers and washing machines usually need a water temperature of 80 °C and 60 °C, respectively, and send marginally lower temperatures to the drains. A general rule is that the gray water can deliver 5 to 10 °C lower temperatures than the input temperature. Various studies have shown that gray water can provide a temperature range of 30 to 35 °C when harnessed on site.

2.6.4 Existing System - Tromsøbadet

The newly built swimming pool in Tromsø utilized the methods explained in this section. Instead of spilling all heated water from showers and filter cleaning, the

water is cleansed and is reused to replace the evaporated water in the pools. With using this method, the facility can save both water usage and energy. [37]

The estimated savings from both water fees and energy is estimated to be one million kroner. By utilizing the excess heat from the heated water in the pools, it is estimated that the system will be able to save energy equivalent to 400 000 kWh every year.

The system will also utilize the heat from gray water from showers and sinks with a heat pump.

For periods where the production of heated gray water is higher than the demand, 12 m^3 of thermal storage tanks will be used to store the heated water for showers and sinks. The gray water, stored in another tank, is first used to directly heat up the cold supply water. Then the gray water is used as a heat source in a heat pump to heat up the water further for shower use and thermal storage. This can be shown in the schematics of the system shown in figure 2.19.

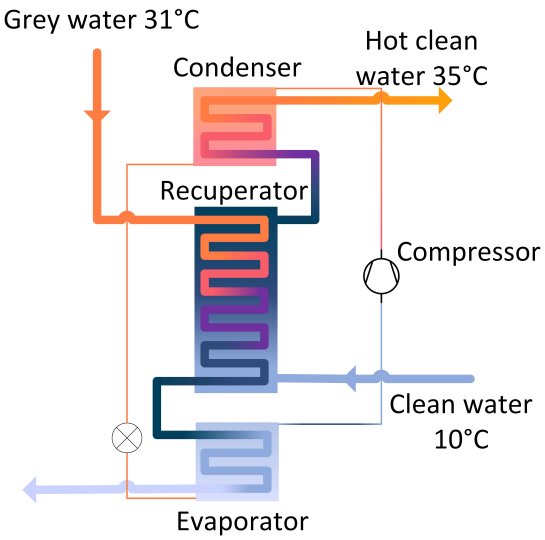

Figure 2.19: *Schematics of heat pump system at Tromsø pool*

Based on an assumption of an energy saving of about 1.2 million kroner, Enova has provided a support of 3.35 million kroner.

Relating Cost to Waste Heat Utilization

According to Enova, a state enterprise supporting measures to enable effective and environmentally friendly energy supply, a lot can be saved by converting the waste from gray water to a heat source. First of all, it is a free heat source. Secondly, by installing equipment for recycling this heat, Enova will sponsor up to 2500 NOK. [67]

The electricity cost for heating of water can be lowered by between 15 % to 40 %. An average sized family in Norway uses approximately 5000 kWh for heating of water every year, according to Enova. With a gray water heat recovery installation, and assuming 1 kWh costs 1 NOK, til electricity bill for heating of water will be lowered from 5000 NOK to 600 to 2000 NOK.

2.7 Heat Pumps

Some of the most urgent threats facing our planet, are those connected to the production and use of energy [60]. The demand for energy is only growing, so in order to keep the environmental impacts low, the effectiveness of produced energy has to be better. Not only is the annual energy demand increasing, but there will also be a higher power demand. This means we will need larger systems that are able to handle higher power demands. This section contains information about heat pumps in general, how they can contribute to meeting higher energy demands. It will also include some specific information about different heat pumps and different refrigerants.

2.7.1 Heat Pumps in General

The greatest trait of a heat pump, is that it manages to get more energy out of a heat source than originally seemed possible. This is done through a process that will be explained a bit further into this section, but it means that a heat pump can cover a demand much higher than the power it requires. This ability makes the use of heat pumps to replace heaters running purely on oil or electricity one of the main measures to ensure a more sustainable energy deliverance [60].

Heat pumps exploit natural temperature differences to slightly rise the temperature of a circulating refrigerant, before compressing it to a higher temperature level. This means that no electricity goes directly to the production of heat, but instead is used for the work load of the compressor.

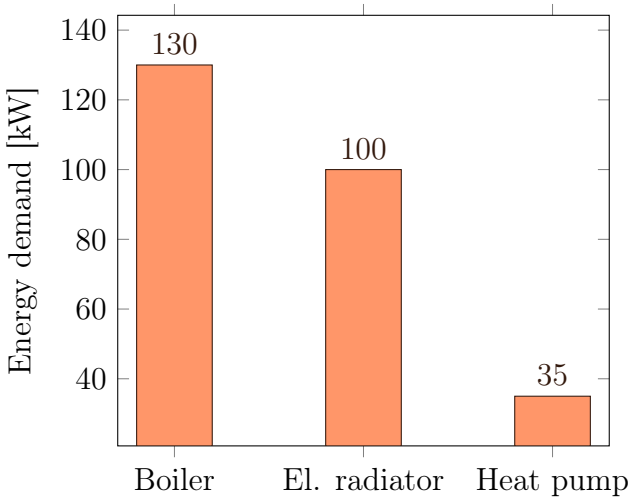

Figure 2.20: *Typical energy demands for different methods of 100kW heat production*

The use of heat pumps is an efficient way to produce energy for space heating, heating of DHW and space cooling. Figure 2.20 shows the principal of this. The energy delivered by the systems is 100 kW, and the graph shows how much energy the different systems need in order to cover this. Using equation 2.18, the efficiency, η

[−], of the boiler, electrical radiator and heat pump are 0.78, 1.0 and 2.9, respectively.

$$\eta = \frac{\text{delivered energy}}{\text{used energy}} \tag{2.18}$$

A boiler system includes a lot of heat losses, which makes it consume more energy than it delivers. This is the reason why boiler systems are energy demanding. The electrical radiator has approximately no losses and is therefor 100 % efficient. The heat pump produces more energy than it consumes, and has thereby an efficiency of more than 100%.

This efficiency of a heat pump, and thus the energy used, is dependent on the refrigerant, which will be discussed in more detail in section 2.7.2. The energy savings, however, can be as large as 50 to 80 % compared to that of conventional heating systems [60].

Industrial heat pumps (IHP) are heat pumps that use excess heat from other industrial processes. Regular heat pumps use heat sources like geothermal wells or water basins. IHP are preferred due to their high COP as a result of low temperature lifts. They also usually have low installation costs, and the distance between the heat source and sink is generally short. [56]

The Process of a Heat Pump

The concept of a heat pump, is to transfer heat from one place with low temperature, to another place with higher temperature. According to the 2$^{\text{nd}}$ law of thermodynamics, this is not possible in a natural manner. However, with the help of compressors, valves and heat exchangers, heat pumps are able to do it none the less. [58]

The main components of a heat pump that need to be present in order for the process to work, are pipes, one compressor, one expansion valve, and two heat exchangers, also referred to as a condenser and an evaporator. Other components, like accumulation tanks and additional heat exchangers could also be present to get even higher efficiencies.

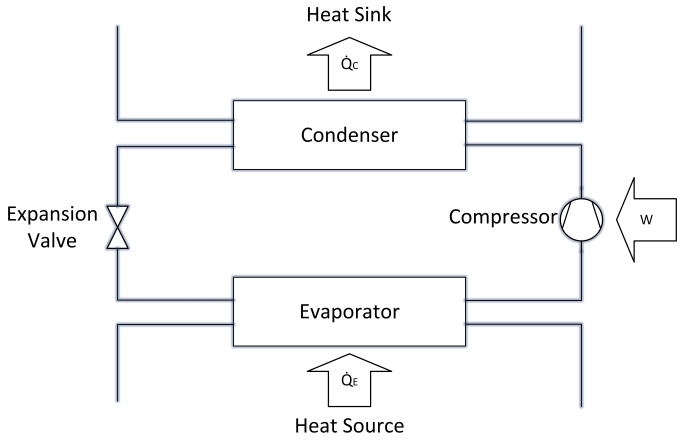

Figure 2.21: *The simplified process of a heat pump*

Further, a heat pump consists of three main circuits. These are the low temperature side, also referred to as the heat source, the high temperature side, referred to as the heat sink, and a refrigerant circuit. Figure 2.21 shows the composition of a heat pump, where the refrigerant circulates between the condenser and evaporator.

As seen in the figure, the evaporator draws energy, $\dot{Q}_E$, from the heat source, and the condenser delivers energy, $\dot{Q}_C$, to the heat sink. In the condenser, the refrigerant cools down and condenses while delivering heat to the high temperature side liquid. In the evaporator, the refrigerant warms up and evaporates while receiving heat from the low temperature side liquid.

To make this happen, the compressor and expansion valve regulate the pressure levels of the refrigerant. This to make sure the evaporation temperature in the evaporator is lower than the heat source temperature. Similarly for the condenser, they work together to make sure the condensing temperature is higher than the heat sink temperature. The supplied energy, $\dot{W}$, in the compressor is the only non-natural energy transfer happening in the heat pump.

Heat Pump in ph-Diagram

The process shown in figure 2.21, can also be represented by the ph-diagram shown in figure 2.22. This diagram follows a refrigerant cycle of ammonia, with the specific enthalpy, h [kJ/kg], plotted against the corresponding pressure, P [bar]. Specific enthalpy represents the energy present in a system as a result of the pressure and temperature of the system. The figure is plotted in the simulation tool DaVE, which will be explained more in depth in chapter 3. [58]

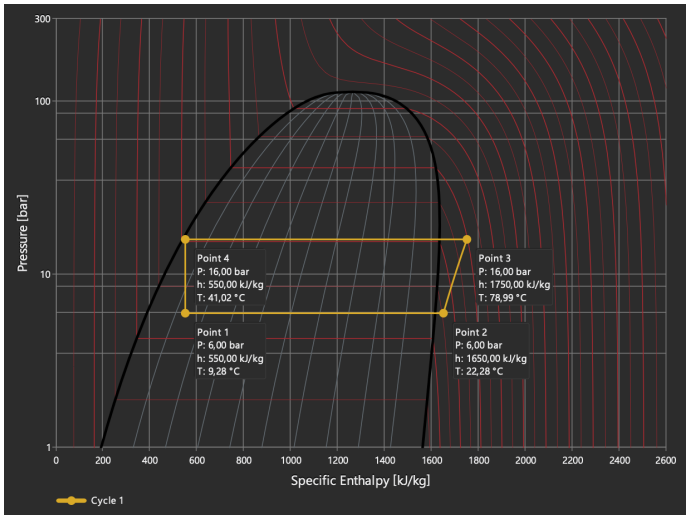

Figure 2.22: *The heat pump process in a ph-diagram*

This diagram represents the phases the refrigerant goes through in the heat pump. The dome in the middle represents the two-phase stage, being both liquid and gas. The red lines represent constant temperature levels, with a total difference of 20 K between each line. Where the black and red line meet to the left of the dome, everything is liquid. Moving along the red line to the other side of the dome,

more liquid turns into gas without changing the temperature, until everything is gas on the right side of the dome.

In the figure, the refrigerant warms and evaporates form point 1 to point 2, gaining energy from the heat source at constant pressure. From point 2 to point 3, the compressor compresses the refrigerant, causing T and P to increase rapidly. Then, at point 3, the refrigerant enters the condenser, gas turns into liquid, transfers heat to the heat sink, and cools to a lower temperature at constant pressure from point 3 to point 4. Finally, the refrigerant enters the valve where the pressure is relieved, and T drops back to point 1. The enthalpy value, h, however, stays the same between point 4 and point 1.

In figure 2.22, it can also be seen that point 2 is slightly extended into the gas region. This is to ensure that only gas enters the compressor. Liquid is not compressible, and if liquid is to enter the compressor, the efficiency will drop. Therefore, it is often common to have a superheat, ΔT_{SH} [K], of about 5 K, meaning having a temperature of the fluid at 5 K higher than the evaporation temperature for that pressure level.

Energy Evaluation

Figure 2.21 and 2.22 indicates that, for a heat pump delivering heat, the delivered energy at the high temperature side, corresponds to the supplied energy in the compressor and the drawn energy from the low temperature side combined. This is also illustrated by equation 2.19. [56]

$$\dot{Q}_C = \dot{Q}_E + \dot{W} \quad \text{[kW]} \tag{2.19}$$

This equation shows that the heat transfer rate in the condenser, $\dot{Q}_C$ [kW], equals the heat transfer rate in the evaporator, $\dot{Q}_E$ [kW], and the work performed on the system, $\dot{W}$ [kW], combined.

In real life, there will be losses in the compressor, causing it to deliver less energy than what it requires. Isentropic efficiency, η_{is} [–], is the ratio between the power input in the compressor and the power input from the compressor to the heat pump process.

Usually, for heat pumps used for buildings, it is true that a heat pump that can cover 50 % of the peak demand can also cover 90 % of the total demand.

Coefficient of Performance

To evaluate how well a heat pump operates, the efficiency of the system needs to be calculated. The efficiency of a heat pump is determined by the coefficient of performance (COP). This value states the ratio between useful heating or cooling provided, Q, and the amount of work needed, W. Thus, the COP for a heating process can be calculated by equation 2.20.

$$COP_H = \frac{Q_C}{W} \tag{2.20}$$

Equation 2.21 shows the COP for a cooling purposes. For both equations, the higher the COP value is, the less energy demand is needed in the compressor for

the system to deliver the necessary energy. However, to compensate for this, more energy is needed from the energy source.

$$COP_C = \frac{Q_E}{W} \tag{2.21}$$

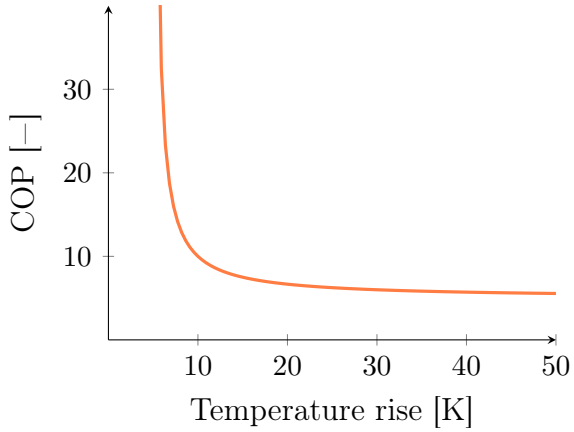

Figure 2.23: *Theoretical COP related to the temperature rise of the heat pump*

There is a close relationship between the temperature rise within the refrigerant and the COP value. This i shown in figure 2.23, where the graph indicates the lower the temperature difference between the evaporator and condenser, the higher COP values can be reached [58].

2.7.2 Choosing a Refrigerant

When designing a heat pump, it is important to evaluate which refrigerant, or working fluid, to use. The working fluid is the carrier of thermal heat within the heat pump system, ensuring heat transfer from the heat source to the heat sink. When choosing a refrigerant, a couple of factors need to be taken into consideration. These include environmental and safety properties, but also physical, thermal and practical properties, as well as its cost and availability. [59]

In the beginning of heat pump history, natural gases like CO_2 and NH_3 were used. In the 1930s, synthetic media like CFC and HCFC were introduced and were widely used instead. This worked for a while, but then awareness of the impacts these fluids had on the environment was set in focus, and the interest in natural refrigerants arose again. In 1995, a ban of CFC gases was formed, and in 2015 HCFC gases were prohibited as well.

Pressure Conditions

When deciding on a refrigerant, it is important to use one that has a saturation temperature and pressure that is within the use area of the heat pump [58]. This means finding a refrigerant where the critical pressure and its corresponding critical temperature does not limit the temperature delivered by the heat pump. This is

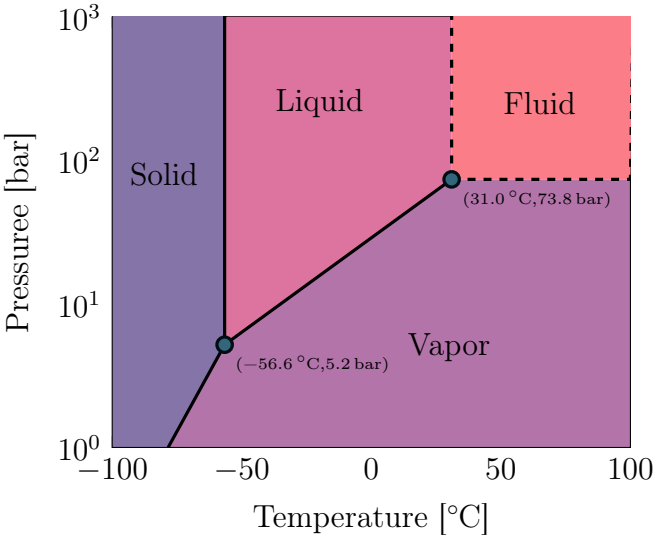

Figure 2.24: *Phase diagram for CO_2*

because above the critical point, no liquid can exist, which can limit the efficiency [39].

Figure 2.24 shows the concept of the critical point. There are two points here to pay extra attention to, the triple point and the critical point. All media have a phase diagram like this, but this one is an example of what it looks like for CO_2. Within the different areas, only one state can exist. The separation lines, however, represents areas of phase shifting, where more than one can exist, and at the two points, three different states can exist.

The vapor area of the diagram is where the medium is in gas form, but is below the critical temperature. This means that the medium can change phase into liquid if the pressure is increased, but the temperature stays the same.

Another factor to evaluate, is that the evaporation pressure also has to be higher than the ambient pressure in order to ensure outflow during a possible leakage. The condensation pressure is also limited by the components of the heat pump [58].

Another critical consideration, is the ratio between the evaporation and condensation pressure. This ratio is crucial when it comes to the energy and space efficiency of the heat pump.

Ozone Depletion and Global Warming Potential

When evaluating the environmental impact of a refrigerant, two different characteristics are central. These are ozone depletion potential (ODP) and global warming potential (GWP). ODP is the medium's ability to degrade the ozone layer. The value is compared to CFC_{11} which has the value of 1.0. Media with high ODP are usually also greenhouse gasses. [44]

To evaluate the greenhouse potential of a medium, GWP is used. This estimates the amount of heat in the atmosphere the gas is able to trap. This value is compared to the GWP of CO_2, which has the value of 1.0. Gases with high GWP might not have any ODP value, which is why both values have to be taken into consideration.

Review of Refrigerants

Table 2.12 show a couple of refrigerants and their values corresponding to those that have been presented in this section. Only the critical points for refrigerants commonly used are presented [39].

Table 2.12: *Some refrigerants and their corresponding values*

Type	ASHRAE	ODP [–]	GWP [–]	T_{crit} [°C]	P_{crit} [°C]
CFC	R12	1.0	10 200	-	-
HCFC	R22	0.05	1760	-	-
HFC	R410	0	2090	71	49.0
CO_2	R744	0	1 (0)	31.1	73.8
NH_3	R717	0	0	132.3	113
HC	R290	0	4	-	-
H_2O	R718	0	0	273.9	221

When CO_2 is used in a heat pump, it is usually a natural gas that is already existing in the atmosphere. The GWP is therefore negligible, hence the (0) in the table.

2.7.3 CO2 as Refrigerant

The discovery of how harmful synthetic refrigerants can be, has led to an renewed interest in natural refrigerants for heat pumps. Natural refrigerants, like water and CO_2, are eco-friendly, non-toxic, non-flammable, cheap and easy to access, which are very preferable qualities [51]. This section will therefore present properties of CO_2 and the use of it in heat pumps for cooling and heating.

Properties of CO2

The most remarkable feature of carbon dioxide (R744, CO_2), that makes it so applicable for heat pumps, is that it has a low critical temperature of 31.1 °C [46]. This makes the CO_2 heat pump valid to operate in a transcritical manner, a process which will be explained more in depth later in this section.

In addition, CO_2 requires heat pumps to have a high operation pressure under normal conditions, much higher than heat pumps running on other refrigerants. What this means in practice is that these heat pumps require a smaller volume of working fluid for covering the same demand as other heat pump refrigerants, resulting in a more compact solution with smaller components [58]. Being a natural refrigerant, CO_2 is also considered both environmentally friendly and safe.

However, the high operating pressures CO_2 require, also bring some challenges. It is the cause of the main disadvantage of CO_2 as a refrigerant, being it's huge expansion losses compared to other working fluids.

Transcritical Process

In regular heat pump processes, the whole process is kept below the critical point, and mostly within the phase shifting area. The process of heat exchange on the high pressure side of the refrigerant is therefor a condensing transformation of gas to liquid, which is why this heat exchanger used in these processes is typically called a condenser. The heat transfer is mostly latent and the temperature level stays unchanged for most of the process. [39]

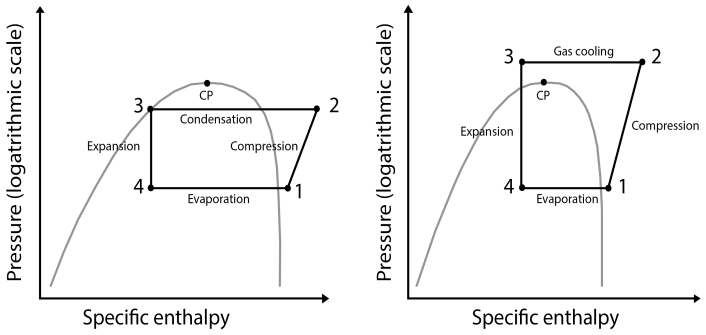

Figure 2.25: *ph-diagram for subcritical and transcritical heat pump processes*

In a transcritical process, on the other hand, the process is no longer limited by the critical point, and the cooling process takes place above it in the ph-diagram [39]. This phenomenon is shown in figure 2.25, where the difference of the regular, or subcritical, and the transcritical process is shown in ph-diagrams. Gas is the only thing existing in this process, which means there is no substance change here, but cooling of gas. The high pressure heat exchanger of a transcritical cycle process is therefore called a gas cooler.

2.7.4 Ammonia as Refrigerant

Ammonia (R717, NH_3) has been used as a refrigerant for a long time, especially in bigger refrigeration systems. Even from before the CHC gases were banned, ammonia was know to have much better thermodynamic properties. Now that environmental impacts and energy efficiencies are getting on the agenda, ammonia is getting an even better reputation as a refrigerant. [58]

As for the functional properties of ammonia, the critical pressure is measured to be 113.3 bar with a critical temperature of 132.3 °C. Which is shown in table 2.12 earlier in this section.

One unfortunate downside to ammonia, is that it causes copper to corrode in humid conditions, which can cause damages in the compressor. Another very important downside to ammonia, is that the medium is both toxic and flammable. It also has a quite distinct smell that can cause panic, but at the same time makes it easy to tell if there is a leakage.

2.7.5 Hydrocarbon as Refrigerant

Hydrocarbons have a lot of favorable thermal and environmental properties, making them good refrigerants in heat pumps. The most used hydrocarbon for this use, is propane (R290, C_3H_8). [58]

The use of propane needs to be highly regulated, due to its high explosion danger at relatively low concentrations. However, its not regarded as a toxic gas, since it is not dangerous in concentrations below the low explosion limit.

2.8 Thermal Energy Storage

The demand for heating and cooling within a building varies with time. The changes in this demand can be on hourly, monthly or seasonal basis. Because of this, it can be quite difficult to predict what the profile for the demand will look like in the future. In addition, designing a system able to cover any demand of the future in real time, can be quite expensive and space demanding. In a society where the energy demand is constantly increasing, a future system able to cover all the demand peaks, without particularly stressing the grid, can therefore be quite useful and profitable. This is why thermal energy storage (TES) can be a good supplement to an energy system for a building.

TES is a form of energy storage, utilizing the thermal properties of fluids. A conventional way of storing energy, is through charging a battery, with the help of electricity. TES, however, stores thermal energy that can be used later for either heating or cooling purposes. The method is typically used for storing energy for buildings and industrial processes. [50]

This can be done by heating or cooling a material, storing it, and finally reversing the process for a time when it is needed. Doing this is called sensible heat storage (SHS). Another way of exploiting TES, is changing the phase of a material, for instance from liquid to solid, and changing it back again when the energy is needing. This process is called latent heat storage (LHS) [12].

In TES, it is important to know the energy, Q kJ, required to heat a substance of mass, m kg, and specific heating capacity, c_p [kJ/kg K], from a low temperature, T_1 [°C], to a high, T_2 [°C]. This can be calculated using equation 2.22.

$$Q = m \cdot c_p \cdot \Delta T \qquad \text{[kJ]} \quad (2.22)$$

This equation is quite similar to equation 2.7. The difference is that here, the total amount of energy needed to heat up a mass is calculated, rather than the effect a moving liquid can cause. Q differs from $\dot{Q}$ with not being dependent on time or speed. Table 2.13 shows some c_p values and densities for some commonly used materials [23]. Q can also be presented in kWh, by dividing the amount by a factor of 3600.

One way of using SHS for heat storage, is storing hot water in highly isolated tanks. Water has the advantive properties of being both cheap and free of toxins, which is why it in most cases is the preferable choice. The most preferable property of water, is that it has one of the highest specific heats for liquids in ambient temperatures. Even though many solids have even higher specific heats, water still is

Table 2.13: *Some densities and specific heat values for different substances at a temperature of 300 K and under atmospheric pressure*

	Density ρ [kg/m^3]	Specific heat c_p [kJ/kg K]
Concrete	2300	0.970
Insulation	44	2.020
Sandstone	2200	0.712
Gravelly Earth	2050	1.84
Clay	1458	0.879
Water, fluid	997	4.179
Water, vapor	25.6	1.868
Ammonia	0.689	2.158
CO_2	1.77	0.851
Air	1.16	1.007

quite a good medium because it being a liquid makes it is easy to transfer between places.

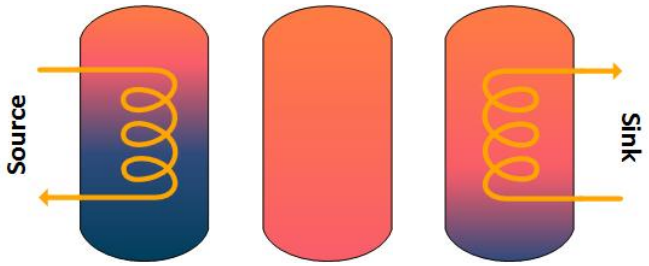

(a) *Charging* ***(b)*** *Storage* ***(c)*** *Discharging*

Figure 2.26: *TES tanks during charging, storage and discharging*

The three main stages of a typical TES process, being charging, storing and discharging, can be shown in figure 2.26, respectively [12]. Sensible TES consists of a storage medium, a container and input/output devices. Further in this report, TES will indicate SHS.

Figure 2.26 also shows the tank when it is, respectively, close to empty, full and close to full. The best scenario is having a tank that is close to full so that any excess heat can be stored, and the load is not too much to handle. In real life scenarios, the tank will change between all three states.

2.9 Cost Related to Electricity

Electricity prices are calculated based on several variables. Electrical power is traded on the spot market by wholesalers, and a spot price is determined on when and how

much is traded. A residential consumer has the choice of entering into a various set of pricing models, and they can decide on which service provider to buy from. Nord Pool provides statistics for spot prices. [9]

In addition to the variable spot price provided by a service provider, a consumer will have to connect to the local electrical grid. The local power supplier will charge a fixed price for connection to the grid, then a variable price for consumption of MWh, and a consumption fee based on MWh consumed. Equation 2.23 shows how to calculate the total cost of electricity. [43]

$$C_{tot} = GR_{fixed} + (GR_{var} \cdot E) + (GR_{fee} \cdot E) + SP \cdot E \,[\text{NOK}] \quad (2.23)$$

In this equation, total cost, C_{tot} [NOK], is dependent on the energy consumed, E [kWh], the fixed grid rent, GR_{fixed} [NOK], the variable grid rent, GR_{var} [NOK/kWh], the variable grid fee, GR_{fee} [NOK/kWh], and the spot price, SP [NOK/kWh].

Trondheim has a local district heating system, and prices are set by Statkraft and calculated similarly. Prices are based on spot price, in addition to system connection price. Both are dependent on consumption. According to the Energy Law in Norway,§5-5, district heating cost are not allowed to be higher than the electricity cost. [8]

A district heating system using a heat pump and excess heat from e.g. cooling of a ice rink, will demand less power than using electricity as sole energy source. This will provide savings which must be compared to the investment cost of a district heating system.

$$C_{reduced} = C_{elec} - C_{comp} \quad [\text{NOK}] \quad (2.24)$$

The equation 2.24, shows the possible savings, $C_{reduced}$ [NOK] when comparing the cost of space heating using electricity, C_{elect} [NOK], and the energy cost of using a heat pump for space heating, C_{comp} [NOK].

The same equation can be used to find savings for using a heat pump to heat DHW compared to only using electrical power to heat DHW.

To find the today's value of the future savings, Net Present Value is the most common formula to use. The net present value, NPV [NOK], is the today's value of future cash flows, so in this thesis it will show today's value of the future savings. The calculation of NPV is shown in equation 2.25

$$NPV = \sum_{t=1}^{n} \frac{R_t}{(1+i)^t} \quad [\text{NOK}] \quad (2.25)$$

NPV is dependent on the time periods, t [–], the discounting rate of return on an alternative investment, i [–], and the net inflows and outflows for a single period, R_t [NOK].

Chapter 3

Method

This chapter begins with presenting the programs used in this thesis. Then, the building project at Tungaveien 1 at Leangen in Trondheim will be introduced, and the different options for the energy system that will be evaluated will be presented. Further, the method for evaluating the energy demands will be presented. The next sections will go through the different heat sources that could be used, and how the heat pump will be simulated. Finally, the cost analysis will be presented.

3.1 Programs

SIMIEN

SIMIEN is a simulation program used to generate accurate energy profiles for buildings. The model is simplified so all areas, zones, within the building are treated alike, e.g. variations from bathrooms, internal loads, temperature profiles are not separately considered. Other specifications like construction details and energy systems are also included in the tool. Through a simulation of the building, SIMIEN is able to pull an energy profile, presenting energy demands and yearly usages of the different energy suppliers. In this thesis, SIMIEN is used to estimate the energy profile and the thermal comfort profile. These estimates are used in the calculations and dimensioning of the heat pump. SIMIEN is downloaded through RemoteApp from NTNU.

Dymola

Dymola is a collection of modeling and simulation tools used to visualize complex computerized version of real life systems under different conditions. The program can be used to build heat pumps in a detailed manner, with specifications for all components within it, and simulate and investigate its behavior with different set points, limitations and other conditions. The simulation gives an accurate representation of different variables, including water flows, pressure states and temperatures. Dymola uses the language Modelica, and the TIL library is used as an additional component package. Dymola is a program that have different functions with different licenses. The license provided by NTNU makes the TIL library possible to implement. The program can be downloaded from their website [14].

DaVE

DaVE is an additional application that interacts with Dymola. It uses simulation results from Dymola to design detailed diagrams. In this thesis, pressure points from Dymola is used to make diagrams like ph-diagrams. DaVE is a complimentary program that works with Dymola and is licensed based. The license used for this thesis is provided by NTNU.

CoolPack

Coolpack is a simple simulation tool for refrigeration systems where operations of a heat pump can be evaluated at a detailed level. The tool uses inputs for some of the values, and calculates the remaining values. It also presents a ph-diagram, as well as other state values. The program is run on RemoteApp from NTNUs servers.

Visio

Visio is a drawing program used in this thesis to make figures. Every figure which is not referenced from another source or simulation tool, was drawn in Visio. The program is downloaded through NTNUs RemoteApp function.

COMSOL Multiphysics

COMSOL Multiphysics is a simulation tool used for anticipating the workflow of different scientific problems, like fluid or heat flow. The tool uses the finite element method to solve complex mathematical problems. The finite element method involves dividing the physical domain into a finite number of smaller parts, a mesh, and reduce the problem of fluid flow and heat transfer into simpler mathematical equations related to the boundaries between these parts. COMSOL Multiphysics is used to simulate heat transfer and fluid flow in the gray water tank. Both 2D and 3D representations of the problem are simulated. The program can be downloaded from their website [5].

3.2 Leangen Building Area

Tungavegen 1 at Leangen is an area in Trondheim, located to the East of the city center. The area is characterized by industrial buildings, storage facilities and department stores. In addition, there are some smaller residential buildings. At the moment, a racecourse is placed in the middle of Leangen. The racecourse with surroundings, will for the next 30 years be transformed mainly into a residential area, with some commercial buildings, offices, and a kindergarten. The detailes mentioned for Tungavegen 1 in this chapter, are specified in the plan description written by Asplan Viak [11].

In times when the environment and its impact on the future of our planet is more relevant than it has ever been, it is important for this building area to be as environmental friendly and energy efficient as possible. This will both help with

reaching the sustainability goals, as well as be economically preferable in the long run. Further in this thesis, different methods of achieving this will be discussed.

3.2.1 The Situation Today and Further Plans

The building process will have an incremental progress, meaning not everything will be built at once. It will take several years from the first building process has started, until the last building is completed. [11]

The area will exist of 13 building zones, as illustrated in figure 3.1. Nine of these, referred to in the figure as B1 to B9, consists mostly of residential buildings. BKB1 and BKB2 will mostly consist of service buildings, such as cafes and hair salons, in addition to a kindergarten, a central for waste disposal, and a very small number of apartments. KB consists of only office buildings, and O_BOP is a health and welfare center with 70 assisted living apartments.

Figure 3.1: *Distribution of zones at Leangen building area with local heating pipes*

The area will include 1660 to 1770 apartments, where the average size of an apartment will be 70 m^2. Zone B1 and B2 will also include some terraced houses, which is illustrated in figure 3.1 as small, tightly packed boxes. Every building will also include a basement. These basements will contain the energy centrals with technical equipment, as well as parking spaces and storage areas for bikes, sporting goods etc.

Table 3.1 shows the distribution between the different zones, building type with the corresponding total gross floor area (GFA). The apartment column includes both apartment buildings and terraced houses. The column named "Health" represents the health and welfare center.

Table 3.1: *The GFA of the different zones in m^2*

	Apartments	Services	Offices	Kindergarten	Health	Waste
B1	10 600	-	-	-	-	-
B2	13 200	-	-	-	-	-
B3	11 000	-	-	-	-	-
B4	12 700	100	-	-	-	-
B5	16 000	100	-	-	-	-
B6	29 400	200	-	-	-	-
B7	13 800	-	-	-	-	-
B8	9 000	-	-	-	-	-
B9	22 700	-	-	-	-	-
BKB1	6 600	1900		2 000	-	-
BKB2	9 000	2 100	-	-	-	300
KB	-	-	9200	-	-	-
oBOP	-	-	-	-	12 000	-
Total	154 000	4 400	9 200	2 000	12 000	300

3.2.2 Energy Standards

Due to the long building and planning period for Tungavegen 1, the standards and requirements for the buildings will change and develop. The three building stages at Tungavegen 1 will therefore follow three different standards. The buildings in the first stage will follow the standards from TEK17, the second building stage will follow the Passive House standard, and the last stage will be built after an estimated standard for 2030, referred to as "Estimate 2030+". [11]

3.2.3 Network Structure

The goal for Tungavegen 1, is that every zone will be as close to self providing as possible when it comes to heating.

When looking at figure 3.1 there is a purple line that illustrates the main pipe which will go from the ice rink and follow the planned walking path in a circuit throughout the area. The reason for following the walking path, is that this will give easy access if maintenance is needed. The distribution line will thereby be close to each zone, where an energy central is located. Each zone will have a separate energy central, which will provide the whole zone with energy for space heating and domestic hot water, DHW. The energy centrals are illustrated as a small purple circle in each zone, situated as close to the distribution line or pipe as possible.

3.2.4 Energy Central Structure

The Energy Central is a major part of the echo system to enhance how Tungavegen 1 will optimize the heating capabilities. The Figure 3.2 shows a model of what an

energy central for a building zone could look like. The figure contains three external pipes. Two are connected to the city distribution system for drinking water and sewage, respectively. The third is the circuit pipe from the ice rink.

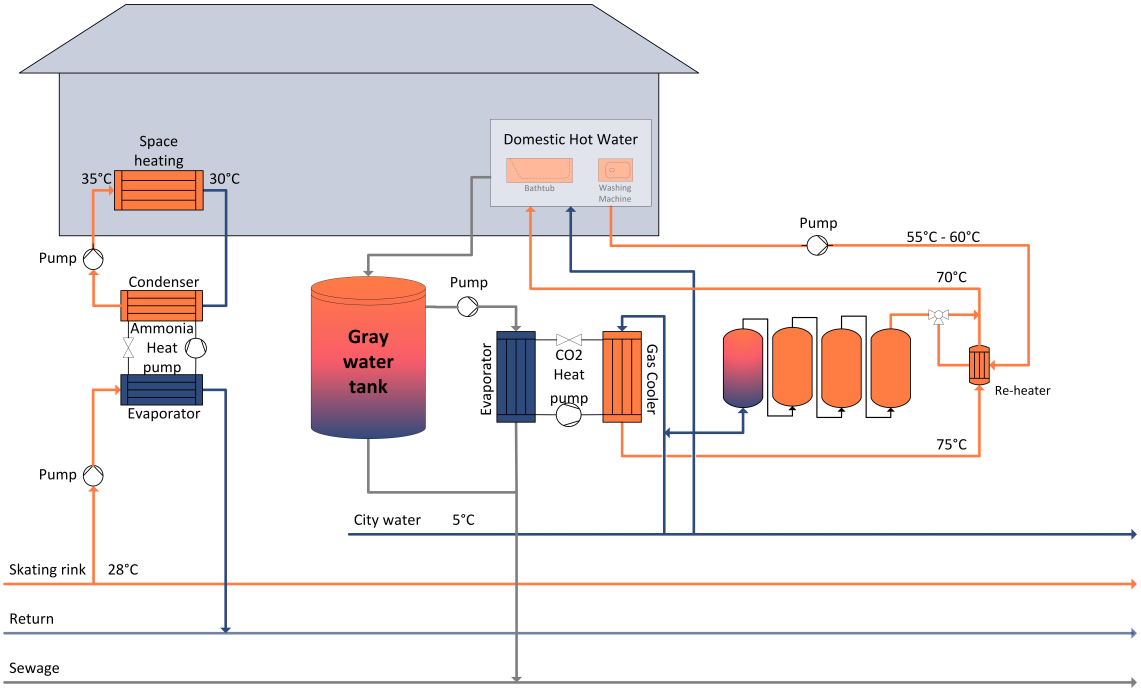

Figure 3.2: *Illustration of what an energy central might look like*

There are two main circuits in the illustration, one for space heating, and one for DHW. Both circuits will utilize the use of heat pumps, in the illustration these are ammonia and CO_2, respectively.

The circuit including the ammonia heat pump will provide space heating. It will pull heat from the low temperature water produced by the ice rink to elevate the temperature in the space heating circuit. The goal is to lift the temperature from about 30 °C to 35 °C. The thesis will evaluate whether this will cover the whole space heating demand.

The second circuit covers the DHW demand. This will primarily be covered by the excess heat from the produced gray water, in combination with the CO_2 heat pump. Together, they heat the 5 °C city water to a temperature of 75 °C to provide DHW. Then both the heated water and the cold city water is used to provide hot and cold water to the buildings. The gray water will then be collected in a tank, to complete the circle.

Every energy central will include four TES tanks, as illustrated. Whenever the production of gray water is higher than the demand of DHW, the TES tanks will be filled. This to make sure as little amount of energy as possible gets wasted.

The details of how the heat pumps work will be explained later in this chapter, but the important difference between them, is the temperatures. The one for space heating will need a much lower temperature rise than the one for DHW, which is why they use different refrigerants.

The aim for this central, as shown in figure 3.2, is for the energy centrals to be

able to completely cover its own heating demand for DHW and that the skating rink will cover the space heating demand. This means that the system will be able to be completely independent of the city network for district heating. The only external energy needed will then be for the circulation pumps within the network, and the compressors in the two heat pumps.

3.3 Energy Demand

The previous section explained how Tungavegen 1 will operate. The following section will go through how the reference zone is used to estimate energy demand for the area. In addition it will go through how SIMIEN is used to generate energy profiles. In the end an overview of possible temperatures for the reference zone are discussed.

3.3.1 Reference Zone

Further in this thesis, section B1 from figure 3.1 will be used as the reference zone. A snapshot of zone B1 is shown in figure 3.3. This means that all further calculations in this thesis, will be done based on information and data for this zone only.

This is also the first zone that is planned to be built, and will thereby be used as a reference for the next stages. As seen in table 3.1, the sizes of the zones at Tungavegen 1 varies greatly. Due to this, the profiles will not be accurate for all building zones. However, the results and experience from zone B1, will give necessary information to enhance the next stages to be more cost and energy efficient, in addition to other more general building enhancements.

Since it is the first zone to be built, it will follow the least strict standard. In the years to come, features and standards will, due to research and new information, evolve further, and the buildings built later will require to follow standards that are more stringent. Energy demand for buildings built later, will reflect this, and the demand will be lower than in the first building stage.

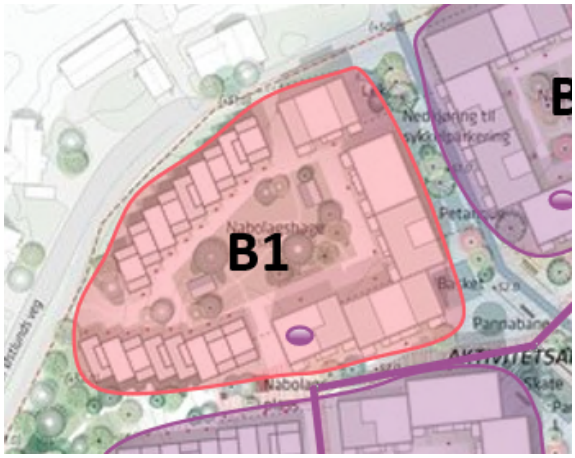

Figure 3.3: *Map over zone B1*

Zone B1 consists of 5 apartment buildings and 17 terraced houses, as illustrated in figure 3.3. The gross floor area (GFA) of the zone is 10 600 m^2, as indicated

in table 3.1, and will not consist of any other building types. The height of the apartment buildings will vary from three to six floors.

Energy Profile

For the energy profile, both values taken from TEK17 and SINTEF will be used and compared. From SINTEF, an excel file has been used [25]. From this file, only heating of space and DHW is provided. Therefore, only these can be compared to the TEK17 standards. Hence, space cooling, cannot be compared with these numbers.

SINTEF has gotten the results based on measurements done on real life buildings. This has been done through the use of a load profile generator developed by SINTEF [30], and based on a temperature profile of an average year in Trondheim.

The results from SIMIEN, on the other hand, are based on the low energy consuming standards from TEK17. The temperature profile is still based on a temperature profile of an average year in Trondheim, but the theoretical standards from TEK17 may differ some from the actual measurements in the load profile generator. The results from both of these will be compared in section 4.1.1.

3.3.2 Model in SIMIEN

SIMIEN is used for the simulation of this reference zone because it is a simple and understandable tool that gives satisfying results. The exact details of the construction is not needed in order to make a virtual model of the area.

In SIMIEN, zone B1 is illustrated as two zone areas, one for the apartments and one for terraced houses, with values corresponding to the first building stage. This is the standards defined in TEK17 [68], as described in section 2.5. As previously mentioned every building will have a basement. Since they will not have direct heating, they are modeled as unheated basements in SIMIEN.

It is an assumption that all rooms within the apartments and terraced houses has the same energy and temperature profiles, which makes it possible to illustrate B1 with two zones in the simulation tool. Further, since a specific energy profile or how the air flows within the various rooms are not within the scope of this thesis, SIMIEN gives a sufficiently detailed report for the building area.

As shown in figure 3.5 the program gives options to which energy supply methods are to be used. For this simulation, district heating is chosen as the main supplier for space heating and cooling, as well as DHW, in cooperation with heat pumps. Electricity is chosen to cover the rest of the energy demand. Other sources like solar power for absorption or boilers are also options that could be implemented.

Specifications for zone B1, both construction wise and energy wise, are shown in tables 3.2 and 3.3, respectively.

Based on this input SIMIEN can generate different reports. In this thesis, the information generated on energy use, energy demand, thermo losses and thermo comfort will be the main focus.

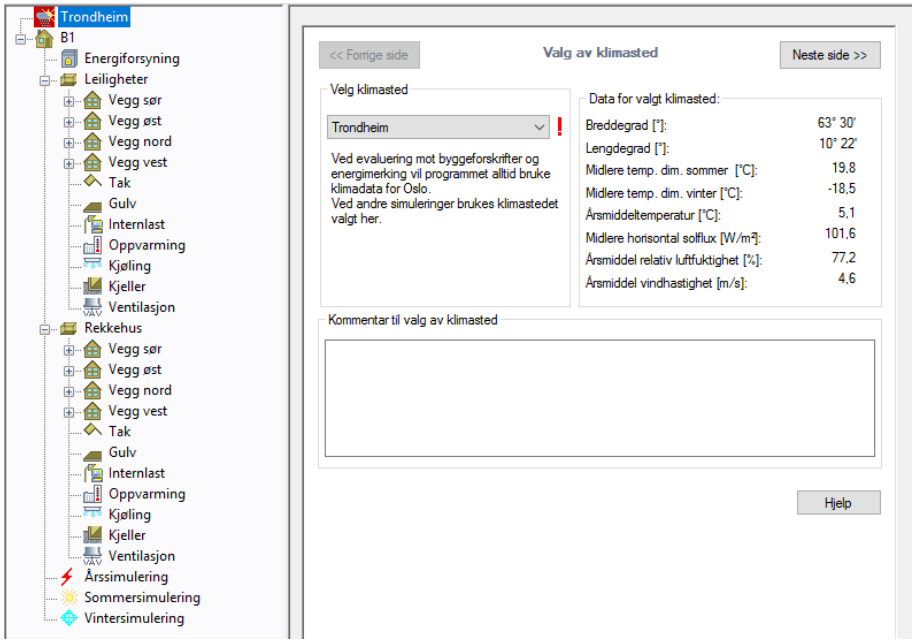

Figure 3.4: *Dashboard on SIMIEN*

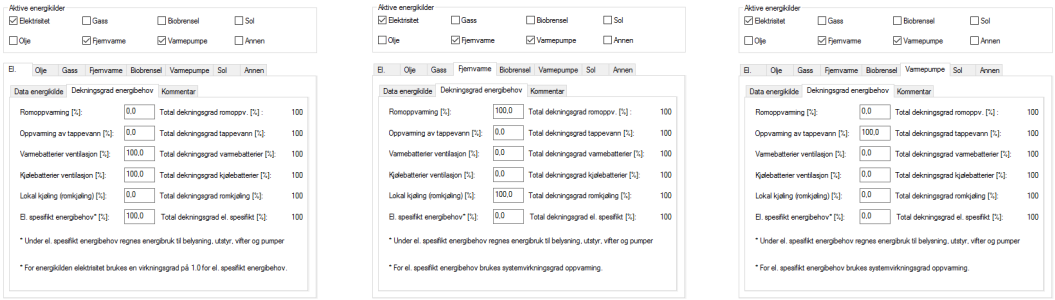

(a) *Electricity* ***(b)*** *District Heating* ***(c)*** *Heat Pumps*

Figure 3.5: *Energy options in SIMIEN*

3.3.3 Supply Temperatures

Keeping consistent temperatures throughout the thesis is crucial to ensure accurate comparisons. Therefore the temperature mentioned below will be used in the models, simulation tools, and calculations.

The space heating is conducted by underfloor heating. In correspondence with section 2.5.2, a water temperature of 35 °C in the supply pipe and an outlet temperature of 30 °C should be enough to keep the desired indoor temperatures.

DHW needs to have a temperature high enough to cover all hot water demands. This includes about 40 °C for showers and faucets, and 60 °C for washing machines. It should also be hot enough to kill all Legionella. The desired temperature for DHW is therefore 75 °C.

The space cooling can be implemented in various ways, which will be explained later/has been explained. To prevent the temperatures from exceeding 24 °C as much as possible, as presented as the preferred solution in section 2.9, the pipe

Table 3.2: *Construction specifications of parameters entered in SIMIEN*

	Apartments	Terraced houses
Apartments per floor	3	1
Floors in building	6	3
Space per apartment	78	70
Total floor space	7020	3570
Total room volume	18954	9639
Exterior wall area	4163	2738
Window/door area	1091	535

Table 3.3: *Energy specifications of parameters entered in SIMIEN*

Energy covered by:	Space heating	Space cooling	DHW	Technical
Direct electricity	0	0	0	100
Heat pumps	0	100	100	0
District water	100	0	0	0

temperatures should keep a temperature of 19 °C. The temperature supply side of the heat exchanger should therefore keep a temperature between 18 to 25 °C.

3.4 Heat Sources

The heat distribution system at Leanegen opens up for integration for weaker and renewable heat sources. This section will go through some possible heat sources that can be integrated in Tungavegen 1. Utilization of heat from gray water will be covered in section 3.6.

3.4.1 Ice Rink

In the vicinity of Tungavegen 1, Leangen Ice Rink is located. This is an indoor hockey arena for nearby sports clubs. The ice rink has it's peak production of ice in the colder months. It is also producing ice in the spring and autumn, but then at a much lower energy consumption. This can be seen in figure 3.6, which is data collected from Leangen Ice Rink about their monthly use [20]. On a yearly basis, this corresponds to 1766 MWh in 2018, and 2265 MWh in 2019. The production of ice leads to a massive amount of energy as explained in section 2.6.1.

Instead of letting this heat go to waste, the heat could be used to heat up the water circuit running through Leangen. This has been looked into in previous master theses, and the excess heat from the skate rink will, presumably, heat the water to a temperature of about 28 °C [61]. However, 28 °C is not sufficient for space heating in the area by it self, as stated in section 2.5.2. Dymola will be used to show how a heat pump can use this water to the required temperature of 30 to 40 W/m^2.

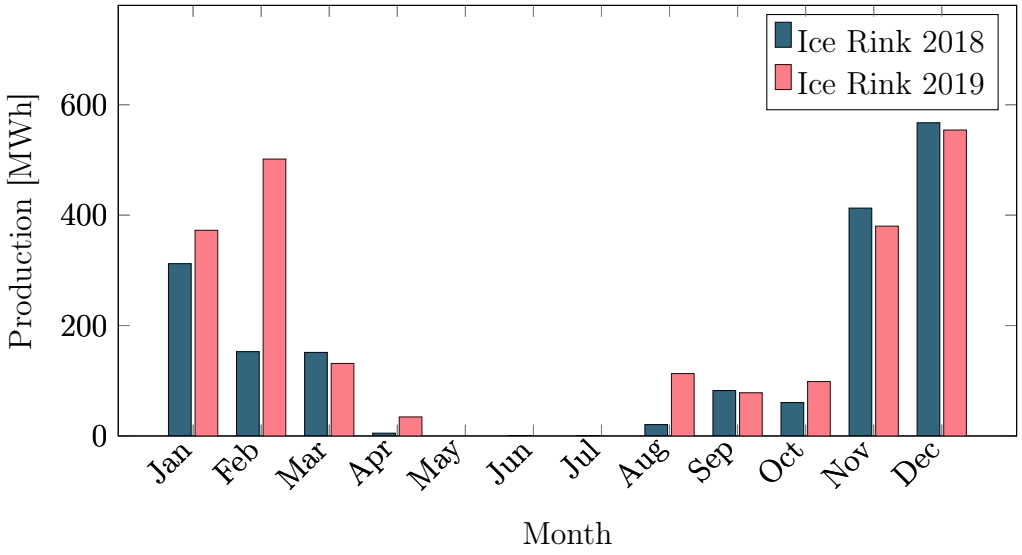

Figure 3.6: *Measured excess energy from ice rink in 2018 and 2019*

3.4.2 Surrounding Factories

Another possible producer of heat as a byproduct are factories, and especially those handling dairy. These have a huge cooling demand, for both processing and storing the products.

Tine Tunga, a dairy factory at Leangen, was contacted about their waste heat. They informed that they currently are planning to invest in an upgraded energy system, enabling them to reuse the excess heat in their own facilities for internal use [53]. Being the largest factory in the area, and the desire to utilize this for their own benefit, it has been evaluated as not relevant for this thesis.

If, however, any of the factories does have excess heat to spare, the heat would be utilized in the same manner as for the ice rink, through a common distribution system through the area.

3.4.3 Gray Water

Every residential building uses DHW in one way or another. The water is e.g. used for cooking, cleaning and washing, and after it has served its purpose, it is discarded in the sewage as gray water. Usually the gray water still has high temperatures and is thereby a resource which is just wasted into nothing.

The thesis will look at a method of using the gray water as a heat source in the process of heating DHW. To do this, the amount of of gray water produced, and the energy potential of this based on the temperature decrease it will get in the evaporator, was calculated. It was calculated for temperature differences of 10 K, 15 K, 20 K and 25 K, with a heat pump with a COP of 3.2.

For consistent comparison, it was assumed that the total energy potential of the gray water, and the total energy demand for DHW, was divided equally through every month, regardless of number of days in the months. This makes it less accurate for every month, but makes for better energy balance calculations.

3.4.4 District Heating

The prime goal of Leangen building area, is that every zone can provide their own energy, with supplement from the nearby ice rink. Trondheim city has a district heating system, providing residential heating throughout the city [65]. Trondheim's local district heating system will, preferably, not be in use. This will be taken into consideration in the in the discussion in Chapter 5. However, if calculations show that this is not going to be possible, the local low temperature district heating system goes right next to the area, making it possible to connect if desired.

3.4.5 Solar Heat Collection

Solar heat is a possible option as an addition to the previously mentioned heat sources. The thesis will look at the data of the possible heat that can be extracted from the sun, to further evaluate if this is a viable option for Tungavegen 1.

The solar radiation information is generated from the Photovoltaic Geographical Information System [36]. On this site, the measured solar radiation in kWh/m^2 for an exact location through the years 2009 to 2016 can be found. Information for later years are not yet published.

In order to calculate how much energy can be utilized from this, the solar radiation can be multiplied with the possible collector area, and the total energy in kWh can be found.

The found results are plotted in a graph, and a line for the average solar radiation each month is drawn. This way, future predictions are more accurate, because the solar radiation varies greatly every year. However, predictions about the future radiations can never be exact, and there are huge uncertainties to this. It is therefore not wise to rely fully on these predictions.

3.5 Heat Pump Models

Heat pumps will be used to utilized energy from weak energy sources, like those mentioned in the previous section. The project at Leangen will in regards to this thesis consist of at least two different heat pumps. One will use CO_2 as refrigerant, while the other will use either ammonia or propane.

The ammonia or propane heat pump is going to be used to rise the temperature of the water in the space heating circuit from 30 °C to 35 °C. The heat source is going to be the 28 °C water from the ice rink. The CO_2 heat pump will use the excess heat from gray water production to rise the temperature of the city water from 5 °C to 75 °C.

The results in this thesis will focus on an ammonia heat pump. The CO_2 heat pump has been examined by another thesis.

3.5.1 Space Heating and Cooling Integration

Figure 3.7 shows two options on how to use a heat pump for room temperature regulations. On the left, the heat pump for cold months with space heating demand,

and on the right, warm months with need for space cooling. The figure shows the use of an ammonia heat pump, but propane could be used as well.

Space heating at Tungavegen 1 will use the water from the ice rink as the heat source. The temperature of the water coming from the ice rink is 28 °C, and with the use of a heat pump, the energy central will be able to elevate the temperature of the space heating water circuit to 35 °C. This is shown to the left in figure 3.7.

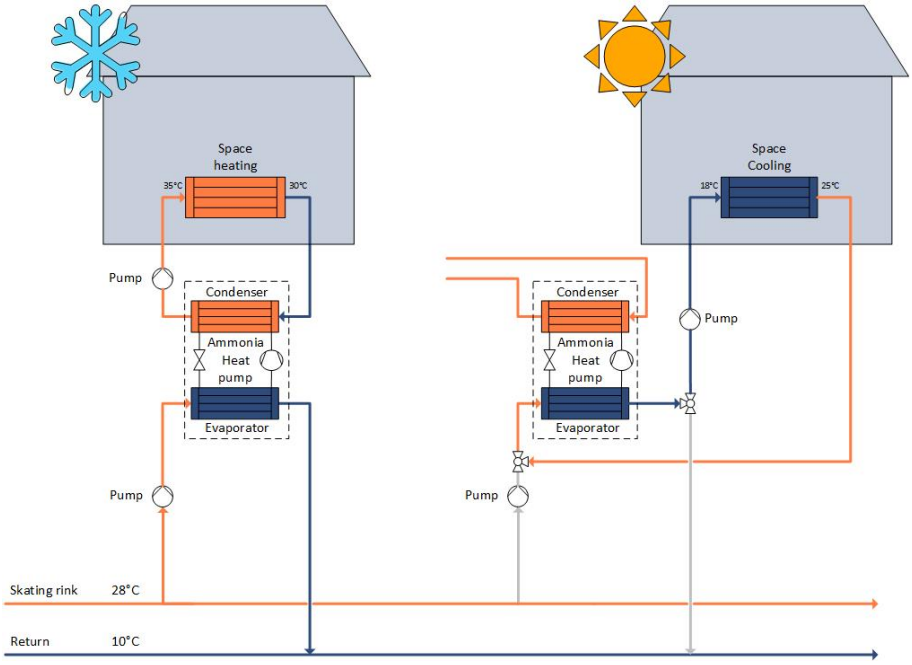

Figure 3.7: *Possible implementation of the ammonia heat pump for summer and winter operation*

During the summer months the space heating demand will be much lower. During these months the heat pump can be switched around, providing space cooling instead. The implementations of this is shown to the right in figure 3.7. In this scenario, the space cooling circuit will work as a heat source to the pump. The heat sink, however, can be the outside air, the return circuit, or any other medium with a temperature lower than the condenser output.

3.5.2 Model in CoolPack

CoolPack is used to simulate the heat pumps in order to get initial conditions which then is used as input to Dymola. It has also been used to compare different values, as well as to cross check different modifications before entering them into Dymola.

For the ammonia heat pump, a regular one-stage cycle with a simple direct expansion evaporator has been used. A superheat of 5 K is also chosen, in order to ensure only gas enters the compressor.

The models in CoolPack are primarily dependent on the delivered heating energy, $\dot{Q}_C$ [W], which is the main input. In addition, the simulation takes the two temperature levels and the isentropic efficiency, η_{is} [−] as input. Together, CoolPack

uses these values to estimate the mass flow of the refrigerant, as well as the different pressure and enthalpy levels.

The strengths of using CoolPack is it's ability to produce good input values to Dymola simulations, and it gives a quick and easy insight into how a heat pump will react to the input values. The downside of Coolpack is that it is highly simplified and gives indicative values only. It cannot give any real details about the different components.

3.5.3 Model in Dymola

Dymola is used to specify the components in more detail than what is possible in Coolpack. In addition, the results from the simulations in Dymola, gives a more detailed picture on how the heat pump works.

The heat pump was modeled in Dymola by a step by step approach.

- Step 1: Optimizing the condenser
- Step 2: Adding valves and accumulation tank
- Step 3: Adding and optimizing the evaporator
- Step 4: Adding the compressor

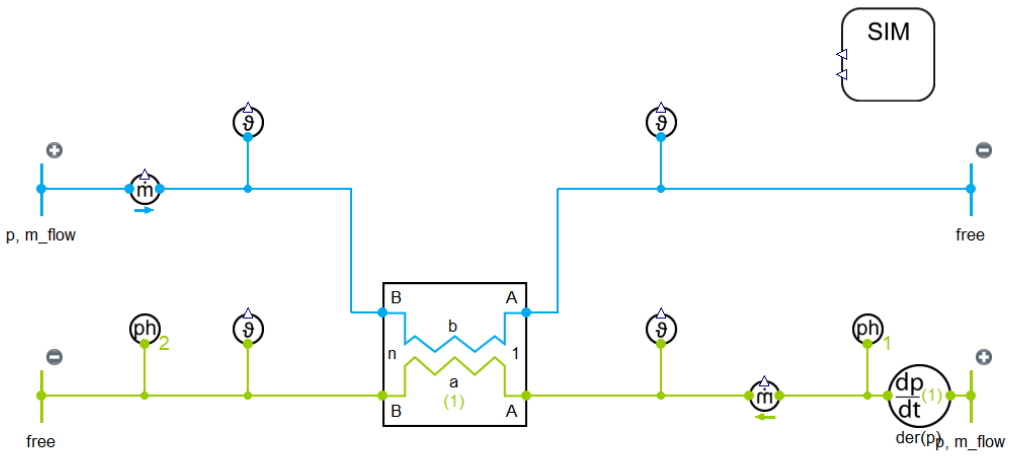

Figure 3.8: *Start of ammonia heat pump in Dymola*

In the first step, the condenser was optimized. Figure 3.8 shows the first step of how the heat pump was set up. The parameters used in the heat exchanger were initialized in CoolPack, and then optimized by try and fail in Dymola. ph-diagrams from DaVE were also used in all the steps in order to make sure the heat pump behaved as it should.

In Dymola, instead of implementing an entire closed circuit, boundary types can be used to represent the liquid flows. The different boundary types can be

defined with up to three parameters, being fixed pressure, mass flow, temperature and specific enthalpy.

The two liquid inlets for water and the refrigerant, respectively top left and bottom right in the figure, are represented by a boundary type with fixed pressure and mass flow rates. As an additional condition, the water side also had a fixed temperature, corresponding to the space heating temperatures. All the boundary condition levels for the water side were found by calculations done for the space heating.

The refrigerant inlet, on the other hand, has fixed enthalpy as the additional parameter. The three boundary conditions for the refrigerant are taken from CoolPack. The outlets for both the water and the refrigerant are represented by free boundary conditions, meaning they will vary based on the settings of the other components.

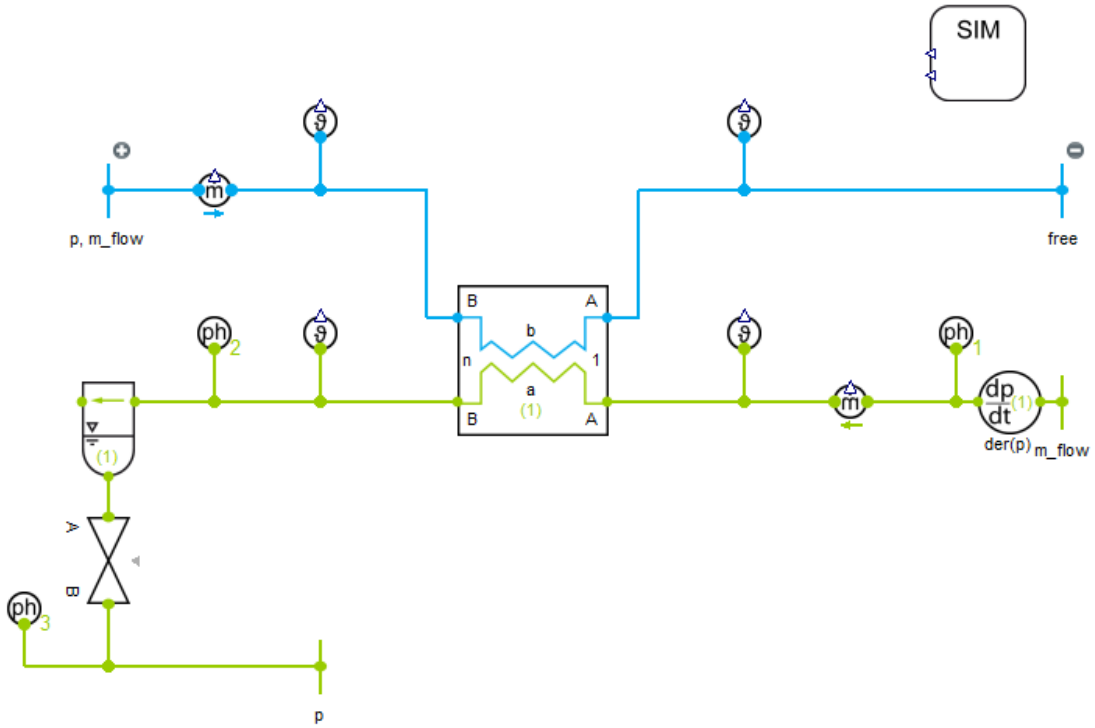

Figure 3.9: *Step 2 of heat pump implementation in Dymola*

The goal of this first step, was to optimize the condenser heat exchanger so that the water side gets the right temperature and energy lift. Plate heat exchangers were used, and most of the default values in Dymola were left unchanged. The size of the heat exchanger was first calculated, and then some of the parameters were adjusted until the heat transfer area was correct. Finally, the rest of the parameters were adjusted until the water side had the needed temperature for the space heating.

The second step, was adding the valve and accumulation tank, as shown in figure 3.9. The size of the accumulation tank was set to 0.6 L, and then the values for the flow through the valve was adjusted until the refrigerant had the expected values simulated by CoolPack.

In the third step, the evaporator was added. Similar to the method for the condenser, but the values here were not as easy to estimate as for the condenser.

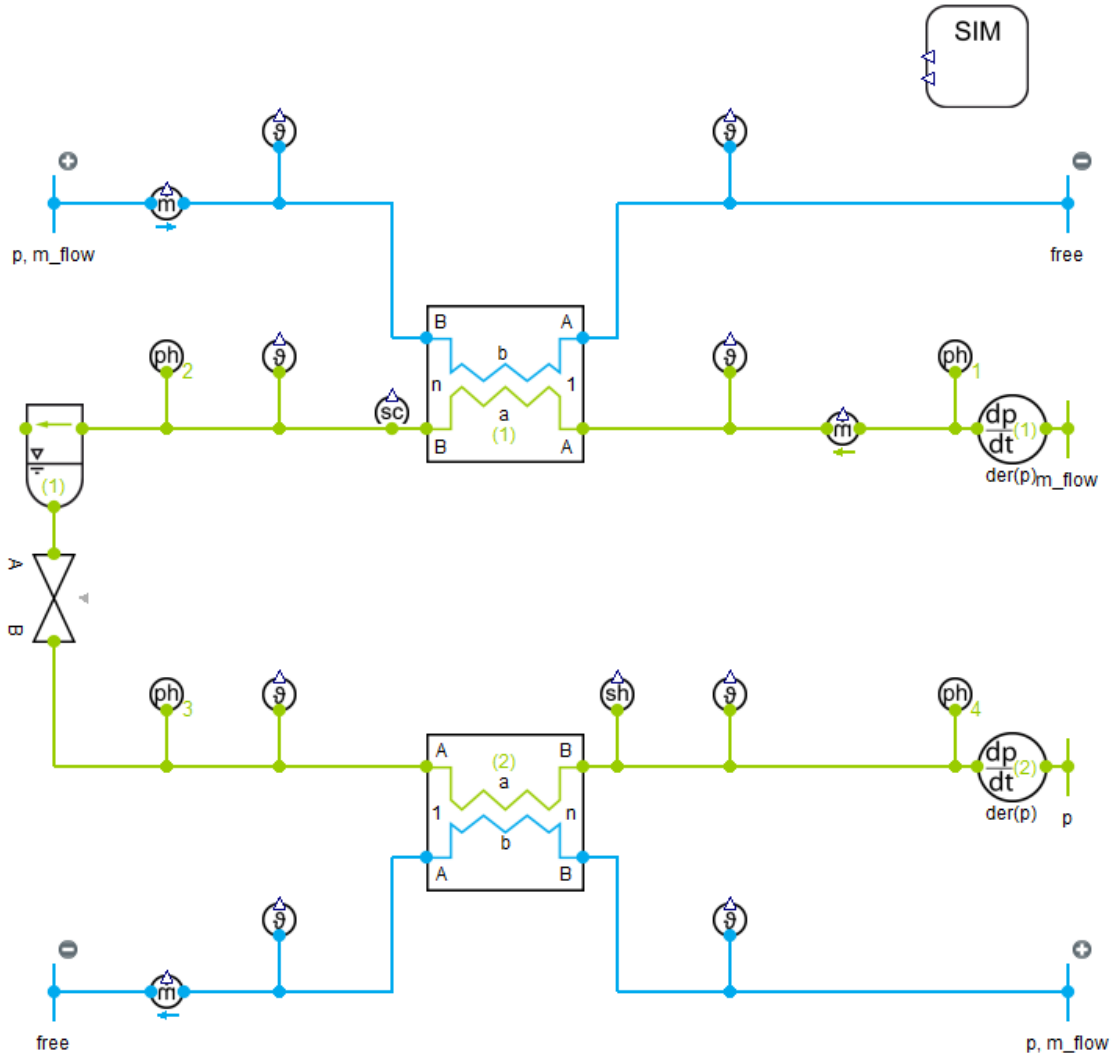

Figure 3.10: *Step 3 of heat pump implementation in Dymola*

The water coming from the ice rink was given, but the return temperature was, for initial simulations, estimated to be 10 K lower. the heat transfer size was first calculated and then the values were adjusted. The size of the evaporator was found with the same approach as for the condenser by theoretical calculations. The rest of the parameters were found by empirical testing.

The fourth step would be adding the compressor, but optimizing this is not part of the scope for this thesis.

3.6 Gray Water

Gray water is the main heat source in this thesis, and will thereby have its own section. It will be evaluated if excess heat from the gray water is enough to cover the heating demand for DHW, with the help of a heat pump.

Every residential building produces gray water, with a water temperature of

around 30 °C. This gray water will be collected into tanks placed into each energy central, which then will utilize the heat within. This means that Tungavegen 1 will need 13 gray water tanks, one for each zone.

Each tank will be large enough to contain 24 hrs of gray water produced for that zone. The sizes of the zones vary greatly which means the amount of produced gray water will as well. However, because the gray water production, as well as the heating demand, is proportional to the number of apartments in a zone, calculating the potential in the reference zone will give a good indication for the potential of the other zones, as well as the size of the different tanks.

3.6.1 Gray Water Implementation

Figure 3.11 shows a possible way to implement the gray water tank into the energy central in order to utilize the excess heat. The dark gray lines represent the flow of the gray water.

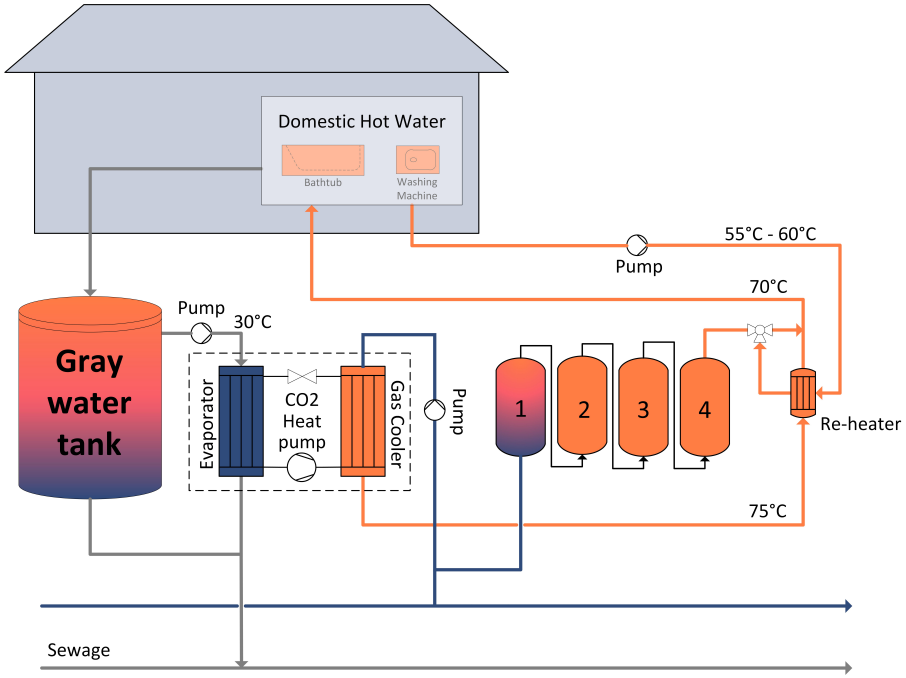

Figure 3.11: *Possible implementation of gray water excess heat utilization*

As shown in the figure, the gray water is first collected in the gray water tank. Then, with the help of a circulation pump, the water enters the evaporator of the heat pump before it is discarded in the sewage. If there is more gray water produced than needed to heat up DHW, the gray water is directly emptied into the sewage.

The heat pump in this process is chosen to be a CO_2 heat pump as shown in the figure. This is because of the high temperature elevation needed in this process. The right heat exchanger was made a gas cooler because the heat pump is working in a transcritical manner.

The DHW starts out as city water, then enters the gas cooler, receives energy until the water reaches a temperature of 75 °C. Further, it goes through the re-heater

heat exchanger. There, the hot water transfers heat to the return water from the building. This to make sure that both water circuits have a temperature of 70 °C.

After the re-heater, the water enters in the TES tanks, or the building. The TES tanks are numbered 1-4 to better understand the water flow. The TES tanks are always full, so whenever DHW is used, tank 1 is refilled with new cold city water. When there is more hot water produced than used, tank 4 is filled. Simultaneously, the water in tank 1 is extracted to circulate in the gas cooler, rather than being discarded.

Finally, the DHW is used in the building before discarded as gray water in the gray water tank. The unused water is ciculated back to the re-heater with a temperature between 55 to 60 °C. There it reaches 70 °C before the loop starts over again.

3.6.2 Energy Evaluation

In order to evaluate whether the gray water holds sufficient energy to heat up the DHW, an estimation of how much gray water B1 produces, is needed. It is assumed that the apartments have an average of two people with normal water usage behaviors living in them. Further, in correspondence with 2.6.3, it is assumed that every person produces 87 L, corresponding to approximately 87 kg, of gray water, with a temperature of 30 °C.

The next step in finding out how much gray water B1 could produce, was to find the total number of apartments. The total GFA of B1 and the average size of each apartment is given by the project holders. To find the number of apartments from this, the total GFA was divided by the average apartment size.

These numbers will be approximate, but will give a good estimate to use in further analysis and calculations.

3.6.3 Space Cooling Integration

Going back to section 3.5.1, it is not very energy efficient to use the outside air as an energy sink for the space cooling process. This would be similar to wasting the heat produced by the ice rink's cooling system, which would not correspond to the goal of making Tungavegen 1 a contribution to the sustainability goals.

Consequently, this thesis will look at the possibility of using the gray water tank as a heat sink when the system is in cooling mode. This is illustrated in figure 3.12. Calculations were done on the tank used for gray water, and the heating transfer capability were calculated. This was done both numerically with the simulation tool COMSOL Multiphysics, and mathematically through calculations and methods presented in section 2.3.

In this figure there are two separate heat pumps. One for the space heating circuit, and one for the space cooling circuit. It was considered to use the same heat pump for both heating and cooling of space. However, this would have required modifications to the heat pump which were too expensive. A cheaper option would be to have two separate heat pumps as shown in 3.12. Further, in this thesis two

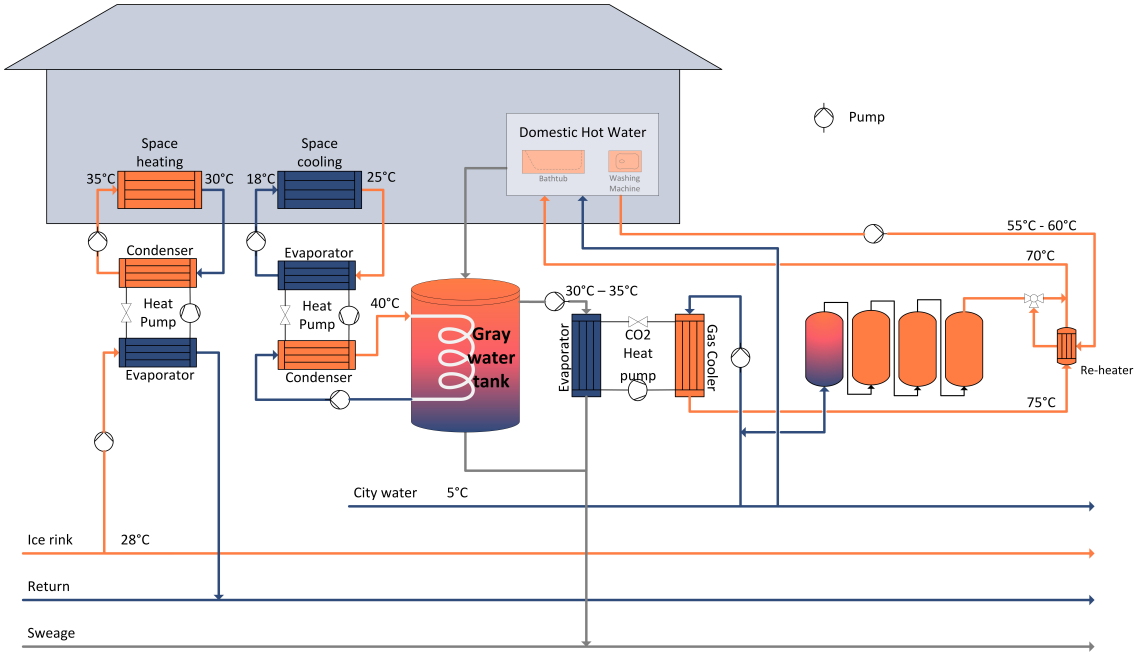

Figure 3.12: *Integration of space cooling with gray water tank as heat sink*

separate heat pumps will be the used option, as this was decided by the project holder.

In the figure, it is shown that the gray water tank is the heat sink for the condenser. This method will be beneficial for the space cooling process and also ensure potential higher temperature in the gray water tank.

In order to find out whether the fusion of gray water and space cooling is a viable investment, an evaluation of the energy transfer from the space cooling circuit to the gray water tank was performed. This was done by simulating the gray water tank in the multiphysics tool COMSOL Multiphysics.

3.6.4 The Gray Water Tank

The gray water tank is a major component of the energy central. In the next section, the gray water tank´s functions will be examined more in depth.

Figure 3.13 shows an illustration of the gray water tank seen from the side, and from above. In this illustration the tank is in a hexagon shape, but other shapes were also evaluated.

The gray water tank system consists of two rooms. One room is the the technical equipment - room A, where all external equipment can be reached. The second room B, is the gray water tank. Both can be accessed by hatches a and b.

The gray water enters the system at inlet 1, then runs through a self cleaning filter c. After being filtered it exits through outlet 2. The self cleaning filter c is able to discard any content not wanted in the gray water tank, disposing it into the sewage. Then the tank fills with gray water. When the heat is needed, the gray water is drawn in at inlet 3 by pump d and circulated in the heat pump. The float e keeps inlet 3 floating right below the water surface making sure that any objects floating in the water top is not drawn into the heat pump at outlet 4. If the tank

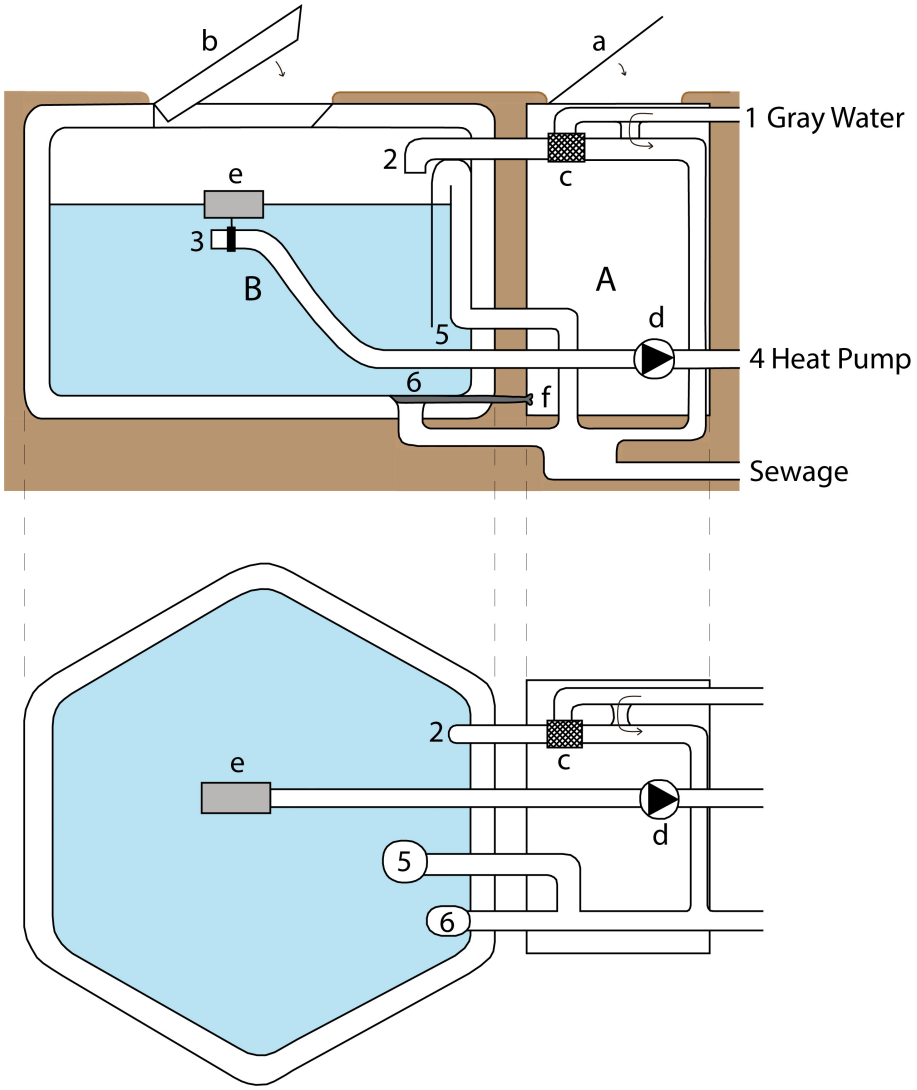

Figure 3.13: *Details of the gray water tank*

gets full, the ground water will enter at inlet 5 and discarded to the sewage. This mechanism makes sure that the colder water which is in the bottom of the tank, is discarded first.

Every once in a while, the tank needs to be cleaned. The process starts by emptying the gray water in the tank by opening hatch f and the water disposes through outlet 6. Then the tank is cleaned by a person entering hatch a performing a thorough wash internally in the tank. When the system is in cleaning mode, the flaps g and h shuts down, directing the gray water directly into the sewage.

The small circles in the walls are the pipes circulating the water coming from the space cooling circuit. The size of the pipes was taken from a product catalog from PipeLife [48]. The chosen pipe size had a diameter of 25 mm and with a wall thickness of 2.3 mm. It was also informed that the pipe has a thermal conductivity of 0.40 W/m K, and a coefficient of expansion of 0.16 mm/m °C.

3.6.5 Model in COMSOL Multiphysics

The gray water tank described in this section was simulated in COMSOL Multiphysics. The size of the tank was set to hold one full day's worth of gray water produced from zone B1.

A step wise approach was used in order to build the tank within the simulation tool. The first step was deciding on the global environment. For this, COMSOL Multiphysics' axis symmetric functionality was used. This enabled a relatively simple geometry while simulating a complete tank in 3D. This method was time efficient and produced simulation results relatively quickly. A downside was that all the geometric elements were circular. Hence, the coil inside the walls was simulated as circular pipes and not connected as a spiraling coil. As this simulation was performed to determine heat flux between the coil and the walls circling the gray water, this simplification was accepted.

Another weakness with the model, is that the gray water was simulated as a body of water with no inlet or outlet flows. Gray water will be produced unevenly over a 24 hours period, while gray water will be consumed at a steady rate over the same time period to produce DHW.

While the simulations start with a complete body of gray water with a temperature of 30 °C, this will never be the actual gray water temperature, other than right after the space cooling is started for the season or the tank is refilled after maintenance. In addition, simulation lengths of more than 12 hours will not represent real conditions, as newly produced gray water at 30 °C regularly is added to the gray water tank, and the hottest gray water at the top of the tank will be drained. Both of these will be lowering the overall average gray water temperature.

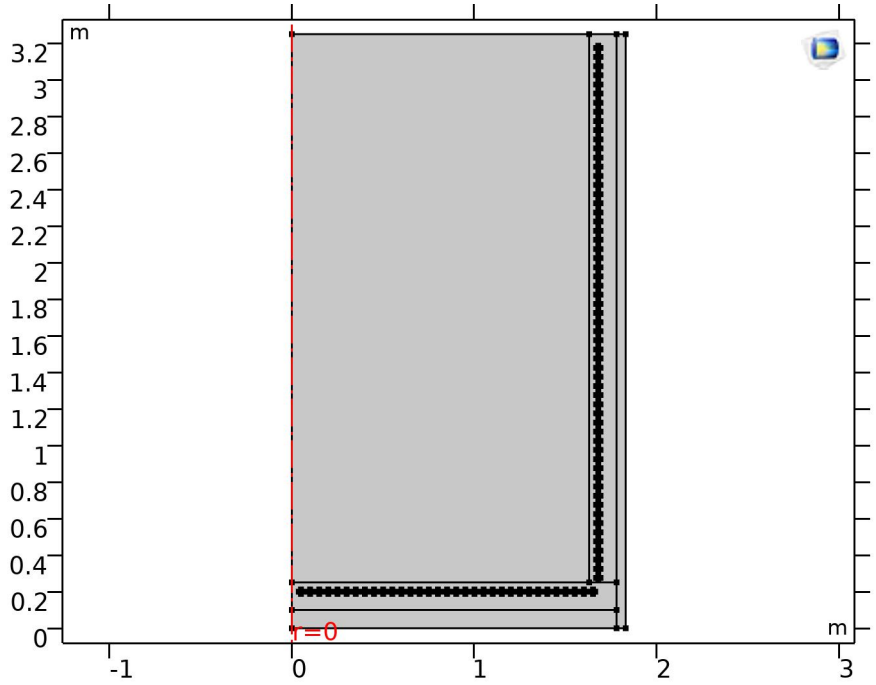

Figure 3.14: *The base case model of the gray water tank in COMSOL Multiphysics*

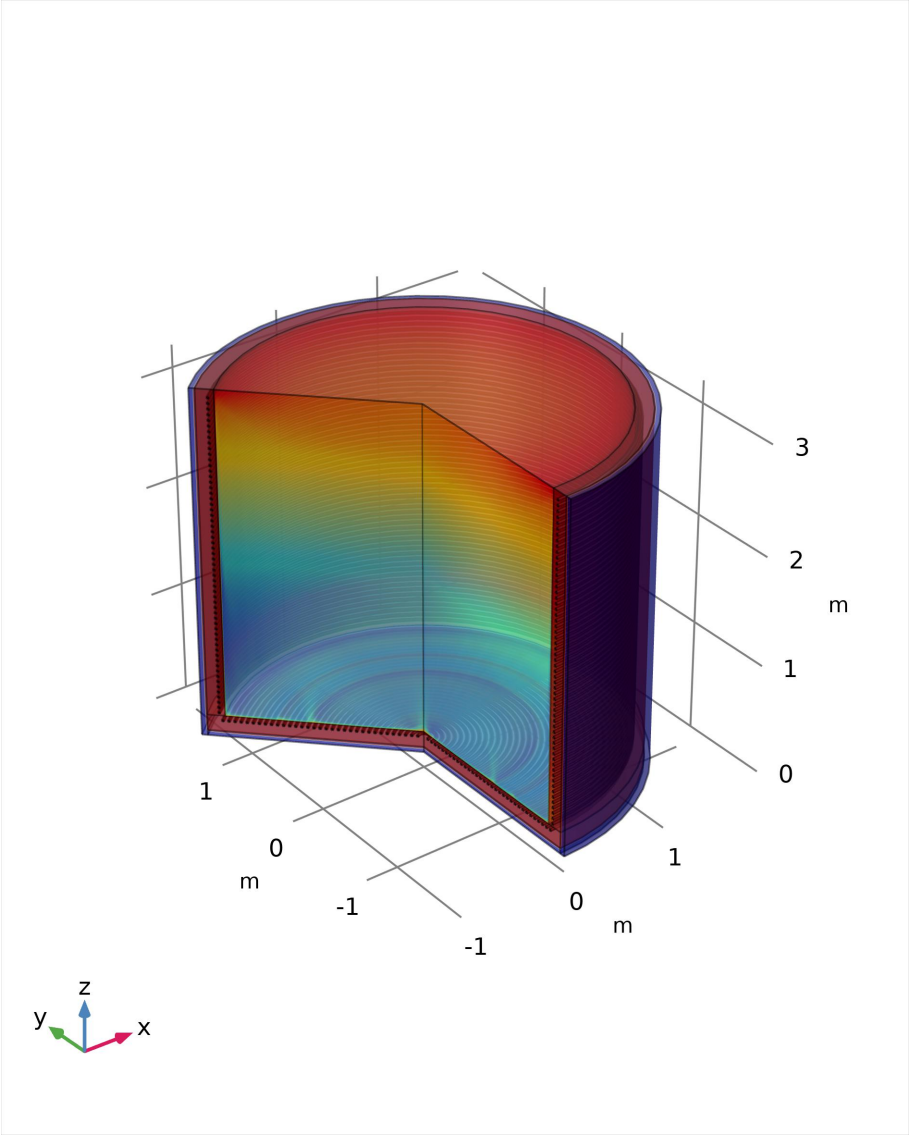

Figure 3.15: *3D representation of the base case model of the gray water tank in COMSOL Multiphysics showing surface temperatures at 270 min into the base case simulation*

In order to minimize the limitations by the lack of in- and outlet flows, the simulations were focused on conditions after the initial 200 min. and up to a period of 720 min., or 12 hours. During these 520 min., the simulations would represent the real conditions as close as possible.

Next it was decided to use heat transfer in fluids, with laminar flow as sub-physics. Laminar flow was added to simulate the flow inside the gray water tank, while heat transfer in fluids was used to simulate the heat flux between the different domains, gray water fluid, solid walls and the surroundings. For the heat transfer in fluids, COMSOL Multiphysics' built in external natural convection heat flux was used for both outer and inner walls and the bottom of the tank. For the pipes, internal forced convection was used.

The third step was to define exact geometry and materials for the simulation. The full sized tank was built with concrete walls and insulation between the tank

and outside gravel. COMSOL Multiphysics' built in materials were used for both Concrete, liquid water, and insulation. Structural steel was used for the steel tank simulation. The pipes simulating the coils with hot water coming from the space cooling system, were integrated into the concrete walls and bottom, 5 cm into the material seen from the inside gray water tank wall. The concrete thickness was set to 15 cm, and 5 cm for the insulation. The distance between the pipes was set to 5 cm both in the wall and in the bottom. The number of pipes were 59 in the wall and 33 in the bottom. All the pipes were included in the simulations, while the heat flux mathematical calculations only considered the 59 wall pipes. The complete model produced by COMSOL Multiphysics, is shown in 3.14, and a 3D representation is shown in 3.15.

The fourth step was to determine the mesh for the finite element method simulation. COMSOL Multiphysics' auto generated mesh was used for this. A number of various mesh properties were adjusted to optimize the simulation for time and accuracy, and several simulations failed to converge and did not yield results. For the base case, the auto generated coarser mesh was used. This caused a finer mesh around smaller physical details and at the boundary between the solid and fluid domains, and a much coarser mesh for the larger body of gray water away from the solid wall and bottom. Figure 3.16 shows both the complete mesh for the base case, and a detailed view of the mesh at the bottom right corner of the 2D model in COMSOL Multiphysics.

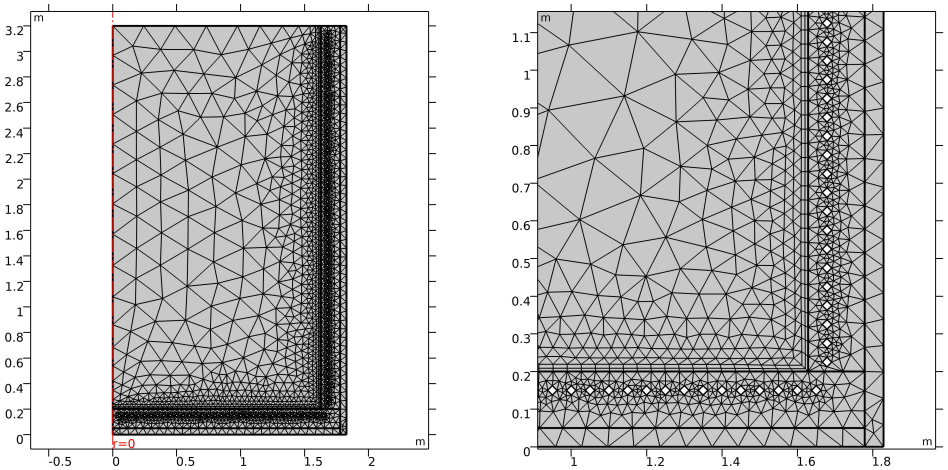

(a) *Whole Mesh* ***(b)*** *Detailed Mesh*

Figure 3.16: *Whole mesh and detailed mesh for the base case*

The final step was to select a study-type. A time-dependent solver for heat transfer and laminar flow was chosen. Multiple simulation lengths were carried out to get an initial understanding of the dynamics of the gray water tank.

In order to simulate close to actual conditions as discussed earlier in this section, 720 minutes was chosen as the simulation run length. Within this 12 hour time period, three time snaps were chosen as focus points. These were 200 min., 360 min., and 720 min. With a 720 min. run length, most simulations took from three to eight hours to complete, with the longest simulation lasting 18 hours. The

simulations were run on a DELL Latitude laptop with an 8 core x64 Intel i7 2760QM 2.4 GHz CPU and 8 GB RAM running 64-bit Microsoft Windows 10 OS [10].

Several simulations were run in order to determine the effectiveness of heat transfer between the pipes and concrete as well as the concrete and gray water. Both pipe diameter, the number of pipes, and wall material was altered in separate simulation runs.

Initial values

COMSOL Multiphysics provides a way to specify initial values for the different domains in the model. For the laminar flow study, initial values for the flow inside the gray water tank were set to zero for all simulations. For the heat transfer in fluids study, the different domains were given different initial temperatures. Initial temperatures used in the different simulations are shown i table 3.4.

Table 3.4: *Initial Values in COMSOL Multiphysics*

Parameter	Value
Initial temperature gray water, Tgw [°C]	30
Initial temperature pipes, $Tpipe$ [°C]	Simulation specific
Initial temperature solid wall, $Tpipe - 2$ [°C]	Tpipe - 2
Initial temperature insulation, $Tgravel$ [°C]	10

3.6.6 Comparisons

Four models with different geometry were simulated in COMSOL Multiphysics and compared. This was to find out which parameters play the biggest roles, and to see how the tank is best built. All simulations with changes were compared to the base case. The base case was built as explained in the previous section. All other simulations had only one changed parameter from this base case.

The second simulation had larger pipes. The larger pipes in the simulation were chosen to align with the next size up from PipeLife product line. This is the pipe with diameter of 32mm and wall thickness of 3mm.

In the third simulation, the pipes in the bottom of the concrete tank were removed, with exception of a few pipes close to the wall. This was to see whether or not the heating from the bottom changed the water flow within the tank, and thereby ruined the natural convection. Figure 3.17 shows the six pipes that were kept in the bottom concrete for the simulation with fewer pipes.

In the final simulation the concrete tank was replaced by steel. This was to see the major change happening with a tank material with higher thermal conductivity.

These cases were compared in three different areas. The first was the water temperature of the gray water. The water temp was measured at 4 different locations and plotted in a graph. Figure 3.18 shows the locations of the four points. The comparisons between simulations were done at the top middle point 2 as this represented the temperature in the body of gray water furthest away from any warmer solid wall, as well as being closest to the gray water outlet.

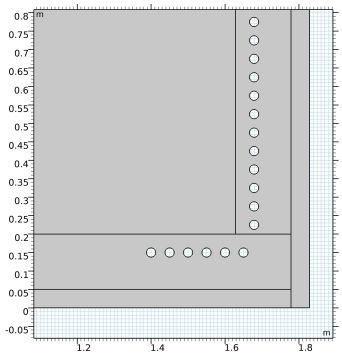

Figure 3.17: *The model gray water tank for the third simulation run with fewer pipes in the bottom concrete in COMSOL Multiphysics*

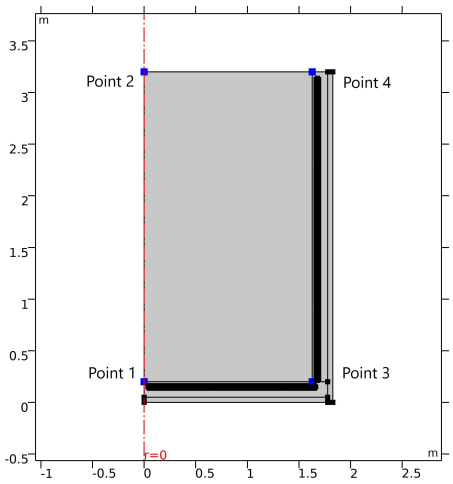

Figure 3.18: *The four points (blue dots) where temperatures were compared in the gray water tank in COMSOL Multiphysics*

The normal total heat flux was also derived from the simulations and compared. Normal total heat flux, Φ [W], is evaluated by COMSOL Multiphysics as the heat transfer rate, φ [W/m^2], over the total area of a boundary, perpendicular to the plane of the boundary. Normal total heat flux from the pipes to the wall, from the wall to the gray water, and from the wall to gravel were acquired and plotted in a graph. In addition, the difference between the first and the two latter was calculated and plotted in the graph as well.

3.19 shows the boundaries that were used for the normal total heat flux values in the simulations.

The third comparison was made on the water flows happening in the tank.

Snapshots from three different time periods, respectively, 200 minutes, 360 minutes and 720 minutes were taken and compared.

Different Coil Temperatures

Different temperatures of the water in the pipes representing the coil was also simulated in COMSOL Multiphysics. The temperatures tested were respectively 10 K, 20 K, and 30 K higher than the temperature for the base case. No other adjustments

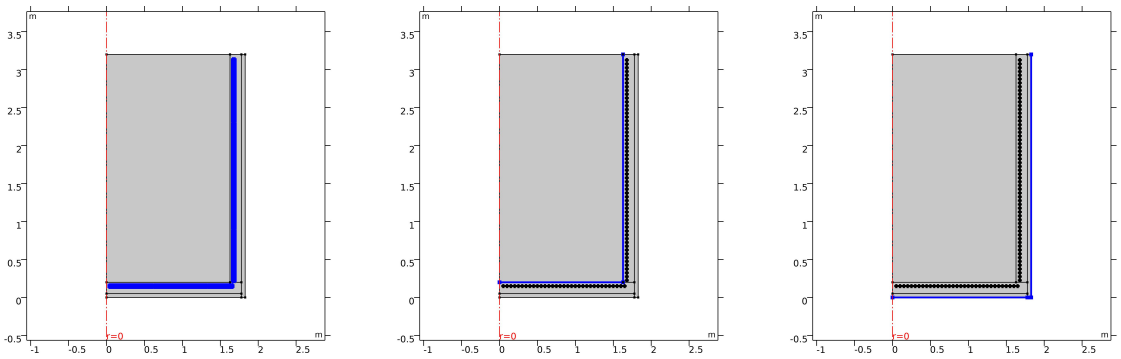

(a) Heat Flux Pipes *(b) Heat Flux Gray Water* *(c) Heat Flux Gravel*

Figure 3.19: *The three different boundaries (blue) examined for Normal total heat flux from the COMSOL Multiphysics simulations*

were made. This comparison was to see how much impact it would have to design a heat pump with a higher condensation temperature. Temperatures at the top middle point (Point 2) was once again used to compare the temperature development over time in the base case to the three other simulations. Normal total heat flux between the three boundaries, pipes, concrete wall and outside gravel as shown in 3.19 were compared for the three simulations.

Table 3.5: *Variable parameters in the COMSOL Multiphysics simulations that were different from Base Case*

Simulation	Variable	Base Case Value	Simulation Value
Larger Pipes Case	Pipe Diameter, D_{pipe} [m]	0.025	0.032
Fewer Pipes Case	Number of bottom pipes	33	6
Steel Tank Case	Tank material	Concrete	Steel
50 °C Case	T_{pipe} [°C]	40	50
60 °C Case	T_{pipe} [°C]	40	60
70 °C Case	T_{pipe} [°C]	40	70

Table 3.5 gives an overview of the variables that were changed between the various simulations.

3.6.7 Pressure Drop Calculations

It is of importance to determine the pressure drop within the pipes in the tank walls. This is needed to regulate the correct circulation pump pressure, and also to avoid too high pressures.

The heating capacity of the condenser for the space cooling circuit was found with SIMIEN. Further, an assumption was made that the water circuit gets a 10 K temperature rise in the condenser, regardless of the condensing temperature. With

this information, and given the pipe parameters, the mass flow and velocity of the water was calculated.

The dynamic viscosity was found using a temperature in accordance to the base case introduced earlier in this section. The rest of the calculations were performed based on the equations from section 2.4.

It was further tested if more parallel coils in the tank would provide a lower pressure drop. The numbers of parallel coils tested were one, two, three, and four.

Finally, the pressure drop in different bends were evaluated, and pressure drop were calculated for different geometric forms. The forms tested were circular, quadratic, hexagon, and octagon.

The pressure drop was then used to find out how much circulation pump power was needed in each case.

3.7 Cost Analysis

To evaluate which system would be most cost effective, and if the energy methods presented in this thesis are competitive, a cost evaluation was performed. The calculations were done for reference zone B1, and were based on it's energy profile produced in this thesis.

3.7.1 Cost for Different Heat Sources

For space heating the following was looked at:

- Using electricity for space heating as sole energy resource
- Using the local district heating system for space heating
- Using excess heat from Leangen Ice Rink together with a heat pump for space heating

To calculate cost, spot prices were found in Nord Pools price statistics for the Trondheim area [9]. The prices vary greatly through the years, so an average for the past 16 years was used. The prices are shown in table 3.6, and prices are given in NOK/MWh.

Further, the grid rent was calculated using the variable price per MWh used. The fixed yearly price was not taken into account in the calculations, as this would be included for everyone as all are connected to the electricity grid. Prices for network rent was based on input from nve.no and Trønderenergi, fall 2020.

To find prices to use the local district heating system, prices from Statkraft Fjernvarme for the Trondheim region, per September 1st 2020 was used. [57]

Taking the cost of electricity, reduced by cost of using a heat pump for the excess heat from the ice rink gave the cost reduction for space heating. Same was done for cost of the local district heating system, reduced by cost of using heat pump for the excess heat from the ice rink.

The cost from the local district heating system and electricity did not vary significantly, hence, calculations for electricity was used. [61]

For heating of DHW the following options were looked at:

Table 3.6: *Historic Spot Prices Trondheim*

Year	Price per year	Unit
2019	379.56	[NOK/MWh]
2018	423.44	[NOK/MWh]
2017	275.40	[NOK/MWh]
2016	266.01	[NOK/MWh]
2015	189.80	[NOK/MWh]
2014	263.57	[NOK/MWh]
2013	303.43	[NOK/MWh]
2012	235.66	[NOK/MWh]
2011	370.63	[NOK/MWh]
2010	465.44	[NOK/MWh]
2009	310.97	[NOK/MWh]
2008	421.26	[NOK/MWh]
2007	236.79	[NOK/MWh]
2006	394.64	[NOK/MWh]
2005	235.30	[NOK/MWh]
2004	243.75	[NOK/MWh]
Average 16 years	313.48	

- Using only electricity for heating of DHW
- Using a heat pump with gray water as the heat source to heat DHW

Energy demand for DHW and space heating for the reference zone B1 was simulated in SIMIEN and the results were used for the calculations.

3.7.2 Cost of Investment

To find out how long it would take to make an investment of a system for a central heat pump and gray water for zone B1 positive, a set of investment cost estimates for the system was set from 10 MNOK to 2 MNOK. The intervals was set to 2 MNOK to do the calculation. The analysis was simplified to make an indication of how big an investment could be, as this thesis is not evaluating cost of systems. To simplify, only variable cost for electricity were taken into account. The financial investment cost was not taken into the consideration, thus the interest was set to zero.

As an alternative to find today's value of future savings, the Net Present Value model was used. Life expectancy was set to 10, 20 and 30 years to see the different impact of the NPV. The discounted interest rate was set to 2, 5 and 10 percent.

Chapter 4

Results

In this chapter, the results from all the simulations done in this thesis will be presented and commented. This includes results from SIMIEN, COMSOL Multiphysics, Dymola and Coolpack, as well as the calculations made. These results will reflect upon the energy potential of Tungavegen 1, in addition to the opportunities the various methods bring. The utilization of gray water and the ice rink water as heat sources will also be explored in this chapter, and the different methods of doing it will be evaluated. Results from the integration of the ice rink circuit in the gray water tank will also presented. The last part of this chapter will finalize the cost analysis.

4.1 Energy Demand for Reference Zone

In order to evaluate the potential of the building area at Tungavegen 1, the SIMIEN simulation of the reference zone explained in section 3.3.1 must be inspected. This section will therefore present the results from this simulation in SIMIEN. Both in terms of the energy profile, and the thermal conditions experienced by it's users, which are both readable in SIMIEN.

4.1.1 General Energy Demand

In order to evaluate the energy demand of Tungavegen 1, the reference zone B1, is simulated in SIMIEN. The function for simulating a whole year is used. In this particular thesis, the heating demand for space heating and cooling, and heating of DHW is of most interest. The results of these particular factors are shown in table 4.1, both the specific demand, and the total demand throughout the year. In addition peak demand is derived from the input in the simulations, and shown in the table.

The peak demand for space heating is 332 kW. From SIMIEN, it is also shown that a heat pump with a capacity of 140 kW is able to cover 90 % of the total energy demand of 313 MWh. The heat pump for the space heating will therefore be dimensioned to cover a peak of 140 kW. For space cooling, a heat pump with a cooling capacity of 112 kW will cover a similar share of the energy demand.

Table 4.1: *Results from SIMIEN simulation*

	Specific demand [kWh/m^2]	Energy demand [MWh]	Peak demand [kW]
Space heating	29.5	313	332
DHW	30.0	317	-
Space cooling	10.6	112	231

The energy profile given by SINTEF, is as shown in table 4.2. In the table, only heating demands are listed, and it does not include space cooling demands.

Table 4.2: *Energy demand for the reference zone, B1, from SINTEF*

	Specific demand [kWh/m^2]	Energy demand [MWh]	Peak demand [kW]
Space heating	31.8	337	209
DHW	30.0	318	54
Total heating demand	61.8	649	250

For an easy overview, table 4.3 is made to compare the specific heating demands for the three sources of the values. The similarities presented in this table will be discussed in the next chapter.

Table 4.3: *Specific energy demand from different sources compared*

	TEK17 [kWh/m^2]	SIMIEN [kWh/m^2]	SINTEF [kWh/m^2]
Space heating	30.0	29.5	31.8
DHW	29.8	30.0	30.0
Space cooling	-	10.6	-

Figure 4.1 shows the distribution of energy demand within the building. The total annual energy demand calculated in this simulation is 1114 MWh, which corresponds to a specific heating demand of 105.2 kWh/m^2. From the pie chart, it is shown that space heating and DHW covers a share of 28 % each.

Figure 4.2 shows a more detailed profile of the energy demand throughout the year. As shown in the figure, the energy demand for space heating varies greatly, with the highest demands in January and December, and no demand during the summer months. The opposite is true for space cooling, which is highest during the summer months, and turned off during the winter.

The loads of DHW, fans, lighting and technical equipment are the same every month throughout the year.

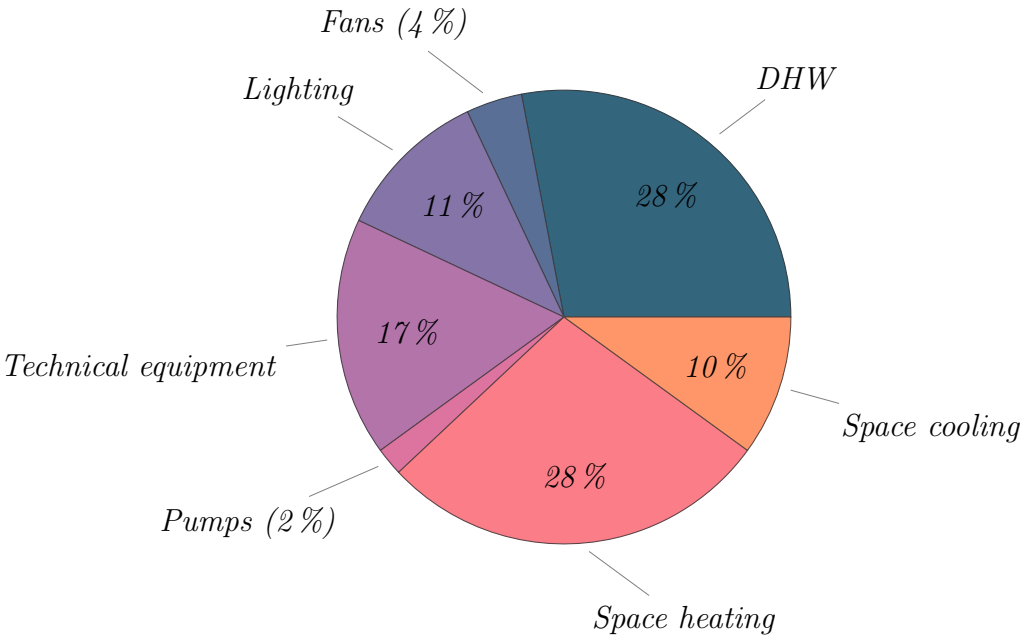

Figure 4.1: *The energy demand of zone B1, as calculated by SIMIEN*

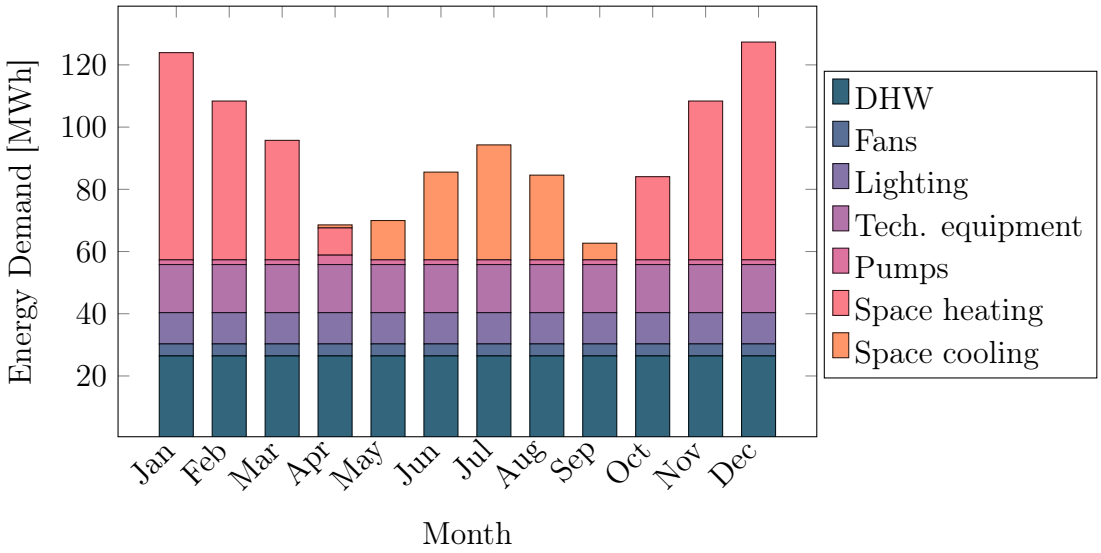

Figure 4.2: *Monthly energy use for the different factors at zone B1*

4.1.2 Energy Balance

The heating demands presented in the previous section are widely dependent on the thermal losses in the building. In figure 4.3, these heat losses for the reference zone are presented as fractions of the total amount of the thermal transmittance in the building, which SIMIEN shows to be 0.64 $\mathrm{W/m^2K}$. The majority of thermal losses are through transmission losses, and losses related to external surfaces and thermal bridges. All transmission losses equals to a 63 % share of the total heating losses.

For the SIMIEN model, there are three different sources for delivering and providing energy. These are electricity, district heating and heat pumps, as represented

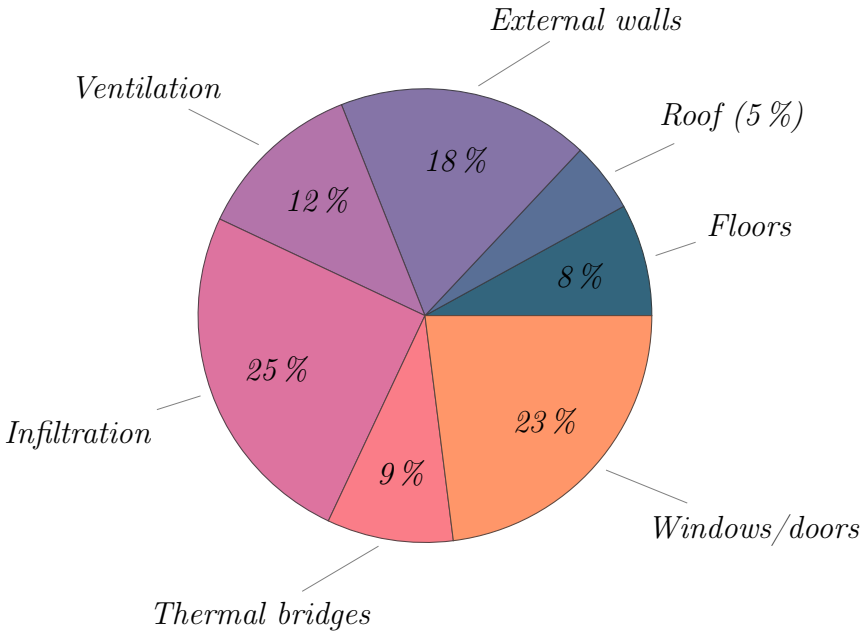

Figure 4.3: *The distribution of heat losses in zone B1 simulated in SIMIEN*

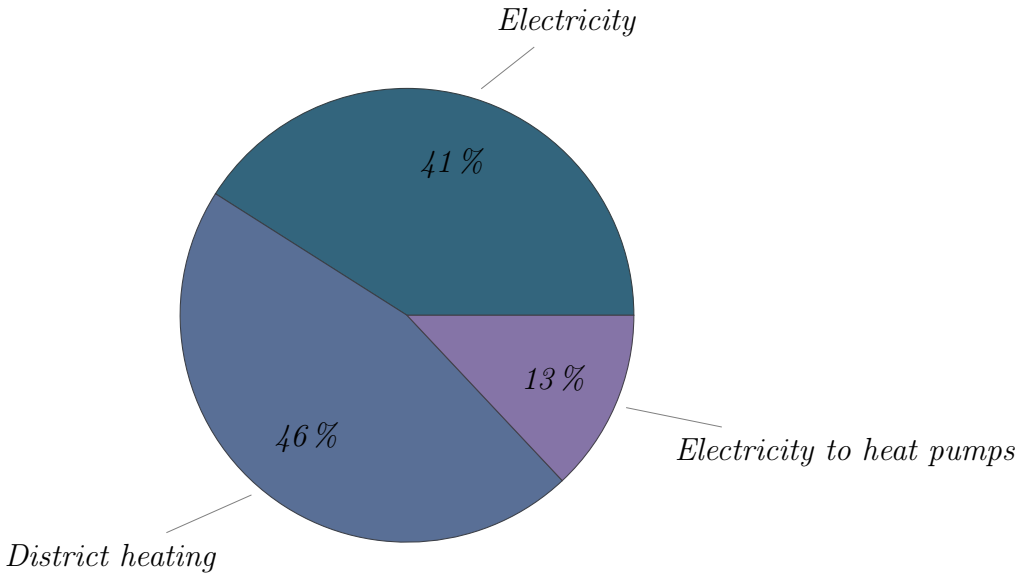

Figure 4.4: *Energy delivered to B1, as calculated by SIMIEN*

in figure 4.4. This chart shows the energy delivered to the building, but does not reflect the actual energy used.

The total delivered energy to the building, is 916 MWh, corresponding to a specific energy delivery of 86.5 kWh/m^2. The difference between used and delivered energy is calculated in equation 4.1.

$$\Delta Q = Q_{used} - Q_{delivered} = 1114 - 916 = 198 \qquad [\text{MWh}] \quad (4.1)$$

This means that the heat pump provides an additional 198 MWh to the delivered energy to zone B1. From SIMIEN, it is simulated a total work demand for the heat pump of 122 kW, which is 13 % of the total energy need as shown in figure 4.4. From equation 4.2, the COP is calculated to be 2.6.

$$COP = \frac{Q_C}{W} = \frac{Q_E + W}{W} = \frac{198 + 122}{122} = 2.6 \qquad [-] \quad (4.2)$$

4.1.3 Indoor Environment

Figure 4.5 shows the maximum, minimum and average operative temperatures occurring in the apartments for zone B1 every month throughout the year. The figure shows that the temperature never exceeds about 23 °C, nor falls lower than 19 °C

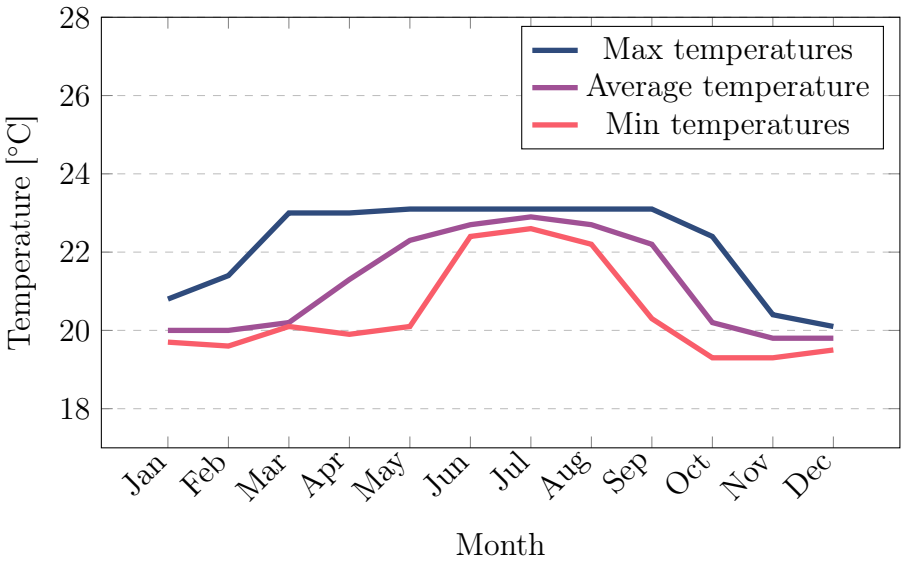

Figure 4.5: *Indoor operative temperatures through the year in the apartment buildings*

During months with space heating, the average temperatures are mostly kept below 22 °C, which is in correspondence with the recommendation from TEK17 presented in section 2.5.3. The maximum temperatures, however, are above 22 °C through the months of March to October.

From the summer and winter simulations in SIMIEN, the PPD and PMV values resulting from the temperatures presented in figure 4.5 can be found. During winter time, PPD and PMV values varies around 30 % and -1 respectively. The summer simulation shows a better result, where the PPD and PMV varies around 5 % and 0 respectively.

4.2 Heat Sources

This section will go through the possible amounts of energy that can be taken from the heat sources discussed earlier. The two main sources of energy is the water circuit from the ice rink, and the gray water produced. In addition, it was looked at how much potential solar power has for Tungaveien 1. The gray water tank, and the potential of integrating it with the space cooling process, will have it's own section, but calculations of how much potential the gray water holds will be showed here.

4.2.1 Ice Rink

Getting a solution where the ice rink is the heat source for Tungaveien 1 to work, would mean cooperating with the ice rink and making a more complex solution where a distribution system within the building area and the ice rink is integrated.

Figure 4.6 shows the produced energy from the ice rink in 2018 and in 2019, compared to the needed space heating in zone B1 gotten from SIMIEN. The produced energy is much higher than the needed energy. However, the heated water from the ice rink is going to be distributed in the whole area of Tungaveien 1, so the needed energy for the whole are will be bigger.

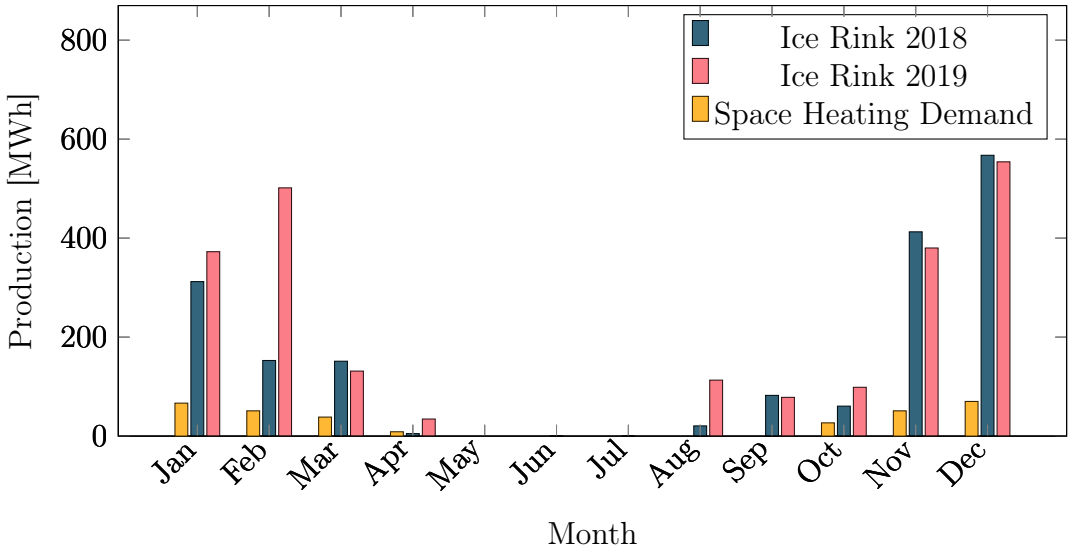

Figure 4.6: *Measured excess energy from ice rink in 2018 and 2019 in comparison with the monthly space heating demand*

The heat pump will have a size of 140 kW. With a heat pump with a COP of 3.2, an energy need per month for space heating of Q_{SH} [MWh], the needed energy from the ice rink every month can be calculated by equation 4.3.

$$Q = Q_{SH} - \frac{Q_{SH}}{3.2} \quad \text{[MWh]} \quad (4.3)$$

Table 4.4 shows the available energy from the ice rink, the energy demand for space heating, the needed amount of energy in compressor for a heat pump with a COP of 3.2, and how much energy is needed from the heat source to cover the

Table 4.4: *Annual energy demand for space heating*

	Available heat [MWh]	Demand [MWh]	Compressor [MWh]	Heat source [MWh]	Share [%]
January	373	67	21	46	12
February	502	51	16	35	9
March	131	38	12	26	20
April	34	8.8	2.8	6	18
May	0	0	0	0	0
June	0	0	0	0	0
July	0	0	0	0	0
August	113	0	0	0	0
September	78	0	0	0	0
October	99	27	8.4	18.6	19
November	380	51	16	35	9
December	554	70	22	48	9
Total	2264	313	98	215	-

demand. Finally, the far right column, shows how big of a share of the energy from the ice rink water is needed in zone B1. This value stays between 9 % to 20 % throughout all of the months.

4.2.2 Gray Water

There are 10 600 m^2 of GFA for residential space in zone B1. The average size of each apartment is 70 m^2, giving about 151 apartments in total. Each apartment has an average of two people living in them, and each person produces 87 kg of gray water. This makes a total of 26 274 kg.

If assuming the gray water will decrease with 10 K, and the specific heat capacity for water is 4.18 kJ/kg K, the total amount of heat possible to extract from the gray water is shown in equation 4.4.

$$Q = 26\,274 \cdot 4.18 \cdot 10 = 1\,098\,000 \qquad [\text{kJ}] \quad (4.4)$$

It is wanted to get the amount this amount in kWh.

$$Q = \frac{1\,098\,000}{3600} = 305 \qquad [\text{kWh}] \quad (4.5)$$

Hence, 305 kWh is the amount of gray water produced for zone B1 during one day. In order to get an indication for how efficient the method of using gray water is, it is of interest to know the amount produced during each month on average, and one year. The gray water production is constant throughout the year. Equation 4.6

show that during one year, zone B1 is able to produce 111 MWh.

$$Q = 305 \cdot 365 = 111\,325 \qquad \text{[kWh]} \quad (4.6)$$

On average every month, this is becomes 9.28 MWh, as shown in equation 4.7.

$$Q = \frac{111}{12} = 9.28 \qquad \text{[MWh]} \quad (4.7)$$

The energy demand for DHW of every month is found to be 26.44 MWh in SIMIEN. Figure 4.7 shows the above calculations performed on systems where the temperate of the water in the evaporator decreases with 10 K, 15 K, 20 K, and 25 K, respectively.

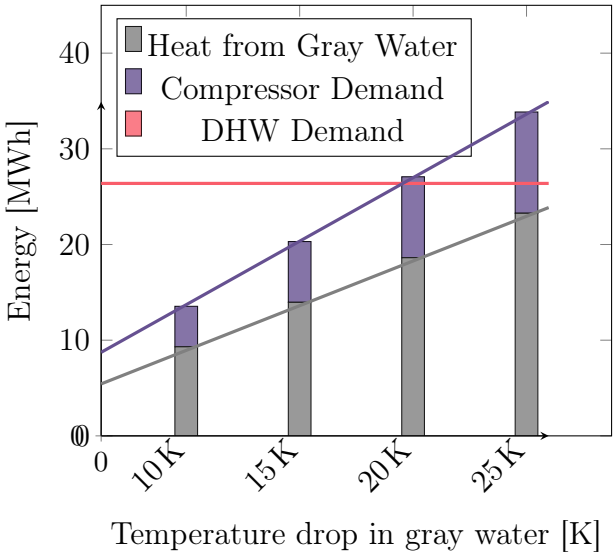

Figure 4.7: *Monthly energy available from gray water with a heat pump compared to the DHW demand*

From the graph, it can be found that with a temperature difference of 19.58 K, the energy demand of 26.44 MWh will be covered, with a heat pump with a COP of 3.2. The energy taken from the heat source is then 18.18 MWh, and the needed energy in the compressor is 8.26 MWh.

4.2.3 Solar Radiation

Solar radiation can be used to supplement the previous methods of providing heat for Tungavegen 1. Figure 4.8 shows the potential in solar radiation generated from the Photovoltaic Geographical Information System, as explained in section 3.4.5.

The graph shows the average amount of solar radiation at the Leangen Area through the specific months during the years 2009 to 2016. There is not much to gather during the dark winter times, but in the summer every m^2 of solar panel could potentially provide between 100 to 200 kWh.

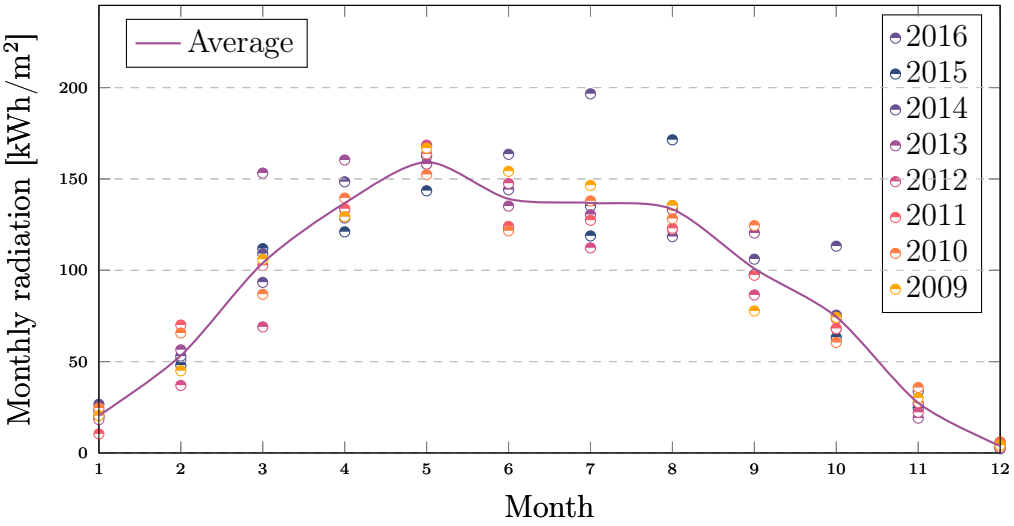

Figure 4.8: *Solar radiation through 2009 to 2016 at Leangen*

4.3 Ammonia Heat Pump

This section presents the results from the simulations done for the ammonia heat pump used for the space heating circuit. First, the results from CoolPack will be presented, both the input values, and the values simulated. These values were used as initial values in the Dymola model, which is also presented in this section. Two models will be presented, one based on the optimal COP, and the other on the optimal superheat in the evaporator. Finally, ph-diagrams produced in DaVE for the two Dymola simulations is presented.

4.3.1 Model in CoolPack

The input values used in CoolPack for the ammonia pump, are shown in table 4.5. The heating capacity of 140 kW was taken from the energy evaluations, where is was found that a heat pump with a heating capacity of this value would be sufficient to cover 99 % of the space heating command. The isentropic efficiency was chosen as a standard for compressors. The evaporation and condensing temperatures were found through iterations.

Table 4.5: *Data input in CoolPack*

Parameter	Value
Evaporation temperature, T_E [°C]	40
Condensation temperature, T_C [°C]	15
Heating capacity, $\dot{Q}_C$ [kW]	140
Isentropic efficiency, η_{is} [–]	0.75

The most important outputs from CoolPack are shown in table 4.6. The evaporation temperature was found to be 124.3 kW, which represents how much energy

will be needed from the heat source. The work performed by the compressor on the heat pump process was found to be 16.91 kW, including losses. The mass flow was simulated to be 0.1122 kg/s.

Table 4.6: *Data output from CoolPack*

Parameter	Value
Evaporator transfer rate, $\dot{Q}_E$ [kW]	124.3
Work performed by compressor, $\dot{W}$ [kW]	16.91
Mass flow, $\dot{m}$ [kg/s]	0.1122
COP [–]	7.348
Evaporation pressure, P_E [bar]	7.31
Condensation pressure, P_C [bar]	15.59
Temperature point 3, T [°C]	87
Temperature point 2, T [°C]	38

Two other values worth mentioning from the CoolPack simulation, is that the temperature on the inlet of the condenser, in point 3, was 87 °C. The temperature at the outlet of the condenser, in point 2, was 38 °C. The condensing temperature was 40 °C, which means point 2 is inside the liquid phase region, and not the two-phase region.

These three values were later used to build the heat pump in Dymola. CoolPack also calculated the COP to be 7.348. This was not directly used in Dymola, but used as a reference.

4.3.2 Heat Exchanger Calculations

The calculations in this section, are based on the theory and equations presented in section 2.3.6. They are made in order to find out how much heat transfer area each of the heat exchangers must have, in order to provide enough energy to the space heating circuit. The input values were based on the findings from CoolPack, and were used as a base for how the Dymola model would look.

Condenser

The first step in determining the size of the condenser, was calculating the T_{lm}. The water in the space heating circuit will decrease with 5 K, so the inlet and outlet temperatures of the condenser was 30 °C and 35 °C, respectively. With CoolPack the condensing temperature was estimated to be 40 °C, and further try and fail with Dymola, found the temperature drop of the ammonia through the condenser to be 65 °C to 35 °C. T_{lm} was then found to be 13.95 K using equation 4.10, with the help of equations 4.8 and 4.9.

$$\Delta T_1 = T_{hi} - T_{co} = 65 - 35 = 30 \qquad \text{[K]} \quad (4.8)$$

$$\Delta T_2 = T_{ho} - T_{ci} = 35 - 30 = 5 \qquad [\mathrm{K}] \quad (4.9)$$

$$\Delta T_{lm} = \frac{\Delta T_1 - \Delta T_2}{\ln \Delta T_1 / \Delta T_2} = \frac{30 - 5}{\ln (30/5)} = 13.95 \qquad [\mathrm{K}] \quad (4.10)$$

Further, the U-value was then evaluated to be $490\,\mathrm{W/m^2\,K}$ from equation 4.11. Standard values within Dymola for U-values, thicknesses, and thermal conductivity were used.

$$\begin{aligned} U &= \frac{1}{\frac{1}{U_{water}} + \frac{d_{steel}}{k_{steel}} + \frac{1}{U_{ammonia}}} \\ &= \frac{1}{\frac{1}{1000} + \frac{0.00075}{20} + \frac{1}{1000}} = 490 \end{aligned} \qquad [\mathrm{W/m^2\,K}] \quad (4.11)$$

Finally, since the condenser is going to deliver 140 kW, the heat transfer area of the condenser must be $20.5\,\mathrm{m^2}$, as found with equation 4.12.

$$A = \frac{\dot{Q}}{U \cdot \Delta T_{lm}} = \frac{140}{0.490 \cdot 13.95} = 20.5 \qquad [\mathrm{m^2}] \quad (4.12)$$

Through iterations, the heat exchanger for the condensing unit was adjusted until the heat transfer area was exactly $20.5\,\mathrm{m^2}$.

Evaporator

The same approach was used for the evaporator in order to find the heat transfer area. The water coming from the ice rink has a temperature of 28 °C. The evaporation temperature was found from CoolPack to be 15 °C. The temperature of the ammonia will receive a 5 K higher temperature. T_{lm} was found using equation 4.15 to be 7.21 K.

$$\Delta T_1 = T_{hi} - T_{co} = 28 - 18 = 10 \qquad [\mathrm{K}] \quad (4.13)$$

$$\Delta T_2 = T_{ho} - T_{ci} = 20 - 15 = 5 \qquad [\mathrm{K}] \quad (4.14)$$

$$\Delta T_{lm} = \frac{\Delta T_1 - \Delta T_2}{\ln \Delta T_1 / \Delta T_2} = \frac{10 - 5}{\ln (10/5)} = 7.21 \qquad [\mathrm{K}] \quad (4.15)$$

The U-value can be evaluated from equation 4.16, which is introduced in equation 2.6 from section 2.1.4.

$$\begin{aligned} U &= \frac{1}{\frac{1}{h_{water}} + \frac{d_{steel}}{k_{steel}} + \frac{1}{h_{ammonia}}} \\ &= \frac{1}{\frac{1}{1000} + \frac{0.00075}{20} + \frac{1}{1000}} = 490 \end{aligned} \qquad [\mathrm{W/m^2K}] \quad (4.16)$$

Since the condenser is going to deliver 140 kW and the COP is estimated to be 3.2, the evaporator will need a heat transfer rate of 96 kW, as shown in equation 4.17.

$$\dot{Q}_E = \frac{COP - 1}{COP} \cdot \dot{Q}_C = \frac{3.2 - 1}{3.2} \cdot 140 = 96 \qquad [\text{kW}] \quad (4.17)$$

The heat transfer area of the evaporator must be 27.2 m^2, as shown in equation 4.18.

$$A = \frac{\dot{Q}_E}{U \cdot \Delta T_{lm}} = \frac{96}{0.490 \cdot 7.21} = 27.2 \qquad [\text{m}^2] \quad (4.18)$$

Mass Flows

The c_p of ammonia varies greatly with the pressure and temperature levels, which makes it difficult to calculate the mass flow. The mass flow rate for ammonia was therefore found with CoolPack to be 0.1122 kg/m, and with try and fail in Dymola finalized to be 0.122 kg/s.

The mass flow for the two water circuits is easier to calculate because the temperature differences are quite small, and the c_p does not change too much. The condenser is going to deliver 140 kW to the water circuit, which will receive 5 K. Equation 4.19 shows that the mass flow must be 6.699 kg/s in order to achieve this heat transfer.

$$\Delta m = \frac{\dot{Q}_C}{c_p \cdot \Delta T} = \frac{140}{4.18 \cdot 5} = 6.699 \qquad [\text{kg/s}] \quad (4.19)$$

The evaporator will provide 96 kW to the ammonia circuit, assuming the same COP as from the energy evaluations. The water coming from the ice rink is 28 °C. Assuming the return temperature will be around 18 °C, the mass flow of the water should be

$$\Delta m = \frac{\dot{Q}_C}{c_p \cdot \Delta T} = \frac{96}{4.18 \cdot 10} = 2.297 \qquad [\text{kg/s}] \quad (4.20)$$

4.3.3 Model in Dymola

There are two figures, figure 4.9 and 4.10, presented in this section from the Dymola simulation of the ammonia heat pump. One shows the results of the heat pump with the calculated values, and the other with slightly adjusted variables. Both illustrations show the whole heat pump, but without the compressor or controlling system.

The space heating circuit has a mass flow of 6.699 kg/s, and gets a temperature lift from 30 °C to 35 °C. This is the case for both scenarios, and corresponds to a $\dot{Q}_C$ power amount of 140 kW. From the figures, it can be read that the condensation pressure is 15.81 bar, and the evaporation pressure is 7.29 bar.

Figure 4.9 shows what the ammonia heat pump looks like after the final simulation with the calculated values. $\dot{Q}_E$ is 96 kW for this simulation, and as seen, this is

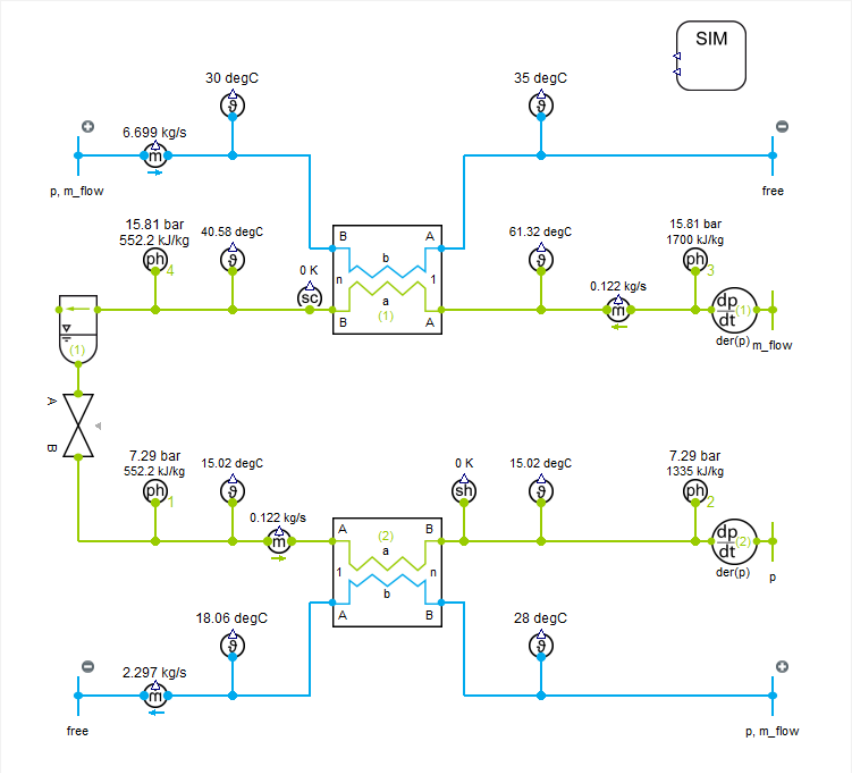

Figure 4.9: *Final result of the ammonia heat pump in Dymola with a $\dot{Q}_E$ of 96 kW*

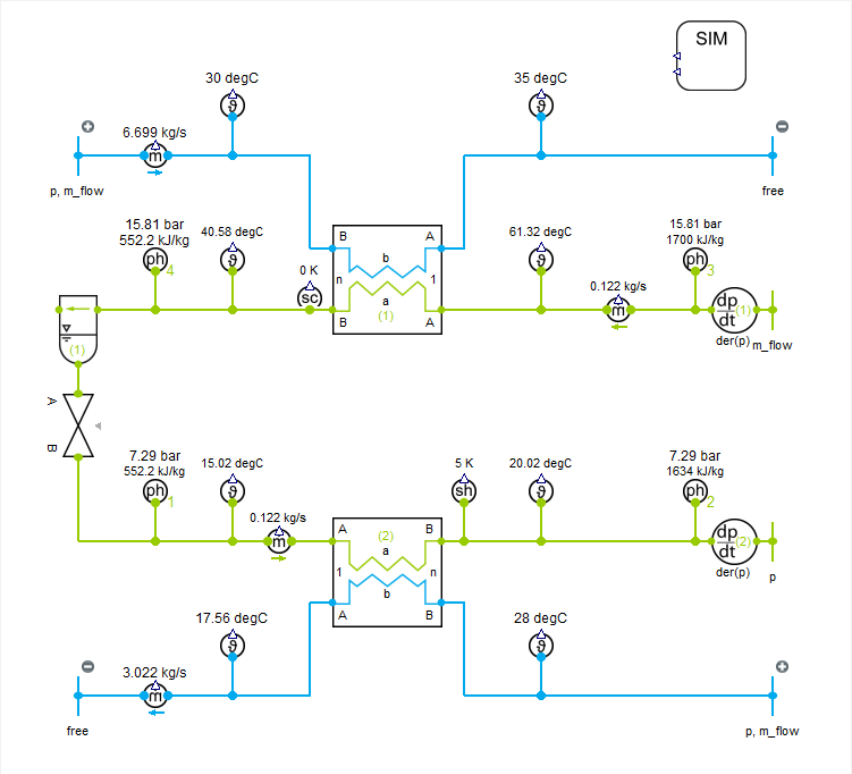

Figure 4.10: *Final result of the ammonia heat pump in Dymola with a $\dot{Q}_E$ of 132 kW*

not enough to get a ΔT_{SH}, or superheat, of 5 K. The work performed on the system in this scenario is 44 kW, corresponding to a COP of 3.18, as shown in equation 4.21 and 4.22.

$$\dot{W} = \dot{Q}_C - \dot{Q}_E = 140 - 96 = 44 \quad [\text{kW}] \quad (4.21)$$

$$COP = \frac{\dot{Q}_C}{\dot{W}} = \frac{140}{44} = 3.18 \quad [-] \quad (4.22)$$

Figure 4.10 shows a representation of the ammonia heat pump where ammonia at the outlet of the evaporator has reached a temperature of 5 K above the saturation temperature for evaporation. To reach this, the heat source circuit has a mass flow of 3.022 kg/s, and reduces the temperature of the water from 28 °C to 18.04 °C. This corresponds to an power amount of 132 kW.

$$\dot{W} = \dot{Q}_C - \dot{Q}_E = 140 - 132 = 8 \quad [\text{kW}] \quad (4.23)$$

$$COP = \frac{\dot{Q}_C}{\dot{W}} = \frac{140}{8} = 17.5 \quad [-] \quad (4.24)$$

The work performed by the compressor in this scenario is 8 kW, which gives a COP of 17.5, as shown in equation 4.23 and 4.22.

4.3.4 DaVE Diagram

The ph-diagrams generated in DaVE, are shown in this section, both for the heat pumps with $\dot{Q}_E$ of 96 kW and 132 kW.

Figure 4.11 shows the final result in DaVE, for the heat pump that reached 96 kW in the evaporator. As seen in the figure, point 2 is far from the wanted separation temperature. It indicates that much of the fluid is still in liquid form.

Figure 4.12 shows what the cycle looks like for the heat pump that delivers 132 kW. Here, point 2 is located outside of the two-phase dome, and only gas exists. It can also be seen that there is enough ΔT_{SH} to have everything in gas form.

From the two ph-diagrams, the figures show that the evaporation temperature is 15.02 °C and the condensation temperature is 40.58 °C for both. These values are very similar to the once found with CoolPack.

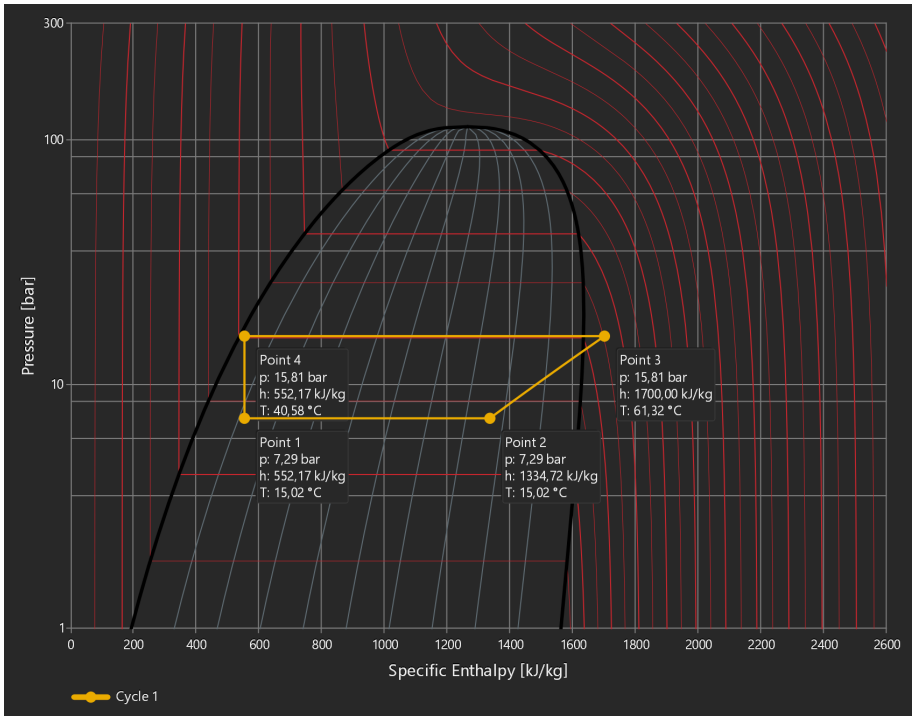

Figure 4.11: *Final result of the ammonia heat pump in Dymola with $\dot{Q}_E$ of 96 kW*

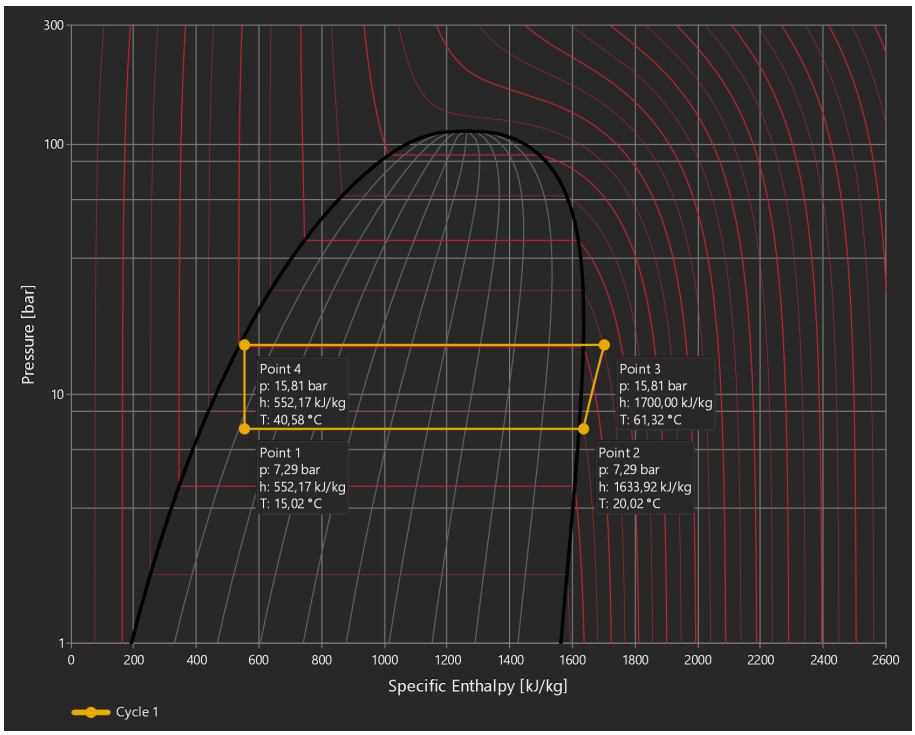

Figure 4.12: *Final result of the ammonia heat pump in Dymola with $\dot{Q}_E$ of 132 kW*

4.4 Gray Water and Space Cooling Integration

This section presents the simulations done with the gray water tank in the simulation tool COMSOL Multiphysics. The first sections present the simulations done with the base case and the three modifications. The next sections does the same for the simulations where only the temperature in the pipes are changing.

4.4.1 COMSOL Multiphysics Simulation Parameters

As shown in section 3.6, the total amount of gray water produced over a period of 24 hours is 26 274 kg. In order to hold this volume for one day, the tank needed to be able to hold approximately 26 m^3 of gray water. For the gray water tank simulations, the volume was set to 25 m^3. The height to width ratio of the tank needed, was a trade off between depth needed to be excavated, and the size of the trench. It was decided to have approximately the same width as depth, and a 3 m high tank was chosen. The width of the tank was calculated to be 3.26 m, hence a radius of 1.63 m. Table 4.7 gives the resulting calculated parameters that were used for the gray water tank.

Table 4.7: *COMSOL Multiphysics simulation parameters*

Parameter	Value
Height of tank, H_{gw} [m]	3
Volume of tank, V_{gw} [m^3]	25
Concrete thickness, d_c [m]	0.15
Insulation thickness, d_c [m]	0.05

4.4.2 The Four Initial Simulations

As explained earlier, the first evaluations made on the gray water tank, was how much the geometry plays a role in the potential of the gray water tank and space cooling integration. The four initial simulations made were the base case, larger pipes, fewer pipes in the bottom, and steel material. Here, the results from these simulations in regards of temperature, water flows, and heat flux will be presented.

Temperature Comparison

Figure 4.13 shows the temperature development in the gray water tank for the four simulations, over a duration of 720 min. Each of the figures shows the temperature development at the four points described in section 3.6.6, and shown in figure 3.18.

The graph for the steel tank case simulation in figure 4.13d, is plotted alone on a different scale on the y-axis, because the temperature gets much higher much quicker for this simulation compared to the other three. The time scale is the same for them all.

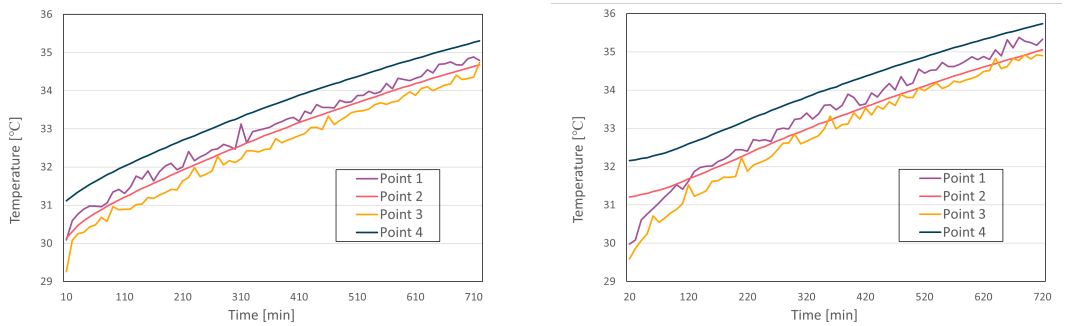

(a) Base Case *(b) Larger Pipes*

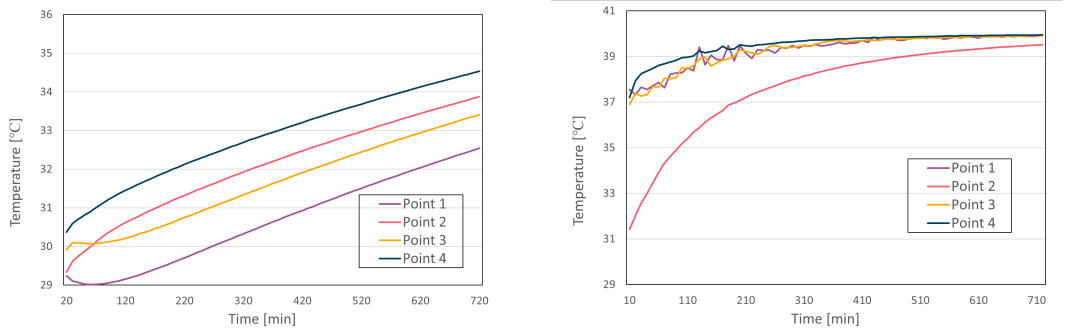

(c) Fewer Bottom Pipes *(d) Steel Tank*

Figure 4.13: *Comparison for the temperature graphs in the gray water tank*

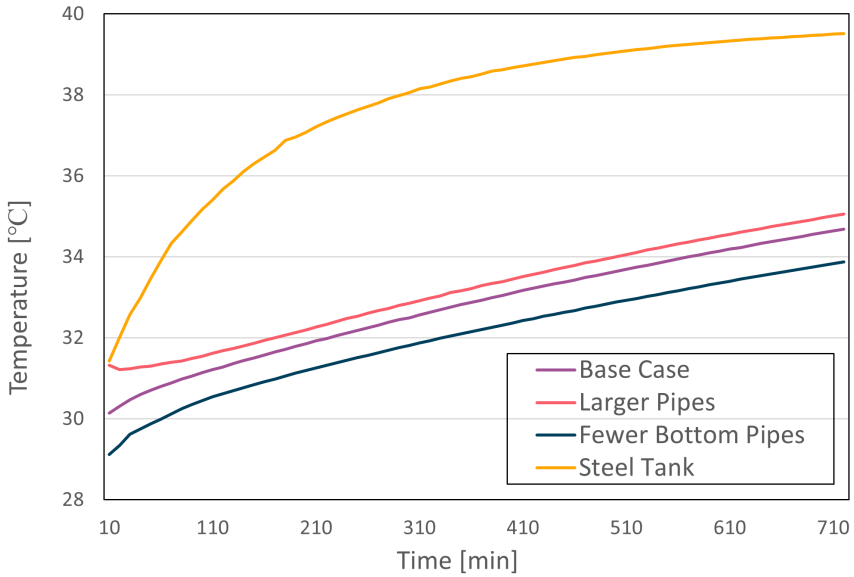

Figure 4.14: *Temperate comparisons at Point 2 between the four initial simulations*

All of the four graphs, show steady increasing temperatures at all four points. The increase is gradually slowing over time for all simulations. For the steel tank simulation, the increase in temperature in the beginning is much faster than for the other simulations. In this case, the temperatures level out to 40.0 °C after approximately 300 min at all the points, except for the top middle point (point 2) that is still at 39.4 °C after 720 min.

The top middle point (point 2), is the only point not close to any of the walls or the bottom, and it is the only point that is simulated to have a steady and smooth temperature rise in all four simulations. In the base case, figure 4.13a, and larger pipes case, figure 4.13b, both bottom points and in the steel tank case, figure 4.13d, also the top point by the outer wall (point 4), show erratic developments. In the fewer bottom pipes case in figure 4.13c, all four temperatures show smooth increases.

Figure 4.14 shows the temperature development of all four simulations at Point 2 as explained in figure 3.18. Initially, the gray water temperature was 30 °C for all simulations. While the steel tank simulation yielded a rapid increase and reached 34.9 °C after 90 min, 37.6 °C after 240 min, and a final temperature of 39.5 °C after 720 min, the other three simulations had all slower temperature increases. The final temperatures after 720 min were 34.7 °C for the base case, 35.1 °C for the larger pipes case, and 33.9 °C for the fewer pipes case.

Heat Flux

Normal total heat flux, from now represented as Φ [kW], was derived from the same simulation runs. Figure 4.15 shows Φ for the four initial simulations. All simulations show that Φ from the pipes representing the coils, is highest in the beginning, and falls quickly during the first 200 min. After 200 min, the graph levels out as Φ from the pipes, approach the value of Φ from the wall into the body of gray water. From this point onward, from 220 min to 720 min, the fall is steady and less steep.

In all simulations, the normal total heat flux from the insulation into the outside gravel was around 0.70 kW, ranging from 0.67 kW for the fewer pipes in bottom case, 0.69 kW for the base case and larger pipes case, and 0.71 kW for the steel tank case.

Figure 4.15 also plots the difference between normal total heat flux from the pipes, and the sum of normal total heat flux into the body of gray water and the outside gravel. The difference is high in the beginning, falls rapidly, and is close to zero from around 200 min until the end. For the steel tank simulation in figure 4.15d, the difference is close to zero from less than 20 min.

The rest of this section will focus on normal total heat flux absorbed by the body of gray water from the tank's inner walls and bottom.

Figure 4.16 shows comparisons of the energy absorbed by the normal total heat flux from concrete wall into the body of gray water between the four simulations.

The steel tank case is different than the three other simulations. Normal total heat flux for the steel tank case starts, at a high of 80 kW and drops quickly to almost zero at 720 min.

The other three cases are similar to each other. They start with values between 12 kW and 16 kW, falls slowly throughout the simulation run length to around 8 kW for them all.

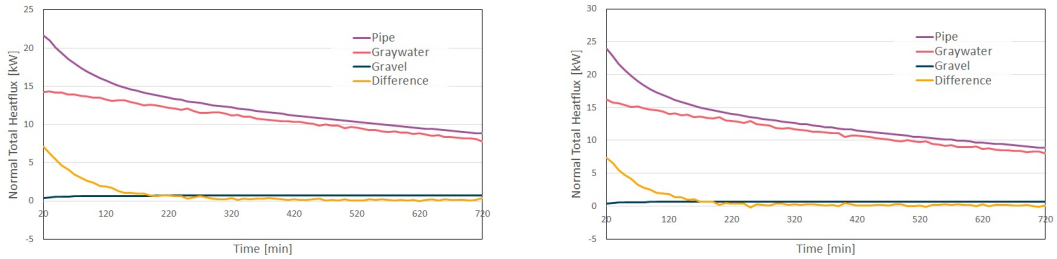

(a) Base Case *(b) Larger Pipes*

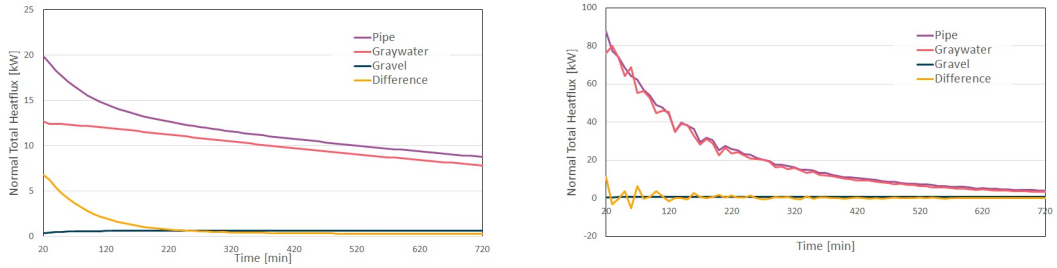

(c) Fewer Bottom Pipes *(d) Steel Tank*

Figure 4.15: *Comparison for the normal total heat flux, Φ [kW], in the four initial gray water tank simulations. All scales are different while the time scale is equal*

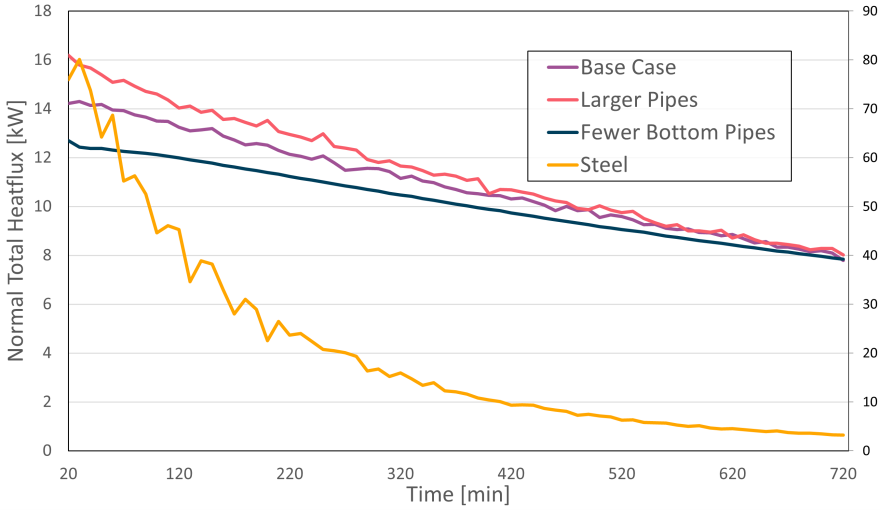

Figure 4.16: *Comparisons of normal total heat flux, Φ [kW], between concrete wall and body of gray water for the four initial simulations. Steel wall simulation is plotted against the right axis*

Table 4.8: *Normal total heat flux received by the body of gray water for the four initial simulations*

Simulation run	Unit	20 min.	200 min.	360 min.	720 min.
Base Case	Φ [kW]	14.2	12.5	10.8	7.8
Larger Pipes Case	Φ [kW]	16.2	13.5	11.3	8.0
Fewer Pipes Case	Φ [kW]	12.7	11.4	10.2	7.8
Steel Tank Case	Φ [kW]	76.0	22.5	12.2	3.2

Table 4.8 shows the values for normal total heat flux for the four simulations at four stages into the simulation runs, 20 min, 200 min, 360 min, and 720 min.

Water Flow Arrows

Figures 4.17, 4.18, 4.19, and 4.20 show the water flow arrows produced by the four simulations at three different time steps, 200 min, 360 min, and 720 min. Common to all simulations, is the rapid flow of gray water rushing up along the hotter wall from the bottom of the tank toward the top. This steady flow of colder water from the bottom being heated by the wall, continues as long as there is temperature difference between the wall and the gray water. The lower the temperature difference between the wall and the body of gray water, the slower the upwards flow. This is particularly evident in the steel tank simulation, as show in figure 4.20

In addition to the outer wall water flow, the base case has turbulent flows towards the bottom third of the tank. The turbulent flow does not alter significantly throughout the 720 min simulation. The larger pipes case in figure 4.18, also has this turbulence at the bottom third of the tank. The rest of the tank is relatively calm.

The steel tank case shows a higher degree of turbulence throughout the simulation. Water velocity is higher along the tank wall, as well as higher turbulent movements particularly in the bottom half of the tank as shown in figure 4.20.

The fewer bottom pipes case is different. The water flow by the vertical wall is similar to the other simulations, while the turbulence is not present as shown in figure 4.19.

4.4.3 Simulations with Different Coil Temperatures

This next section, takes a further dive into the importance of temperature differences. By using two of the same three different areas of comparison, like for the different geometry cases, this section compares what happens when the temperature differences between the gray water and the pipes increases.

Temperature Comparisons

For the three different cases where only pipe temperatures were changed, the temperature developments in the gray water tank's top middle point (point 2) were derived and compared to the base case from the initial simulations. Figure 4.21

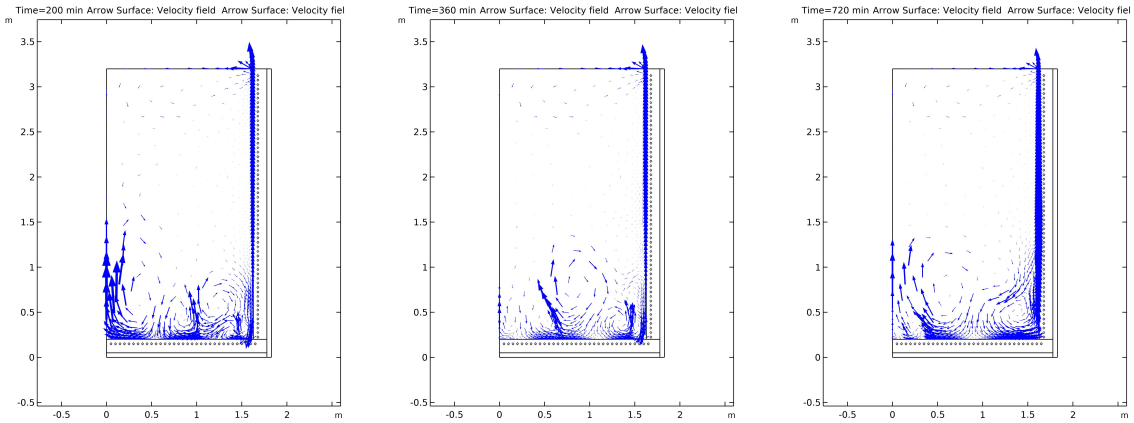

(a) 200 min *(b) 360 min* *(c) 720 min*

Figure 4.17: *Water flow arrows for the base case*

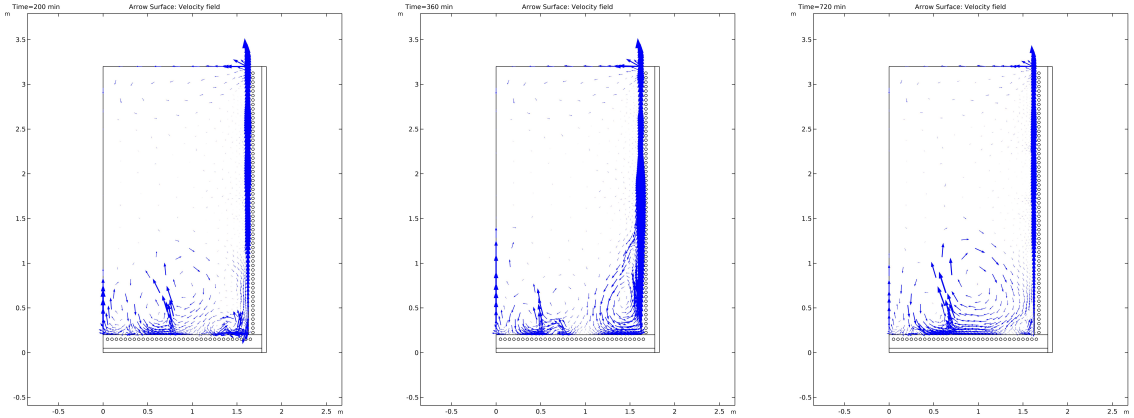

(a) 200 min *(b) 360 min* *(c) 720 min*

Figure 4.18: *Water flow arrows for the larger pipes case*

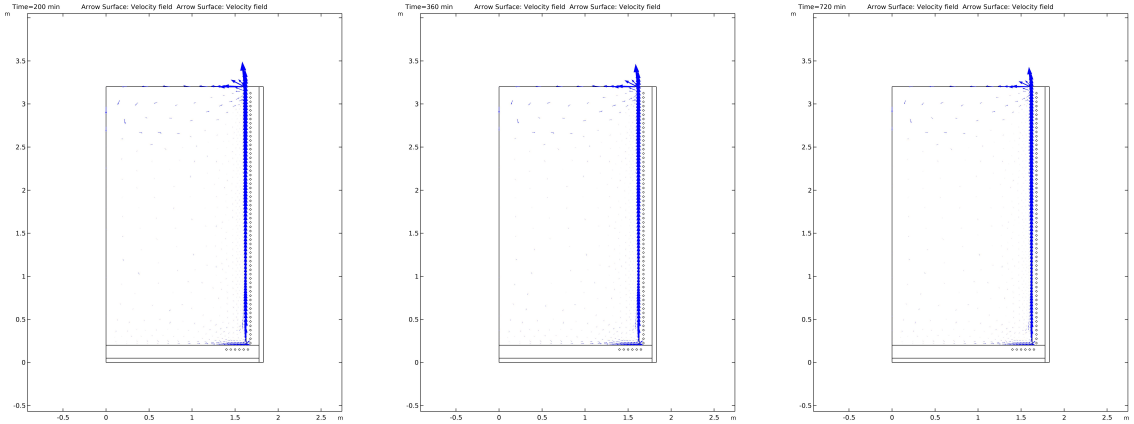

(a) 200 min *(b) 360 min* *(c) 720 min*

Figure 4.19: *Water flow arrows for the simulation with fewer pipes in the bottom concrete*

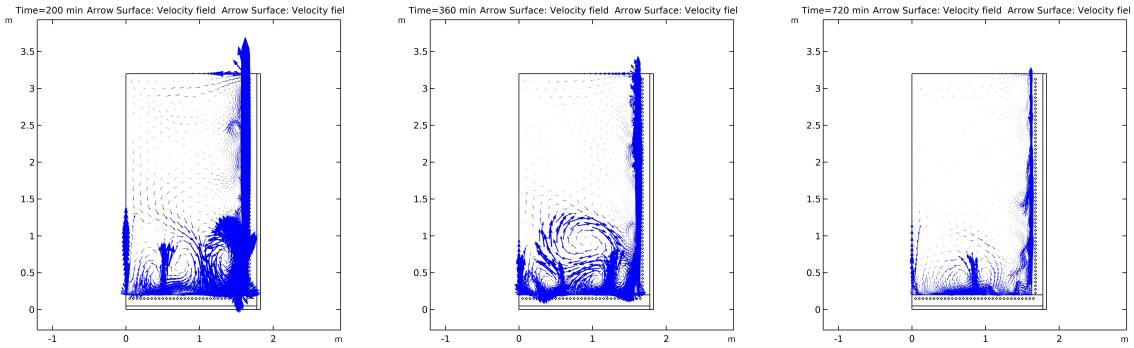

(a) 200 min *(b) 360 min* *(c) 720 min*

Figure 4.20: *Water flow arrows for the steel tank case*

shows the comparisons for the four simulations. Temperatures for all simulations increased steeply in the beginning, while the increase gradually slowed over time. All the simulations started with a gray water temperature of 30 °C, and ended after 720 min at 35.3 °C for the base case, 40.7 °C, 46.1 °C, and 51.2 °C for the other higher temperature cases respectively.

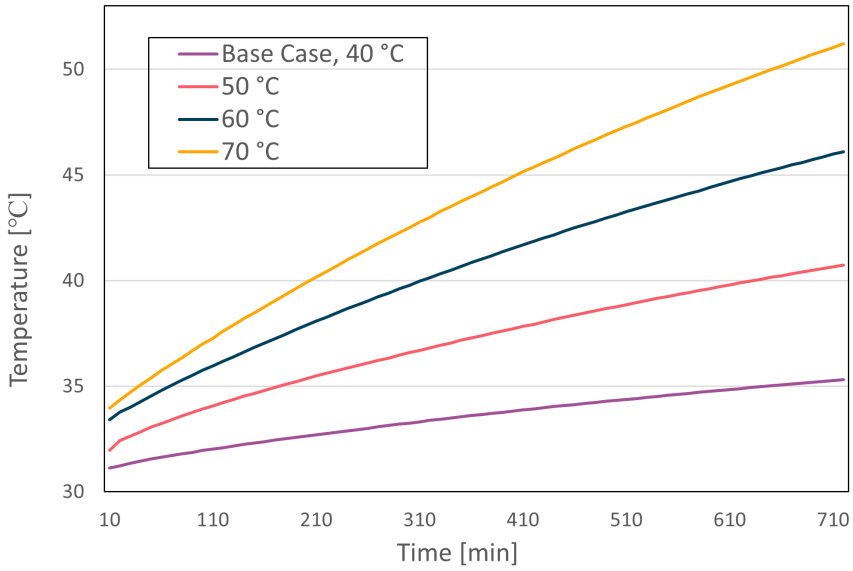

Figure 4.21: *Comparisons of temperature development at evaluation point 2 for the four simulations with different pipe temperatures. Pipe temperatures are 10 K different between simulations*

Heat Flux

Figure 4.22 shows total normal heat flux from the tank structure, wall, and bottom, into the body of gray water for the base case and the three cases with variable pipe temperatures, 10 K, 20 K, and 30 K above base case respectively.

All the three additional cases, yields higher normal total heat flux throughout the simulation runs. The difference is again largest in the beginning and is slowly

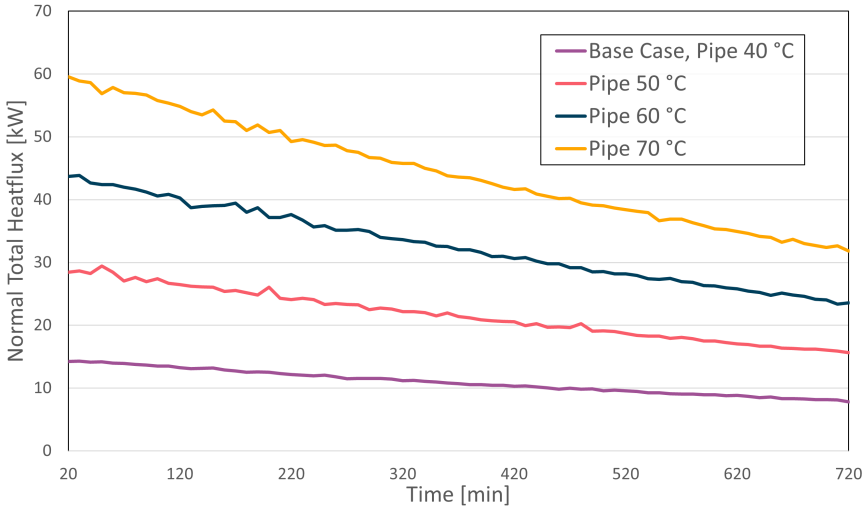

Figure 4.22: *Comparisons of normal total heat flux, Φ [kW], between concrete wall and body of gray water for the four simulations with different pipe temperatures*

Table 4.9: *Normal total heat flux received by the body of gray water for the higher coil temperature simulations*

Simulation run	Unit	20 min.	200 min.	360 min.	720 min.
Base case	Φ [kW]	14.2	12.5	10.8	7.8
50 °C Case	Φ [kW]	28.5	26.1	21.9	15.5
60 °C Case	Φ [kW]	43.7	37.2	32.5	23.6
70 °C Case	Φ [kW]	59.6	50.7	43.8	31.8

reduced over time. After 20 min the 70 °C case yields 59.6 kW compared to 14.2 kW for the base case. After 720 min, the four simulations are still producing significantly different results, varying from 7.8 kW to 31.8 kW, between the lowest base case and the highest 70 °C. Table 4.9 shows the normal total heat flux derived at four points for the four simulations.

The heat loss as derived as negative normal total heat flux from the insulation layer into the outside gravel was higher as the pipe temperature increased. After 720 min. the normal total heat flux into the outside gravel was 0.93 kW for the 50 °C case, 1.18 kW for the 60 °C case, and 1.42 kW for the 70 °C case. This compared to 0.69 kW for the base case.

4.4.4 Pressure Drops

It is assumed that 112 kW is being added to the gray water tank from the space cooling circuit. Using equation 2.7 from section 2.1.4, as shown in equation 4.25, the mass flow is calculated to be 2.68 kg/s. This is assuming the temperature of the gray water is reduced by 10 K in the condenser.

$$\dot{m} = \frac{112}{4.18 \cdot 10} = 2.68 \qquad [\text{kg/s}] \quad (4.25)$$

$$A = \pi \cdot (D/2)^2 = \pi \cdot (0.0204/2)^2 = 0.00033 \qquad [\mathrm{m}^2] \quad (4.26)$$

$$v = \frac{\dot{m}}{\rho \cdot A} = \frac{2.68}{997 \cdot 0.00033} = 8.22 \qquad [\mathrm{m/s}] \quad (4.27)$$

Further, the velocity was calculated to be 8.22 m/s, as shown with equation 4.26 and 4.27.

The diameter of the pipe is going to be 20.4 mm, and the operational temperature is 35 °C. Since it is a liquid, equation 2.11 from section 2.4 can be used, as shown in equation 4.28.

$$\mu = a \cdot 10^{b/(35-c)} = 0.00071849 \qquad [\mathrm{kg/m\,s}] \quad (4.28)$$

The Reynolds number was then calculated, as shown in equation 4.29.

$$\mathrm{Re} = \frac{997 \cdot 5.60 \cdot 0.025}{0.00071849} = 190\,371 \qquad [-] \quad (4.29)$$

The pipes used are plastic, hence $\epsilon = 0$. Coolbrook's equation was then used, in order to find the Darcy friction factor, which was then calculated to be $f = 0.0158$.

Finally, the pressure drop was calculated, and found to be 9880 Pa/m.

$$\Delta P/L = 0.0158 \cdot \frac{1}{0.025} \cdot \frac{997 \cdot 5.60^2}{2} = 9880 \qquad [\mathrm{Pa/m}] \quad (4.30)$$

By adding more parallel pipes in the coil, the pressure drop is able to decrease. Similar calculations as presented above, were performed on coils with 2, 3, and 4 parallel pipes. Table 4.10 shows a summary of these calculations. All the values decrease, with exception of the Darcy friction factor, which increases slightly.

Table 4.10: *Pressure loss for separate pipes*

	Mass flow $\dot{m}$ [kg/s]	Velocity v [m/s]	Reynolds Re [–]	Darcys f [–]	Pressure drop ΔP [Pa/m]
1 coil	2.68	8.22	232 806	0.01580	33 386
2 coils	1.34	4.11	116 403	0.01743	8347
3 coils	0.893	2.74	77 573	0.01898	4492
4 coils	0.670	2.06	58 201	0.02020	2087

As seen in the table, the pressure drop decreases with about 75 % by using two parallel pipes, and 94 % by using four pipes.

Circular Tank

Table 4.11 shows the pressure drop for a circular tank with no sharp edges and one coil. The radius of the coil is 1.63 m, corresponding to one coil being 10.23 m. There are 59 coils, so the total length of the pipe in the coil is 603 m.

With a pressure drop of 33 386 Pa/m, this leaves a total of 20 147 kPa. By dividing the flow on 4 coils, the pressure drop is 2087 Pa/m, and the total pressure drop in the pipes is 1259 kPa.

Table 4.11: *Pressure drop in a circular tank*

	Value
Radius, R [m]	1.63
Circumference, C [m]	10.23
Total pipe length, l_{tot} [m]	603
Pressure drop, ΔP [kPa]	20 147 kPa
Pressure drop, ΔP [bar]	201

Pressure Drop in Bends

For a tank in a hexagon shape, as the tank is illustrated as in section 3.6.4, the pressure drop of every bend is 2866 Pa, as shown in equation 4.31.

$$\Delta P = \zeta_b \frac{\rho v^2}{2} = 0.085 \cdot \frac{997 \cdot 8.22^2}{2} = 2866 \quad \text{[Pa]} \quad (4.31)$$

$$\Delta P = \zeta_b \frac{\rho v^2}{2} = 0.085 \cdot \frac{997 \cdot 4.11^2}{2} = 717 \quad \text{[Pa]} \quad (4.32)$$

$$\Delta P = \zeta_b \frac{\rho v^2}{2} = 0.085 \cdot \frac{997 \cdot 2.74^2}{2} = 318 \quad \text{[Pa]} \quad (4.33)$$

$$\Delta P = \zeta_b \frac{\rho v^2}{2} = 0.085 \cdot \frac{997 \cdot 2.06^2}{2} = 179 \quad \text{[Pa]} \quad (4.34)$$

Since there are 59 rounds of the coil, and 6 bends for each round, the total pressure drop for the gray water tank will be

$$\Delta P = 2.866 \cdot 59 \cdot 6 = 1015 \quad \text{[kPa]} \quad (4.35)$$

The same calculations can be done for a tank in octagon shape, and squared. They will have a ζ_b on 0.075 and 0.1, respectively. Table 4.12 shows the final results for all bends for the different shapes.

Table 4.12: *Pressure loss for separate pipes in bends*

	Velocity $\dot{m}$ [kg/s]	Square ΔP [Pa]	Hexagon ΔP [Pa]	Octagon ΔP [Pa]
1 coil	8.22	3372	2866	2529
2 coils	4.11	843	717	632
3 coils	2.74	375	318	281
4 coils	2.06	211	179	158

Table 4.13 shows the total pressure drop for the different tanks, but represented in bar rather than kPa. A circulation pump must be able to overcome the pressure drops presented, in order to get the wanted flow.

Table 4.13: *Pressure loss for separate pipes total*

	Circular ΔP [bar]	Square ΔP [bar]	Hexagon ΔP [bar]	Octagon ΔP [bar]
1 coil	201	209	211	213
2 coils	50.3	52.3	52.8	53.3
3 coils	27.1	28.0	28.2	28.4
4 coils	12.5	13.0	13.1	13.2

4.5 Cost Analysis

This section provides the results from the brief cost analysis done in this thesis. The two systems put in focus regarding the cost analysis, is the systems that provide energy for space heating, and heating of DHW. The analysis provides an estimation of how much energy is able to be saved by going for the two energy systems, and thus how much can be spent on the investment.

4.5.1 Cost of Different Heat Sources

Using demand input from SIMIEN, and data from Statkraft, Nord Pool and Trønderenergi, costs of the different heat sources were calculated.

The average spot price from Nord Pool for the years going from 2004 to 2019, was 313 NOK/MWh per year. Total variable cost of grid rent and consumption fee per November 2020, was 405 NOK/MWh. With an energy demand of 313 MWh for space heating, total estimated cost is 237 523 NOK per year for zone B1.

Further, using the same calcultation as above, cost of using the local district heating system is 241 442 NOK per year. Because of the marginal price difference of 4000 NOK per year, and due to uncertainty in future prices, going forward, the price for electricity is being used for this cost analysis. Another reason to use the price of electricity is that the prices for local district heating system cannot be higher than using electricity, according to the Norwegian Energy Law.

Table 4.14: *Yearly cost of different heat sources*

Heat Source	Price per year [NOK/MWh]	Demand [MWh]	Total Cost [NOK]
Electricity	758	313	237 523
Local district heating	771	313	241 442
Ice rink	758	98	74 368
DHW with electricity	758	317	240 559
DHW heat pump using gray water	758	99	75 127

When using excess heat from the ice rink at Leangen, the heat pump will need electricity for the compressor. However, the need to meet the demand for space

heating, at the same comfort level, the heat pump will need 98 MWh per year. This cost is estimated to be 74 368 NOK every year.

The second element to evaluate, is the cost of DHW. The demand for DHW, is estimated to be 317 MWh each year. Using the same equation for cost as for space heating, the cost of heating DHW with electricity is estimated to be 240 558 NOK per year. Hence, to meet the same demand while using a heat pump for gray water, the usage is estimated to be 99 MWh per year, with a total price of 75 127 NOK. This is all summarized in table 4.14.

Table 4.15: *Yearly cost savings different heat sources*

Heat Source	Savings [NOK]
Space heating with ice rink	163 431
DHW with gray water	165 431
Total savings	328 586

Table 4.15, shows how much could be saved with the two system. Taking the estimated total cost of electricity and deducting the estimated cost for using a heat pump, the estimated yearly savings could potentially be 163 155 NOK. Further, when estimating cost of DHW by using electricity, minus the cost of using the heat pump on gray water, the estimated yearly savings could be 165 431 NOK. Thereby, the total estimated savings by using excess heat from Leangen Ice Rink, and using gray water to heat DHW, could be 328 586 NOK.

4.5.2 Cost of Investment

Since this thesis is not focusing on a deep dive into the cost optimization of implementing a central heating system, but rather the energy potential, the cost analysis is done on a superficial level. The thesis has not looked into the detailed investment of a system, but rather used two different models.

One of the models is to see how many years it would take for the investment to be positive, given a set of investments costs. The cost was evaluated based on investments from 2 MNOK to 10 MNOK, with increments of 2 MNOK. The investment of discounting rate was set to zero. The other model was Net Present Value (NPV), to find the NPV for three variations of life expectancy and three variations of discounting rates.

With an investment of 10 MNOK, and savings of 328 586 NOK per year, the investment will be positive after more than 30 years. With an invest of 6 MNOK the investment will be positive after 19 years, and with a cost of a system of 2 MNOK the investment is positive after just 7 years. Figure 4.23 shows the different scenarios.

When using the Net Present Value, with a life expectancy of 30 years, and a discounting rate of 2 percent, an investment for a district heating system can be sound up to 7 MNOK. Further, if the interest rate in the market increases to 10 percent, the NPV decreases to 3.1 MNOK. See table 4.16.

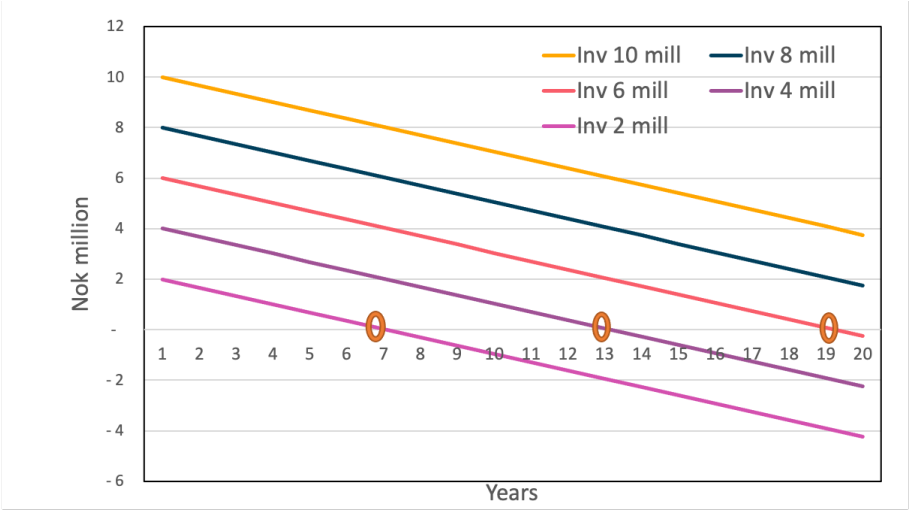

Figure 4.23: *Break Even Scenarios*

Table 4.16: *Net Present Value output*

Years	Discounting Rate		
	2 % [NOK]	5 % [NOK]	10 % [NOK]
10 years	2 952 000	2 537 000	2 019 000
20 years	5 373 000	4 095 000	2 797 000
30 years	7 359 000	5 051 000	3 100 000

Chapter 5

Discussion

This chapter pulls together the the findings from the previous chapter, and provides the discussion needed in order to make a conclusion. First, this chapter will discuss the findings from the energy profile of B1 simulated in SIMIEN. Then, it discusses the different heat sources evaluated in this thesis, before it goes through the findings about the heat pump simulated in Dymola. After that, the findings and potential of integrating the space cooling system circuit with the gray water tank will be discussed. The chapter will complete with a discussion about the costs related to the findings.

5.1 Energy Demand and System Solution

In this section, the findings from the SIMIEN simulation will be discussed. First, the actual energy demand and balance will be in focus, before the reliability of the system based on the perceived indoor environment will be considered.

5.1.1 General Energy Demand

The results from the SIMIEN simulation are similar to the results from the SINTEF estimates. The reason for the SIMIEN results and the results generated by SINTEF of DHW to differ in some way, is that SINTEF's values are based on a standard usage of buildings in the area, while SIMIEN are based on standards from TEK17. However, all three values from SINTEF, TEK17, and SIMIEN, as shown in table 4.3 are quite similar, which indicates that the SIMIEN simulation is reliable.

The DHW heating demand is the same through every month. This is due to the washing demands being constant through the years. In real life, there might be less people home during the summer vacation, resulting in a lower demand. The lighting, fans and technical equipment are also constant throughout the year, while pumps and space cooling only operate through the summer months. This is simply because the cooling equipment are scheduled in SIMIEN only to operate through these specific months.

Of this demand, as seen in the pie chart in section 4.1.1, heating of space and DHW each take up a big share of the energy demand, standing for more than 50 % together. This emphasizes the initial statement about heating in buildings being a

huge consumer of energy, and why finding ways of reducing external sources for this is a valid way of reducing a building's energy footprint.

The reason for there being no heating demand during summer, is that the temperature has been given a set point temperature in the SIMIEN tool during the summer month to 15 °C, which is sufficiently low for it not to turn on during this period. In real life, there might still be necessary to heat up a few rooms, like bathrooms, during this period as well, but this has not been taken into consideration for the SIMIEN energy evaluation of zone B1.

In SIMIEN, a more detailed evaluation of the apartment numbers and sizes was made. Evaluation about the gray water production used an approach where the total GFA was divided by the average area for each apartment at Tungaveien 1. This will still be a valid comparison since the values from SIMIEN are based on the average from TEK17, and not based on the amount of people in each apartment. Since the values in SIMIEN also is so close to what SINTEF has evaluated, it is a valid comparison for how the actual zones will be, regarding the ratio between used DHW and the produced gray water.

5.1.2 Energy Balance

From the SIMIEN results posted in chapter 4 Results, it is shown how much energy supply is needed for zone B1 in order to cover it's energy demand. It is evaluated that the energy used is 1114 kW, and that the energy delivered externally is 916 kW, leaving heat sources supplying 198 kW in the heat pump.

However, this is only true for the heating of DHW, and does not include the fact that space heating will utilize a heat pump as well. The district heating in the report represents the energy coming from the ice rink in the local low-temperature thermal grid, but does not include the energy supplied from the heat pump. This means that the energy taken from the circuit as heat source, will not be equal to the district heating need in the report. Therefore, the total energy delivered in the SIMIEN report, is not accurate for the space heating demand.

As far as heat losses are concerned, plenty of factors can be seen to impact this in the building. However, the majority of the losses are related to the transmission losses. Added together, these stand for more than 50 % of the total heat loss. These could be reduced by adding better windows and better insulation materials to reduce transmission losses. In addition, ensuring a more sealed structure to prevent infiltration will also be beneficial for reducing the losses. Discussing this, however, is not part of the scope for this thesis, and will not be evaluated further.

In section 2.7.1, it is explained that the energy delivered by the different heaters might not be equal to the actual demand within the building. This means that even though the heat pumps only receive 13 % of the total delivered energy to the system, they cover more of the actual energy demanded by the building.

The COP of the heat pump used in SIMIEN is lower than the COP of 3.2 used in the rest of the thesis. This means that the delivered energy shown in SIMIEN will be even lower with a better heat pump. However, this does not affect the energy demands shown in SIMIEN, and the further energy calculations are also not affected either.

5.1.3 Indoor Environment

It is very unfortunate for the energy use of the building that the maximum temperatures in the building is above 22 °C through all the months. This should be looked into in order to get a lower heating demand for the building.

The temperatures are always below 26 °C through the whole year. This is in compliance with TEK17's recommendation of always having indoor temperatures below 26 °C, regardless of the activity performed inside.

Further, they have stated that the temperature should stay beneath 22 °C in periods with heating demand. This is kept through most of the months for the average temperatures. Unfortunately, this is not the case for all the maximum temperatures. The months of March, April, and October are all months with heating demand, and the maximum temperatures are about 23 °C for all of them. This could be avoided by including better regulation and set temperatures in the tool.

The PPD and PMV values are very good during the summer, indicating that the cooling equipment is working properly, and providing a sufficient thermal environment.

For the winter, however, they are not good. The PPD value is 30 %, indicating that the air is too toxicated. This could be addressed by having better ventilation systems. The PMV value of -1 indicated that the inhabitants think it is too cold inside. This suggests that more energy will be used once the apartments are filled with residents.

5.2 Heat Sources

Various heat sources have been evaluated in this thesis. Special notice has been taken towards waste heat production, especially from gray water and the local ice rink. In addition, a brief discussion about the potential in solar radiation will be considered.

5.2.1 Ice Rink

In 2018, Leangen Ice Rink produced 1766 MWh of waste heat. This was not used for anything other than heating up the globe. In 2019 this number was 2265 MWh. That is an insane amount of energy, and it is just wasted.

In order to meet the future energy demands, emissions like these can not happen. From table 4.4 in section 4.2.1, it is seen that the ice rink was able to cover the needed space heating demand in B1 with between 9 % to 20 % of it's total waste in 2019. This means it could deliver energy to between about 5 to 10 zones with the same space heating demand as zone B1.

The energy from the ice rink is, from the estimations done in this thesis, not enough to cover the whole building area at Tungavegen 1. However, it will be enough to cover the first zones to be built. This way, in the beginning, the ice rink can be used to supply space heating, and hopefully trying it out in practice will open up for new discoveries and methods that can be used for the zones to be built later. In addition, technology is getting better and maybe, in the future, it will

ensure that buildings will require less energy while still keeping a sufficient indoor environment.

5.2.2 Gray Water

The produced gray water in zone B1 is shown to able to cover the DHW energy demand if the water decreases by 19.58 K in the condenser, if a heat pump with a COP of 3.2 is used. This means that the water must go from a temperature of about 30 °C to about 10 °C. Using a heat pump with higher COP would mean that the gray water must provide even more energy.

The heat pump used for DHW, is not inspected in this thesis. However, if future analysis shows that it is possible to design a heat pump that can pull 18.18 MWh from the gray water, this would be a great way of covering the DHW demand. It is assumed that the sizes of the apartment in the reference zone is 70 m^2. This is the average of the whole of Tungavegen 1, but since there are terraced houses in B1, the average size of the apartments might actually be higher, and number of people living there might as well. In total, there might be less people actually living in B1. However, it is still a good indication of how big the gray water tanks will be for every zone. A next step here could be doing a deeper analysis of how many people are actually expected to live in B1, or find a estimation of how big the terraced houses will be.

Another consideration to take regarding this system, is that gray water and black water must have separate piping systems. This must be included when planning the building project.

5.2.3 Solar Radiation

The peak of available solar radiation, and the peak of needed space heating is uncorrelated. In the winter when more heating is required, it is dark and thus less solar radiation to be collected. However, some residents might still want heating in the bathrooms, even during the summer. The ice rink is not operational during the summer, so using solar radiation to heat up the thermal grid usually provided by the ice rink, can be a valid option.

Another possibility is to use it as an additional heat source for DHW. This heating demand is estimated to be constant throughout the year, and could potentially mean a smaller temperature drop of the water through the evaporator.

5.3 Heat Pumps

The mass flow of the water through the evaporator was more difficult to determine than for the condenser. The speed of the water from the ice rink is not specified. Further, the return temperature for the low-temperature thermal grid is not specified like it is for the space heating circuit. However, an assumption that the water will reduce the temperature by 10 K is taken, even though it might be different in real life.

Another simplification made, is that losses are not taken into consideration. The compressor, for instance, will most likely not be able to provide the same amount of energy to the refrigerant that it consumes, due to losses. This simplification means that the calculations present a scenario much better than what will be the case in real life.

The DaVE results of the two heat pumps with 96 kW and 132 kW, indicate that the working area chosen might not be optimal for this use. CoolPack, on the other hand, indicates that it should be able to work, but requires the temperature of the refrigerant out of the compressor to be around 87 °C. In addition, it needs the refrigerant to exit the condenser far into the liquid phase.

These high temperatures found from CoolPack is much to high for an optimal, real system. High temperature will first of all provide high losses, which is not wanted. In addition, it is not very smart to have a temperature of 87 °C when the wanted temperature in the space heating is just 35 °C.

The values found in CoolPack makes the ammonia in the condenser have a much higher temperature on the inlet, and a lower one at the outlet, than from the Dymola model. This causes the COP to be much different from the ones calculated from the Dymola file.

5.4 Gray Water

The simulations done with COMSOL Multiphysics showed that energy was used to heat the wall material during the initial part of the simulation runs. This initial condition with a large amount of energy being absorbed by the wall material will, in normal operation, only happen every time the gray water tank is starting up for the season or after a maintenance period. Simulation results after the initial 200 min. should be considered to be closer to normal operational conditions.

5.4.1 Simulation Weaknesses

The gray water tank is simulated without in- and outlet flows. In normal operation, new gray water is added and the warmest gray water is used to produce DHW. Both of these flows will reduce the average gray water temperature in the tank. This thesis has not looked at these in- and outlet flows. However, the simulations between the initial 200 min up to the maximum of 720 min, is likely to be best resembling the normal operational situation.

The simulations have been done on a stationary tank with an initial gray water temperature of 30 °C. In reality, the temperature of the inlet water in the tank will vary depending on what the occupants use. Further work may be needed to determine the actual gray water dynamics for Tungavegen 1.

By using COMSOL Multiphysics 2D axis symmetric functionality, the elements of the geometry were circular. This included pipes inside the walls representing the helix formed coil. As shown in section 4.4.4, several parallel coils may be needed to reduce pressure drops. In addition, the normal total heat flux from the pipes into the wall was simulated. Hence, this limitation should not influence the results significantly.

The pipes were also simulated without a plastic pipe wall. This simplification may influence the heat flux through the plastic wall into the tank wall. Further simulations may be performed to investigate this in detail.

The simulations assume constant temperatures along the whole length of the pipe, while in reality, the pipe temperature is reduced as heat is transferred form the pipe. Further simulations may be needed to determine this effect.

In all simulation runs, the energy transfer from the coils into the body of gray water, grows with the temperature difference between them. The combination of gray water being introduced to the tank quickly, and drained to circulate in the heat pump for DHW, will cause cooler gray water temperatures. This means that the efficiency of using pipes to heat up the gray water, will increase with the need for DHW. Hence, real life will be better than the simulations performed in this thesis.

5.4.2 Turbulence

The turbulence was very different between the simulations. Steel is a material with high thermal conductivity, resulting in a much faster heat transfer. The steel tank is heated up within a few minutes, compared to around 100 - 200 min. for the concrete tank.

This rapid heat transfer, generates turbulence. This is most evident in the beginning of the steel tank simulation in figure 4.20, but applies for the rest of the simulations as well. It is also indicated in the rest of the graphs, where the lines are variable, rather than smooth.

This turbulence can also be caused by the disruption of the natural flows that are caused in the tank. When water is heated at the walls of the tank, it moves upwards until it reaches the surface of the water. There, it is pushed away by the continued upwards water stream, before it is forced downwards in the middle of the tank. The water heated by the bottom pipes will move upwards as well, and work against the down flowing water.

In the case with fewer pipes in the bottom, something different is happening. Instead of the water flows working against one another, the water moving downwards in the middle will continue to the bottom, before being push towards the walls to be heated again. This can be seen in the graphs by this simulation producing smoother lines.

The lack of turbulence may increase the temperature difference between the bottom and top of the tank since water is stirred together by turbulence. Since the hottest water is drained from the top, the configuration with fewer pipes may be more efficient. However, the simulations did not provide significant data to support this, and further work is needed.

5.4.3 Tank Geometry

As the tank is planned now, the introduced water will be entered from the top close to the wall. This might not be beneficial, considering the warm water at the top is what will be extracted to the heat pump.

In addition, the inlet water from gray water will also cause motion in the water, and might also work against the natural flows. Because of this, it might be a better solution have it enter at the bottom.

Another option could be releasing the gray water in the middle of the gray water tank, but still from the top. This way the colder new gray water will better follow with the existing current down in the middle, along the bottom of the tank from center to walls, and follow the warming along the concrete wall bottom to top.

The simulations show that the gray water received from 10 kW up to 50 kW of heat flux depending on the configuration. An alternative tank without pipes would steadily lose heat to the surroundings. This is an argument for why pipes would be beneficial, not only because of the added heat, but also the reduced losses.

5.4.4 Space Cooling Integration

Space cooling is only needed during summer time, and might not even be necessary in Norway during nighttime, due to low temperatures. Because of this, using the gray water tank as a heat sink for the space cooling circuit, will mostly be beneficial for the heat pump, and not for the gray water.

Another solution could be having an external heat exchanger, where the gray water receives energy from the space cooling circuit before it enters the gray water tank. This will ensure a better heat transfer between the two liquids, and might lead to higher efficiency of the system.

A different method that could be evaluated instead of using the gray water tank as a heat sink, could be dumping the heat to the local low-temperature grid. This could be done through a simple heat exchanger, and can thereby provide heat for the water circuit at Tungavegen 1. Since the ice rink is not running during the summer time, the space cooling circuit could provide as a heat sink for the possible space heating instead.

A last remark to consider, is that since temperatures are expected to rise in the decades ahead, and given the world's slow track record of reducing emissions to reach UN's goal of max 2 degrees global warming, the need for space cooling is likely to grow significantly over the next few decades. This will help making the solution to exploit excess energy form space cooling exceedingly profitable.

5.4.5 Pressure Prop

For the pressure drop calculations, it is evident that there is not much difference between the different tank shapes. Choosing the tank that is the easiest and cheapest to produce, is therefore the best option. However, the drop in mass flow the parallel pipes brings, causes the pressure drop for both the per meter and the per bend to decrease drastically.

The pressure drop in the pipes in the bottom are not evaluated here, but since these are equal for all the cases, it will not effect the comparisons.

5.5 Cost Evaluation

One limitation with the cost analysis in this thesis is the lack of detailed insight into the construction costs associated with the various alternatives. Instead of calculating the profitability of the project, the savings associated with the system is calculated giving an indication as to the investment size. The yearly savings is estimated to be 328 kNOK. Translating this to an investment today means making assumptions on interest rates and life expectancy of the system. Given today's volatile financial markets, these calculations are highly uncertain, but is a good starting point to go forward.

Chapter 6

Conclusion

The goal for this thesis, was evaluating different methods for how the building project Tungavegen 1 in Trondheim could be made energy efficient, and at the same time environmentally friendly. This has been looked at from a financial perspective, but also with the United Nations' Sustainability goals in mind. This thesis has provided information and simulated results from different methods, of which two distinct ones have been in focus.

One focus area was using excess heat from Leangen Ice Rink to provide space heating for Tungavegen 1, and the second was using waste heat from gray water to provide DHW. In addition, it has been looked at the possibility of integrating space cooling into the system, and using the excess heat from that as an additional heat source for the DHW.

By this thesis, it can be concluded that Leangen Ice Rink produces more than enough waste heat to cover the space heating demand of zone B1. It is also found that it produces enough excess energy to cover the space heating demand for some additional zones. However, it does not seem like, based on the calculations in this thesis, it will be able to cover the space heating demand for all the zones at Tungavegen 1. It should still be an investment, and when time comes for the later zones to be built, new possibilities of heat sources should be evaluated.

This thesis can also conclude that it is numerically possible to cover the DHW demand with a heat pump and the produced gray water as a heat source. This, however, requires that the evaporator of the heat pump is able to lower the temperature of the gray water with just beneath 20 K.

In order to make this work, the piping system needs to separate the gray water from the black water. This must be taken into consideration when planning the building process of Tungavegen 1.

It can be concluded, by the results found in this thesis, that both methods are beneficial for Tungavegen 1. This seen from both an environmental and an economical viewpoint. They are both able to save almost the same amount of energy in the form of electricity for zone B1, and the total justified investment cost at each energy central can be 6 million NOK if the life expectancy is 19 years or above.

When regarding the integration of the space heating circuit, and using the gray water as a heat sink, integrating the pipes within the walls of the tank is not the

best option. The only exception is if analysis regarding the heat pump used for the space cooling circuit is shown to need high temperatures in the condenser. Instead, an external heat exchanger could be used, making for more efficient heat transfer. Another solution is using the local thermal grid as a heat sink instead. However, what is evident from this thesis, is that, somehow, the energy produced by the space cooling system should not be discarded, but rather used as an heat source another place in the system. If, however, it is decided to go for this approach, parallel pipes should be used, in order to minimize the pressure losses.

All the results from this thesis, show that Tungavegen 1 has the ability to become a sustainable contribution to Trondheim. Using the innovative and smart solutions presented in this thesis, will help saving money, and also help with reaching the United Nations' seventh sustainability goal.

Chapter 7

Further Work

To take the findings of this thesis further, a deeper energy evaluation should be performed. The zone evaluated in this thesis, consists of both apartment buildings and terraced houses. An evaluation of a zone that only consists of apartment buildings could be interesting to look at, to see if there is a noticeable difference.

It should also be performed a better energy evaluation regarding the space cooling system. It is not very common to provide space cooling in residential buildings in Norway, because of the low temperatures. Making a heat pump in Dymola solely for the space cooling should be included in a more extensive evaluation. This would also give a more accurate profile of how much energy the condenser will actually provide.

Looking closer at how much energy it is possible to pull out of the gray water, and how a heat pump should be designed in order to cover the total demand of the space heating, would also be interesting to look at. This thesis has looked at how much the gray water must reduce in temperature, but does not specify how a heat pump should be designed in order to make this happen.

Another way of taking this thesis further, is to look deeper into how an external heat exchanger could be used, rather than integrated pipes in the wall. Either by introducing a heat exchanger before the gray water enters the tank, or discarding that completely and only provide heat in the local thermal grid.

In order to make of use all the resources available at Leangen, a deeper evaluation of the potential of using solar power could be performed as well. A method of doing this is calculating how big of an area would be needed in order to make a significant impact.

The financial analysis has been superficial and the focus has been on mostly technical issues and energy efficiency. It would be of great interest, but also a necessity to do a thorough analysis on cost, savings and return on investment. To do this, more detailed knowledge about market, prices, systems and potential must be acquired.

Bibliography

[1] *Active Solar Heating* [2019], https://www.energy.gov/energysaver/home-heating-systems/active-solar-heating. (Accessed: 2019-11-05).

[2] Antonsson, G., Grote, K.-H. and Antonsson, E. K. [2008], *Springer Handbook of Mechanical Engineering*, Springer.

[3] Berge, E. V., ed. [2014], *Energiforskyning på Furuset*, Future Built.

[4] Cengel, Y. A. and Cimbala, J. M. [2014], *Fluid Mechanics - Fundamentals and Applications*, third edn, McGraw-Hill.

[5] *COMSOL 5.4 for Windows* [2020], https://www.comsol.no/product-download/5.5/windows.

[6] Cubrick, R. [2016], 'Thermally active building systems explained', https://web.uponor.hk/radiant-cooling-blog/thermally-active-building-systems-explained/. (Accessed: 2019-12-15).

[7] Cubrick, R. [2017], 'The benefits of thermally active building systems'.

[8] Data, L. [2020], 'Lov om produksjon, omforming, overføring, omsetning, fordeling og bruk av energi m.m. (energiloven)'.

[9] *Day-Ahead Price* [2019], https://www.nordpoolgroup.com/Market-data1/Dayahead/Area-Prices/NO/Daily1/?view=table.

[10] *DELL Latitude laptop* [2019], https://www.dell.com/.

[11] *Detaljregulering for Tungavegen 1 - Planbeskrivelse* [2018].

[12] Dincer, I. and Rosen, M. A. [2010], Thermal energy storage (tes) methods, *in* 'Thermal Energy Storage: Systems and Applications', 2nd edn, John Wiley & Sons, chapter 3.

[13] *District heating briefly explained* [n.d.], https://www.statkraft.com/energy-sources/district-heating/district-heating-briefly-explained/. (Accessed: 2019-12-02).

[14] *Dymola Software* [2020], https://dymola.software.informer.com/.

[15] *Eco-friendly Supermarkets - an Overview* [2016].

[16] *ectogrid* [n.d.], https://www.ectogrid.com/. (Accessed: 2020-03-23).

[17] *Everything you need to know about HVAC systems* [n.d.], http://twentyonecelsius.com.au/blog/everything-you-need-to-know-about-hvac-systems/. (Accessed: 2019-12-15).

[18] Feilber, N. and Grinden, B. [2006], *Ny kunnskap om fordeling av strømforbruket*, SINTEF Energiforskyning AS.

[19] Gustafossen, J. and Sandin, F. [2016], District heating monitoring and control systems, *in* 'Advanced District Heating and Cooling (DHC) Systems', Woodhead Publishing, chapter 12, pp. 241–258.

[20] Hafner, A. [2020], 'Forbruksanalyse-leangen ishall-2018-2020'.

[21] Hansen, C. H. and Gudmundsson, O. [2018], 'The competiveness of district heating compared to individual heating', *Grøn Energi* .

[22] *Hva er HVAC?* [2015], https://www.itbaktuelt.no/2015/03/27/hva-er-hvac/. (Accessed: 2020-01-15).

[23] Incropera, F. P. and DeWitt, D. P. [2002], *Fundamentals of Heat and Mass Transfer*, fifth edn, John Wiley & Sons.

[24] Ingenieure, V. D. [2010], *VDI Heat Atlas*, second edn, Springer Reference.

[25] Kauko, H. [2019], 'Bra oversikt - varmebehov gjennomsnittsår'.

[26] Kauko, H. L. P. [2017], Development of smart thermal grids, Technical report, SINTEF.

[27] *Krav til passivhus* [2018], https://bygg.tekna.no/krav-til-passivhus/. (Accessed: 2020-01-16).

[28] Lauenburg, P. [2016], Temperature optimization in district heating systems, *in* 'Advanced District Heating and Cooling (DHC) Systems', Woodhead Publishing, chapter 11, pp. 223–240.

[29] Li, H. and Nord, N. [2018], Transition to the 4th generation district heating - possibilities, bottlenecks, and challenges, *in* 'Energy Procedia', Vol. 149, ELSEVIER, pp. 483–498.

[30] Lindberg, K. B., Bakker, S. J. and Sartori, I. [2019], Modelling electric and heat load profiles of non-residential buildings for use in long-term aggregate load forecasts, *in* 'Utilities Policy', ELSEVIER.

[31] Lund, H., Werner, S., Wiltshire, R., Svendsen, S. and ans Frede Hvelplund ans Brian Vad Mathiesen, J. E. T. [2014], 4th generation district heating (4gdh): Integrating smart thermal grids into future sustainable energy systems, *in* 'Energy', Vol. 68, ELSEVIER, pp. 1–11.

[32] Mazhar, A. R., Liu, S. and Shukla, A. [2018], 'A key review of non-industrial greywater heat harnessing', *energies* .

[33] McDonald, A. G. and Magande, H. L. [2012], *Introduction to Thermo-Fluids Systems Design*, first edn, John Wiley & Sons.

[34] McNabola, A. and Shields, K. [2013], Efficient drain water heat recovery in horizontal domestic shower drains, *in* 'Energy and Buildings', ELSEVIER, pp. 44–49.

[35] *Medicon Village - Möten och samarbeten i en innovativ life science-miljö* [n.d.], `https://www.mediconvillage.se`. (Accessed: 2020-03-23).

[36] *Monthly solar irradiation estimates* [n.d.], `https://ec.europa.eu/jrc/en/pvgis`. (Accessed: 2020-02-05).

[37] Nem [2020*a*], *Kulde og varmepumper nr. 1 2020*.

[38] Nem [2020*b*], *Kulde og varmepumper nr. 2 2020*.

[39] n.n. [2008], 'Transcritical refrigeration systems with carbon dioxide (co2)', *Danfoss A/S* .

[40] n.n. [n.d.], Eco-friendly supermarkets - an overview. Published by SuperSmart.

[41] NorskFjernvarme [2013], '4. generasjons fjernvarme', `http://www.fjernvarmedagene.no/index.php?pageID=102&openLevel=36`. (Accessed: 2020-02-17).

[42] Novakovic, V., Hanssen, S. O., Thue, J. V., Wangensteen, I. and Gjerstad, F. O. [2007], *Energy Management in Buildings*, 3 edn, Gyldendal Norsk Foralg AS.

[43] *NVE nettleie statistikk* [2020], `https://www.nve.no/reguleringsmyndigheten/nettjenester/nettleie/nettleiestatistikk/`. (Accessed: 2020-11-01).

[44] Olsson, K. [2007], 'Er ozonlaget reddet'.

[45] ONDA [2020], 'Plate heat exchanger working principle', `https://www.onda-it.com/eng/news/how-a-plate-heat-exchanger-works/plate-heat-exchanger-working-principle`. (Accessed: 2020-02-27).

[46] Papadaki, A. and Stegou-Sagia, A. [2015], Exergy analysis of CO_2 heat pump systems, *in* 'International Journal of Energy and Environment', 2 edn, Vol. 6, International Energy and Environment Foundation, pp. 165–174.

[47] Pfafferott, D. J., Kalz, D. and Lang, J. [2007], *Thermo-active building systems*, FIZ Karlsruhe.

[48] PipeLife [2020], 'Pe 100 rc trykkrør i kveil', `https://catalog.pipelife.com/no`.

[49] Sarbu, I. and Sebarchievici, C. [2017], Solar water and space-heating systems, *in* 'Solar Heating and Cooling Systems', Academic Press, chapter 5, pp. 139–206.

[50] Sarbu, I. and Sebarchievici, C. [2018], 'A comprehensive review of thermal energy storage', *MDPI Sustainability* .

[51] Sarkar, J., Bhattacharyya, S. and Gopal, M. R. [2005], Transcritical co2 heat pump systems: exergy analysis including heat transfer and fluid flow effects, *in* 'Energy Conversion and Management', Vol. 46, ELSEVIER, pp. 2053–2067.

[52] Sartori, I., Wachenfeldt, B. J. and Hestnes, A. G. [2019], Energy demand in the norwegian building stock: Scenarios on potential reduction, *in* 'Energy Policy', 5 edn, Vol. 37, ELSEVIER, pp. 1614–1627.

[53] Schlemminger, C. [2019], 'Tine-meieri leangen'. [email].

[54] SN [2013], *Kriterier for passivhus og lavenergibygninger - Boligbygninger*.

[55] SN [2016], *Bygningers energiytelse - Beregning av energibehov og energiforskyning*.

[56] Soroka, L. B. [2007], *Industrial Heat Pumps*, Leonardo ENERGY.

[57] Sta [2020], *Fjernvarmetariff PT1V til fellesmålte borettslag/sameier i Trondheim*.

[58] Stene, J. [1997], *VARMEPUMPER Grunnleggende varmepumpeteknikk*, 4 edn, SINTEF Energi.

[59] Stene, J. [2019*a*], *Arbeidsmedier (kuldemedier) for varmepumpeprosessen*, NTNU.

[60] Stene, J. [2019*b*], *TEP4260 Varmepumper for bygningsklimatisering*, NTNU.

[61] Sundal, E. V. [2019], Energy flow analysis of a smartthermal grid at leangen, Master's thesis, NTNU.

[62] *Sustainable Development Goals* [n.d.], `https://sustainabledevelopment.un.org/?menu=1300`. (Accessed: 2019-10-09).

[63] Takács, J., Straková, Z. and Rácz, L. [2017], 'Costs analysis of circulation pumps for heating of residential building', *Periodica Polytechnica Mechanical Engineering* **62**(1), 10–15.

[64] Torras, S., Oliet, C., Rigola, J. and Oliva, A. [2016], Drain water heat recovery storage-type unit for residential housing, *in* 'Applied Thermal Engrineering', Vol. 103, ELSEVIER, pp. 670–683.

[65] *Trondheim* [n.d.], `https://www.statkraftvarme.no/om-statkraftvarme/vare-anlegg/norge/trondheim/`. (Accessed: 2019-12-17).

[66] *Underfloor Heating* [n.d.], https://www.netatmo.com/en-gb/glossary/underfloor-heating. (Accessed: 2019-12-15).

[67] *Varmegjenvinning av gråvann* [2016], https://www.enova.no/privat/alle-energitiltak/varmegjenvinning/varmegjenvinning-av-gravann-/. (Accessed: 2020-02-27).

[68] *Veiledning til Byggteknisk forskrift (TEK17)* [2017], https://dibk.no/byggereglene/byggteknisk-forskrift-tek17. (Accessed: 2019-11-21).

[69] Yang, X., Li, H. and Svendsen, S. [2016], 'Alternative solutions for inhibiting legionella in domestic hot water systems based on low-temperature district heating', *Building services engineering research technology* **37**(4), 468–478.

[70] Zijdemans, D., ed. [2020], *Veiledning for vannbåren gulvvarme i boliger og næringsbygg*, Standard Norge.

Acronyms

4GDH 4th Generation District Heating. 6, 7

COP coefficient of performance. 35, 37, 38

DHW domestic hot water. iii, 6, 26, 30, 34, 44, 48–54, 59–61, 64, 70–74, 79, 97, 98, 100, 101, 103–105, 108

GFA gross floor area. xiv, 27, 47, 48, 50, 61, 78, 101

GWP global warming potential. 39, 40

HVAC heating, ventilation and air conditioning. 12, 13

IHP industrial heat pump. 35

LHS latent heat storage. 42

NPV net present value. 44, 71, 98

ODP ozone depletion potential. 39, 40

PMV predicted mean vote. 26, 76, 102

PPD predicted percentage dissatisfied. 26, 76, 102

SFP specific fan power. 24

SHS sensible heat storage. 42, 43

TABS Thermally Active Building System. 12, 13

TES thermal energy storage. 7, 42, 43, 49, 61

Mari Elisabeth Jensvold Ørbæk

NTNU
Kunnskap for ei betre verd